STELLAR ROTATION

EFFECTS OF ROTATION ON COLOURS AND LINE INDICES OF STARS

A Thesis
Submitted for the Degree of
Doctor of Philosophy in the Faculty of Science
Mahatma Gandhi University, Kottayam

by

ANNAMMA MATHEW

INDIAN INSTITUTE OF ASTROPHYSICS
BANGALORE 560034
INDIA

1993 MAY

CERTIFICATE

This is to certify that the Thesis entitled "Stellar Rotation - Effects of Rotation on Colours and Line Indices of Stars" is an authentic record of the research work carried out by Mrs.Annamma Mathew under our supervision and guidance during the period June 1987 - December 1991 in partial fulfilment of the requirements of the degree of Doctor of Philosophy under the Faculty of Science of the Mahatma Gandhi University. The work presented in this Thesis has not been submitted for any degree or diploma earlier. It is also certified that Mrs.Annamma Mathew has fulfilled the Course requirements and passed the qualifying examination for the Ph.D. degree of this University.

Prof.R.Rajamohan
Supervising Teacher

Prof.M.A.Ittyachen
Supervising Teacher

1993 May

D E C L A R A T I O N

I hereby declare that the Thesis entitled "Stellar Rotation - Effects of Rotation on Colours and Line Indices of Stars" is an authentic record of the research work carried out by me under the supervision of Prof.R.Rajamohan, Indian Institute of Astrophysics, Bangalore and Prof.M.A.Ittyachen, Director, School of Pure and Applied Physics, Mahatma Gandhi University, Kottayam. No part of the Thesis has been presented for any other degree or diploma earlier.

Annamma Mathew

Indian Institute of Astrophysics
Bangalore 560034
1993 May

Dedicated

to

my Parents

Acknowledgement

I express my sincere gratitude to Prof.R.Rajamohan of Indian Institute of Astrophysics, Bangalore, for his invaluable suggestions, constant guidance, whole hearted encouragement and inspiration in carrying out every aspect of this work, without which this work could not have been accomplished. I am also grateful to Prof.M.A.Ittyachan of Mahatma Gandhi University, Kottayam, Kerala for his acceptance as my co-guide and for rendering his help towards the success of this effort.

I am extremely thankful to Prof.K.R.Sivaraman, Director, Indian Institute of Astrophysics, Bangalore, for the help in deputation at the Institute, the interest and encouragement shown in the project and for providing all the facilities for completion of this study. I also thank Prof.J.C.Bhattacharrya, former Director of Indian Institute of Astrophysics, for providing all the facilities at the Institute and for the support and encouragement to me during my work.

I am thankful to the University Grants Commission, New Delhi, for their grant under the FIP with which this work was carried out. I thank Rev.Sr.Roseline, the former Principal, Rev.Sr.Cicy, the present Principal and Very. Rev. Msgr. Mathew Pulickaparambil, the Manager of Assumption College, Changanacherry, Kerala for facilitating my deputation under the FIP of UGC from the College and for extending all necessary help in fulfilling this work. I also take this opportunity to thank Mrs.Brigeethamma Devasia, the former Head, Mrs.Leela Francis, the present Head and my teachers and Colleagues of the Department of Physics, Assumption College, Changanacherry for their encouragement.

Dr.J.C.Mermilliod, of the University of Lausanne, Switzerland provided me with the necessary open cluster data. My thanks are due to him. I thank Mrs.Jacqueline D'Souza for assisting me in completion of my thesis. Most of the computations for the data analysis were dome with the help of Mighty Frame Computer of IIA. I am extremely thankful to Prof.A.Peraiah, for making available unlimited computer time and space. I thank Mr.Baba Antony Verghese and Dr.K.E.Rangarajan for the ready help provided by them. I gratefully acknowledge the computer programmes given by Dr.A.V.Raveendran and the ready help whenever needed. Thanks are due to Mrs.Kuriakose, Mr.Moorthy, Ms.Sandra Rajeeva, Mr.S.Rajasekaran, Mr.K.Sasidharan, Mr.Arvind Paranjpye and Ms.Bhargavi for their help. I remember with gratitude the encouragement given by Prof.S.L. Thomas, Dr.Vasundhara Raju, Dr.Prasannalakshmi, Dr.Ingulgi, Dr.Mathew

Verghese Mekkadan Dr.S. Mohin and other friends.

Ms.A.Vagiswari, Ms.Christina Louis, Mr.H.N.Manjunath and other staff of Indian Institute of Astrophysics Library rendered help in making books, journals, references and xerox copies readily available. Mr.M.G. Chandrasekharan Nair did the typing of the entire thesis. Diagrams are drawn by Mr.S.Muthukrishnan. Mr.P.N.Prabhakara made the photocopies. Mr. and Mrs.R.Krishnamoorthy, P. Pose and M.Subramani are responsible for getting the thesis bound. My thanks are due to each of them. I thank again all the staff members of IIA Bangalore for rendering all the help I required.

Finally, I am extremely grateful to my parents, brothers and sisters, my husband and children for their support and encouragement.

STELLAR ROTATION

EFFECTS OF ROTATION ON COLOURS AND LINE INDICES OF STARS

Summary

The effect of rotation on colours and line indices of stars has been a subject of some controversy, though not actually appreciated as such. Empirical calibrations of broad band and narrow band indices available in the literature have all been carried out without taking rotation effects into account. (e.g. u v b y and β by Crawford 1978, 1979). The discordant results in this field until 1970 have been nicely summarised by Collins (1970). The basic reason, that rotation effects on colours and line indices of stars could not be established firmly, seems to be due to the smallness of the effect at moderte rotational velocities. Further, the effects on observed indices by other causes such as duplicity, chemical peculiarity, evolutionary effects and variable interstellar extinction appear to have introduced a large uncertainity in the determination of rotation effects.

The problem is further complicated by the fact that the effects are a function of the mass of the stars. Theoretical work especially by Collins and his collaborators shows that each index is affected differently and very large effects shoud be observable for the A stars even for moderate rotational velocities. Also, there is no observable parameter which is not affected by rotation. The problem gets further confounded by the fact that only $V sin\ i$ is observable and there appears to be no way of determinging V and i independantly.

We decided therefore to take an approach that would take care of most of these complications. We eliminated, in each cluster, known Be stars, double-lined binaries and close visual binaries with $\Delta m < 2.0$ magnitudes. Only luminosity class IV and V stars are considered. Differences between cluster and cluster would also not affect the final results as each cluster is analysed independantly. B and A spectral type stars were analysed independantly. For each cluster, two colour indices were plotted against each other and a second order polynomial fit was derived. The observed minus computed (O-C) residuals in each index was determined and plotted against $V sin\ i$. These rotation effects determined are relative as both indices are affected by rotation.

As interstellar extinction also reddens the stars, the Alpha Persei Cluster was analysed using both observed and dereddened indices. It was found that for Alpha Persei, where non-uniformity of extinction is not large, both reddened and dereddened indices lead to similar results. However, as suggested by Gray and Garrison, we used the observed indices for other clusters as dereddening procedures for A-stars are based on an assumed calibration which may be in error due to rotational reddening.

Evolutionary effects will introduce a scatter if the cluster members are not coeval. This is evident from our results for the Scorpio-Centaurus association. Here the Upper Scorpius members which are younger than the Lower Centaurus and Upper Centaurus subgroups were found to be separated in all diagrams of colour excess due to reddening versus $V sin\ i$ diagrams. Also the scatter for Upper Scorpius was large where the interstellar extinction is highly non-uniform. The Upper Centaurus and Lower Centaurus group which are unreddened, consisting mostly of B2 and B3 type-stars show the reddening effect due to rotation in perfect agreement with theoretical predictions by Collins & Sonneborn (1977) for stars in the similar mass range.

We have established firmly the rotation effects for various mass ranges by analysing a large number of clusters for which sufficient data was available. As the predicted effects are a function of the mass, we analysed all clusters grouping them into three mass ranges corresponding to the spectral type ranges B0-B3, B5-B9 and A3-F0. The predicted indices for these ranges by Collins and his co-workers were analysed the same way as we did our observational data.

In our analysis of the theoretically derived indices we did not assume any distribution in V or i. Instead, for each value of i (30°, 45°, 60° and 90°) we took sixteen values corresponding to ω=0.2, 0.5, 0.8 and 0.9 for the mass range corresponding to the spectral types from B0-B3, B5-B9 and A3-F0 and derived the rotation effects in different planes (such as β, c_1; β,(u-b) etc.). We found that the rotation effects determined from observed data points for clusters, very closely matched the predictions for the various mass ranges. When this work was almost completed, Collins, Truax & Cranmer (1991) published the results of extensive model atmosphere calculations applicable to rotating early-type stars. These indices were also analysed the same way as we did for Collins and Sonneborn (1977) models. On an average the predicted theoretical rotation effects of the two models does not differ appreciably. This work establishes very firmly, for the first time, that not only rotation effects can be discerned from observations but also that the agreement is good with theoretical predictions of Collins & Sonneborn (1977) and Collins, Truax & Cranmer (1991) for rigidly rotating stars.

We derived ZRZAMS by two methods. In the first method we derived the

ZRMS of each cluster using observed slopes of rotation effects. These were superposed to derive ZRZAMS. Similarly theoretical corrections for each star were made to derive ZRMS for each cluster. These were superposed to derive the ZRZAMS as derived from theoretical predictions (for i=60°). The two sets were found to agree with each other. The absolute magnitudes were corrected only using theoretical predictions. The β, M_v relation for ZRZAMS derived by us is in excellent agreement with the values for the lower envelope of B-stars in the β, M_v plane derived by Crawford (1978). This is as expected since the slow rotators in such a plane would lie along the blue envelope. We have established for the first time the empirical zero rotation zero age values for the intermediate band indices u v b y and H_β.

The most dramatic result that we have obtained is that the blue straggler phenomenon in young galactic clusters can be completely interpreted in terms of rotation effects in colour magnitude diagrams at least in the large majority of clusters with ages less than or equal to Hyades.

The effect of rotation on observed colours of stars was considered as a possible cause for the observed position of blue stragglers in star clusters. We find that the observed blueness of the blue stragglers which are intrinsic slow rotators, in the B7-A2 type range can easily be accounted for by such effects. The reddening caused by rotation shifts the entire cluster main sequence away from the zero rotation main sequence leaving the slow rotators behind. The rotation effect in $(u-b)_o$ index reaches a maximum in the B7−A0 spectral type range where all the slowly rotating blue stragglers are also concentrated. It is also therefore not surprising that the majority of these A−type stragglers are found to be CP stars.

Table of Contents

I. INTRODUCTION

The idea that axial rotation could be determined from the measurements of the widths of spectral lines was first put forward by Captain W.de.Abney (1877). Since then many efforts have been made to determine the rotational velocities of various types and groups of stars. (See e.g. reviews by Huang & Struve 1960; Slettebak 1970; Plavec 1970; Abt 1970). Simultaneously attempts were also made to estimate the changes in the structure of the star due to rotation and the observable effects such changes would produce (see e g. reviews by Roxburgh 1970; Kraft 1969; Collins 1970).

Broadly, the main results can be summarized as follows. The early type B, A and F main-sequence stars rotate fairly fast while stars later than F5 are in general, very slow rotators. Amongst the early-type stars, those that are in binaries are slow rotators on an average than similar single stars, mainly due to the synchronization of rotational and orbital periods. The chemically peculiar (CP)stars of the upper main-sequence are in general slow rotators. The differences between field and cluster stars and between cluster and cluster in the observed rotational velocity distribution are caused by differences in binary and CP star frequencies and by the differences in their ages. Even though there seems to be a concensus as far as these results are concerned, the situation regarding the predicted changes in the structure of these stars and their effects on the observable parameters is quite different.

In fact, the results of the analysis of observations by different authors have led to conflicting results on the possible effects of stellar rotation on the observable parameters (see e.g. the review by Collins 1970). As of today, all existing calibrations of various parameters and the estimates of ages of stars from colour magnitude diagrams have all been done completely disregarding the (predicted) effects due to rotation.

The earliest effort in this field seems to be that of Sweet and Roy (1953) who showed that rotation modifies the luminosity of a star and that it could be as large as one magnitude relative to its non-rotating counterpart. Since then Roxburgh, Griffith and Sweet (1965) Roxburgh and Strittmatter (1965, 1966) Hardorp and Strittmatter (1968) and Collins (1963, 1965), Collins and Harrington (1966) Collins and Sonneborn (1977) and Collins and Smith (1985) have considered in detail the expected rotation effects on the various observable parameters of stars.

In general, such predicted effects in colours and the absolute magnitudes of stars and other observable parameters such as the equivalent widths of the lines are not large except in case of extreme rotational velocities. Attempts to verify such predicted effects were made successfully by Strittmatter (1966) in the Praesepe cluster. Strittmatter measured the difference in the observed M_v and the M_v defined by non-rotators at a fixed (B-V). These deviations ΔM_v were found as expected to be proportional to $(V sin\ i)^2$ based on Roxburgh and Strittmatter's (1966) work. These results, however, were questioned by Dickens, Kraft and Krzeminski (1968) and that more accurate data do not show the expected relationship between (U-B) colours and $V sin\ i$.

Kraft and Wrubel (1965) attributed the large spread in c_1, (b-y) diagram in Hyades to rotation effects. Strömgren (1967) pointed out that no rotation effects are discernible in the intermediate band indices while Crawford and Barnes (1974) found that the c_1 index was affected by as much as 0.035 magnitudes per 100 km s^{-1} of $V sin\ i$ in A stars of α-Persei while the values of B-stars showed no such effects. Hartwick and Hesser (1974) found evidence for rotation effects in the c_1 and β indices of field A and F type stars while Rajamohan (1978) found similar evidence for B and A stars of the α-Persei cluster and Scorpio-Centaurus association.

Similarly Guthrie (1963) found that rotation effects are indeed discernible in H_β line strengths at a given (U-B) index. The theoretical predictions by Collins & Harrington (1966) are in good agreement with Guthrie's findings. However, Crawford & Manders (1966) and Petrie (1964) respectively found no evidence for effects of rotation on H_β and H_γ line strengths. Warren (1976) discussed the proposed rotation effects in some detail, for B-stars in Orion, and showed that no systematic effects are present for $V sin\ i$ less than 250 km s^{-1}.

No consistent picture had emerged as on 1987 when we took up this work to investigate systematically the effects of rotation on the colours and line indices of stars. We decided to reinvestigate this problem in galactic clusters and determine, empirically the effects of rotation on the colour and line indices of stars.

In the meantime Gray & Garrison (1987, 1988, 1989) from a refined MK classification of A and F type field stars, showed that indeed rotation effects can be clearly established in the intermediate band indices c_1 & β.

We have approached the problem in the following manner. By (1) Choosing galactic clusters instead of field stars to reduce the scatter that would be introduced by differences in ages of stars (2) Analyzing each cluster independently to minimize any differences that may exist due to zero point differences for different observers (3) Choosing preferably normal main-sequence single stars (4) Allowing each cluster data to define their own relationship between any two indices to avoid use of existing relationships that have been derived without any regard to the rotational velocities of stars.

In Chapter II, we present the results obtained from analysis of selected uvby H_β data of galactic clusters. In Chapter III we analyze the theoretical predictions of Collins and Sonneborn (1977) and compare the results with those obtained from analysis of observation. We use the results of Chapter II and III to derive the zero-rotation main sequence (ZRMS) values for selected clusters and a preliminary Zero-Age Zero-Rotation-Main Sequence (ZAZRMS) in Chapter IV. In Chapter V, we show how rotation can almost completely account for the blue straggler phenomenon. A brief summary of the results is presented in Chapter VI.

II. EFFECTS OF ROTATION ON COLOURS AND LINE INDICES OF STARS

1. Data and Analysis

Before the available data for cluster members can be analysed for rotation effects, the following factors that affect their colours have to be taken into account.

1. Binary nature: This makes the star generally lie above the main sequence defined by non-rotating single stars. This factor, first suggested by Atkinson (1937) for identifying binaries from colour-magnitude diagrams depends on the mass ratio and evolutionary status of the components. Binaries in general rotate synchronously and hence have lower rotational velocities than single stars of the same spectral type. This effect leads to the inverse correlation between mean rotational velocities and binary frequency of clusters found by Abt & Hunter (1962).

2. The chemically peculiar stars are likely to have colours different from normal stars owing to line-blanketting effects. These are, in general, slow rotators and some of them are magnetic and spectrum variables. The binary frequency amongst magnetic stars is very low, whereas almost all Am stars are likely to be in binary systems (Abt 1965).

3. Evolutionary effects: If the sample does not confirm to a homogeneous coeval group, then evolutionary effects (even within the main-sequence lifetime) have to be taken into account as this would introduce a spread in the observed colour-magnitude diagrams. The advantage of analysing cluster data is that this effect would be a minimum, though in some clusters and associations it is known that not all members are coeval.

4. Reddening due to Interstellar Extinction: Extinction and rotation both lead to reddened indices. Since extinction values in literature have all been derived without taking rotational reddening into account it is necessary to reexamine this problem carefully (Gray & Garrison 1989).

5. Large systematic errors in photometry: Eventhough there is no evidence that such systematic observational errors exist, it is worth noticing that Trimble & Ostriker (1978, 1981) found that some unknown effect exists which complicates the analysis of cluster data for discriminating between double and rotating stars. We plan to overcome this problem by analysing each cluster independently.

The errors in photometry are of the order of ± 0.01 magnitudes. The errors in $V sin\ i$ generally quoted are of the order of 10%. However, according to Collins the errors in $V sin\ i$ derived by conventional methods for stars rotating close to break-up speeds can be as large as 40%. In general, such stars will be classified as Be and they have not been included in the analysis.

In principle it is difficult to determine rotation effects on Colours as theory predicts that almost all observable parameters including the V-magni-tude of the stars are affected by rotation and the magnitude of this effect depends, for each star, on its mass m, rotational velocity V and the inclination 'i'of the rotation axis to the line-of-sight. Thus, two objects of differing masses can have identical colour indices due to their differences in V and i (see eg. Collins & Smith 1985). Therefore, in principle, it is difficult to correct for rotation effects from the observed distribution in colour-colour plots as V and i are unknown and all observable parameters are affected to a larger or smaller extent.

Another problem is the role of interstellar extinction as both rotation and extinction lead to reddened indices. The determination of the extinction values will be uncertain especially when both effects are comparable and the individual extinction values for each star will be highly uncertain, if rotation effects are not allowed for. Also, as pointed out by Gray & Garrison (1989), the system calibration and dereddening procedures, especially for A stars, are themselves affected by rotation which then would cast some doubt in the determination of colour excess due to extinction. Thus, in order to derive the intrinsic parameters for a calibration of indices, we need to correct for extinction and rotation but the calibration procedures depend on an assumed relationship that has not taken rotation into account. Also, only $V sin\ i$ is observable whereas to calibrate we need to know the individual values of V and i. Also quantities such as the mass of the star, which are unaffected by rotation are unknown. Theory also predicts that rotation effects vary as a function of mass and each index varies differently [Collins & Sonneborn (1977), Collins & Smith (1985)].

Our approach to this complicated problem was the following. The effect of rotation is to displace the main sequence of a cluster of coeval stars from its non-rotating counterpart and broaden it by about twice the displacement (Collins & Smith 1985). The maximum shift of a single star depends on the maximum rotational velocity that the star can rotate with; this corresponds to the balance between the centrifugal force and gravity at the equator. The distribution of the cluster stars in the band between its Zero Rotation Main Sequence (ZRMS) and the Critical Velocity Main Sequence (CVMS) depends on the spread in the true rotational velocities of stars. This spread is not sensitive to 'i' (Collins & Sonneborn 1977, Collins & Smith 1985).

Therefore one can expect, for a Maxwellian distribution in V and i, the spread to be dependent on the observed projected rotational velocity $V sin\ i$ as only few objects will be at the tail end of such a distribution. Even though the effects of the rotation of stars are non-linear in V and $V sin\ i$, such non-linearities are important only for stars rotating close to their break-up speeds (ω=1.0). Only early B-stars rotate close to their break-up speeds and such objects can be generally recognised by the emission phenomenon associated with them. The maximum observed rotational velocities for others correspond to $\omega \leq 0.9$ (Rajamohan 1978). Hence if Be stars are excluded, then the rest of the objects can be expected to show a deviation from the ZRMS which will depend, linearly on the average observed rotational velocities of stars (Collins & Harrington 1966; Mathew & Rajamohan 1990). But the position of the ZRMS is unknown. Hence the following procedure was adopted.

We eliminated, in each cluster, known Be stars, double-lined binaries, and close visual binaries with $\Delta m < 2.0$ magnitudes. Only stars of luminosity class IV and V were considered. In a colour-colour plot, we assume that these apparently single stars will define an average sequence parallel to the ZRMS. A single intrinsic line that defines this mean relationship also defines the average shift of the main sequence for the mean observed rotational velocities of the cluster members. The advantage of this method is that while we use all stars to get a statistically significant sample, the intrinsic differences in the angular momentum distribution at different masses will not affect the results significantly. Difference between cluster to cluster would also not affect the final results as each cluster is analysed independantly.

B and A type main sequence members were analysed separately. For each cluster, two colour indices were plotted against each other and a second order polynomial fit was derived. The observed minus computed (O-C) residuals in each index were determined and plotted against $V sin\ i$. The rotation effects determined are relative as both indices are affected by rotation. Errors in photometry and $V sin\ i$ determinations can not completely account for the residual scatter in all these correlation diagrams.

A list of clusters with available uvby, H_β and $V sin\ i$ data was provided by Dr.J.-C.Mermilliod of the University of Lausanne, Switzerland. We analysed the data of most of these clusters in which a statistically significant sample of single main-sequence members with known $V sin\ i$ values were present. The references to the cluster data utilised in this study are given in Table II–1. Detailed description of the analysis of a few selected clusters are given. A final summary of the results of all the clusters analysed is given in Table II-16 and results for all the indices for a few selected clusters in Table II–17.

Table II–1. References to cluster Data

Cluster	Data	Reference	Cluster	Data	Reference
α-Persei (mel 020)	u v b y H_β	Crawford & Barnes (1974)	Coma	u v b y H_β	Crawford & Barnes (1969)
	U B V	Mitchell (1960)		U B V	Johnson & Knuckles (1955)
	Vsin i	Kraft (1967)		*Vsin i*	Kraft (1965)
	ST	Morgan Hiltner & Garrison (1971)		ST	Mendoza (1963)
Pleiades (mel 022)	u v b y H_β	Crawford & Perry (1976)	Cep OB3	u v b y H_β	Crawford & Barnes (1970)
	U B V	Johnson & Mitchell (1958)		U B V	Blaauw, Hiltner & Johnson (1959)
	Vsin i	Anderson, Stoeckly & Kraft (1966)		*Vsin i*	Garmany (1973)
	ST	Mendoza (1956)			
Hyades (mel 025)	u v b y H_β	Crawford & Perry (1966)	NGC 1039	u v b y H_β	Canterna & Perry (1979)
	U B V	Johnson & Knuckles (1955)		*Vsin i*	Ianna (1970)
	Vsin i	Kraft (1965)		ST	Ianna (1970) Abt & Levato (1977)
	ST	Morgan & Hiltner (1965)			
Praesepe (NGC 2632)	u v b y H_β	Crawford & Barnes (1969)	NGC 1976	u v b y H_β	Warren & Hesser (1977)
	U B V	Johnson (1952)		*Vsin i*	Abt, Muncaster & Thompson (1970) Mc Namara & Larson (1961)
	Vsin i	Mc Gee, Khogali, Baum & Kraft (1967)			
	ST	Bidelman (1956)		ST	Abt & Levato (1977)
Sco-Cen	u v b y H_β	Glaspey (1971)	NGC 2264	u v b y H_β	Strom, Strom & Yost (1971)
	U B V	Moreno & Moreno (1968)		*Vsin i*	Vogel & Kuhi (1981)
	Vsin i	Rajamohan (1976) Slettebak (1968) Uesugi & Fukuda (1982)		ST	Yong (1978)
	ST	Garrison (1967)			

Table II–1. Continued

Cluster	Data	Reference	Cluster	Data	Reference
NGC 2281	U B V	Pesch (1961)	NGC 6633	u v b y	Schmidt (1976)
NGC 2287	u v b y H_β	Nissen (1988)	IC 2391	u v b y H_β	Perry & Hill (1969)
		Eggen (1974, 1981)		*Vsin i*	Levato (1974)
	Vsin i	Levato & Garcia (1984)		ST	Perry & Bond (1969)
	ST	Hartoog (1976)			
NGC 2422	u v b y H_β	Shobbrook (1984)	IC 2602	u v b y H_β	Hill & Perry (1969)
	U B V	Hoag et al (1961)		U B V	Braes (1962)
		Smyth & Nandy (1962)		*Vsin i*	Levato (1975)
	Vsin i	Dworetsky (1975)			
NGC 2516	u v b y H_β	Snowden (1975)	IC 4665	u v b y H_β	Crawford & Barnes (1972)
	Vsin i	Abt & Clements (1969)			
	ST	Abt & Morgan (1969)		U B V	Hogg & Kron (1955)
		Hartoog (1976)		*Vsin i*	Abt & Chaffee (1967)
NGC 3532	u v b y	Eggen (1981)			
NGC 4755	u v b y H_β	Shobbrook (1984)	IC4756	u v b y H_β	Schmidt (1978)
	U B V	Perry, Franklin, Landolt & Crawford (1976)		*Vsin i*	Schmidt & Forbes (1984)
	Vsin i	Balona (1975)		ST	Herzog, Sanders & Seggwiss (1975)
	ST	Feast (1963)			
		Schild (1970)			
NGC 6025	u v b y	Kilambi (1975)			
NGC 6281	U B V	Feinstein & Forte (1974)			
NGC 6475	u v b y H_β	Snowden (1976)			
	Vsin i	Abt & Jewsbury (1969)			

2. Alpha-Persei: B Stars

2.1. The effect on c_1 and β in the β, c_1 plane

Table II–2 lists the relevant data for the main-sequence B stars in α-Persei. The identity number is that of Heckmann et al (1956). The last column indicates the stars whose colours are likely to be affected for reasons other than rotation, such as binary nature and chemical peculiarity. The remarks are taken from the original papers that list the data and also from the Bright Star Catalogue (Hoffleit & Jaschek 1982). As the colours of only the double-lined spectroscopic binaries and close visual pairs with $\Delta m < 2.0$ magnitudes are likely to be affected seriously, we include in general the rest of main sequence members to determine the effects of rotation. The β, c_1 values of Ams that are not SB2's or close VB's are also included.

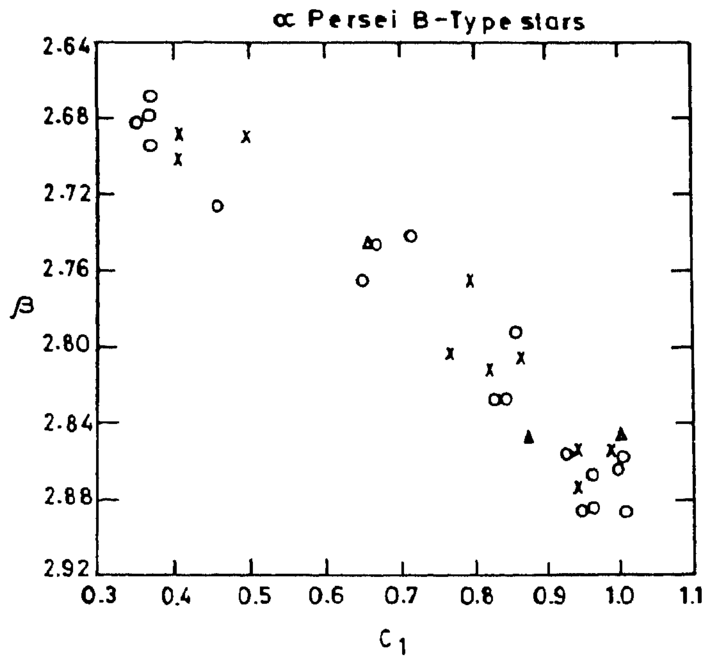

Fig II–1 : *The β, c_1 plot for B-stars in α-Persei cluster. Open circles - single stars : crosses - binaries and radial velocity variables : Triangle - emission lined star.*

A plot of β vs c_1 of α-Persei B stars given in Table II–2 is shown in Fig II–1. A second order polynomial was fitted to the data for the 23 apparent normal B stars and for each star, a calculated c_1 and β value was derived using the polynomial coefficients for its observed β and c_1 respectively. These (O-C) residuals in c_1 and

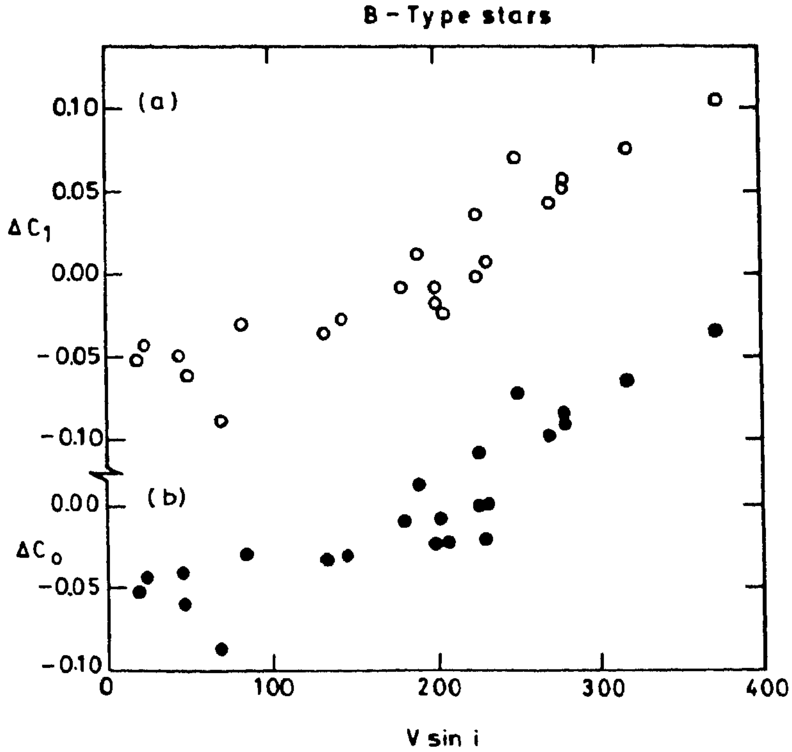

Fig II–2 : *The deviations derived for the reddened (open circles) and dereddened (filled circles) from the observed mean relation in the β, c_1 and β, c_o plane for the B-stars of α-Persei are plotted against $V sin\ i$.*

β derived for each star are given in Table II–3 and are plotted as open circles in Fig II–2 (a) and Fig II–8 respectively. A linear fit to the data points give

$$\Delta c_1 = 0.454(\pm 0.032) \times 10^{-3} V sin\ i - 0.084(\pm 0.006), \tag{1}$$

$$\Delta\beta = -0.162(\pm 0.013) \times 10^{-3} V sin\ i + 0.029(\pm 0.003). \tag{2}$$

This was repeated by using the indices corrected for interstellar extinction. The dereddening procedure which we have followed is the one given by Crawford & Barnes (1974). A linear fit to the derived residual gives:

$$\Delta c_o = 0.442(\pm 0.033) \times 10^{-3} V sin\ i - 0.032(\pm 0.007), \tag{3}$$

$$\Delta\beta = -0.150(\pm 0.013) \times 10^{-3} V sin\ i + 0.028(\pm 0.003). \tag{4}$$

The residuals in c_o are plotted against $V sin\ i$ in Fig II–2b.

Table II–2. Data for α-Persei B-type stars

No	BD	MK	V	(B-V)	(U-B)	β	(b-y)	m_1	c_1	$V sin\ i$	Remarks
167	48°862	B9.5 V	7.94	0.121	0.03	2.887	0.074	0.137	0.945	20	
212	49 876	B9 V	7.15	0.040	−0.11	2.807	0.046	0.106	0.865	280	
285	47 792	A0 p	8.09	0.214	0.15	2.848	0.144	0.135	0.999	35	Ap, SB?
333	50 731	–	7.19	0.034	−0.19	2.794	0.050	0.096	0.762	230	
383	49 899	B3 V	5.15	−0.061	−0.55	2.683	0.005	0.074	0.356	145	
401	49 902	(B5 V)	5.04	−0.080	−0.49	2.668	−0.005	0.083	0.393	320	
423	48 886	A0 Vn	7.64	0.073	0.01	2.856	0.057	0.127	0.990	280	
557	48 899	B5 V	5.26	−0.076	−0.52	2.688	−0.009	0.087	0.407	250	SB
575	51 728	A0 V	7.85	0.104	0.04	2.886	0.075	0.131	0.965	85	
581	48 903	B9 V	6.99	0.015	−0.15	2.813	0.024	0.115	0.821	200	
625	47 817	B9.5 V	7.63	0.114	0.04	2.875	0.086	0.128	0.940	25	SB?
675	48 913	B7 V	6.06	0.651	0.16	2.726	−0.027	0.104	0.462	70	
692	47 821	B9.5 V	7.49	0.034	−0.02	2.856	0.028	0.136	0.947	340	SB
729	47 826	(B9 V)	7.72	0.113	0.03	2.868	0.080	0.126	0.962	225	
735	47 828	B8.5 Vn	6.83	−0.016	−0.19	2.766	0.018	0.104	0.795	375	
774	48 920	B5 V	4.97	−0.092	−0.54	2.702	−0.027	0.095	0.407	200	SB1
775	47 831	B8.5 V	7.26	0.047	−0.16	2.804	0.057	0.100	0.786	200	
780	49 938	A1 Vn	8.09	0.166	0.11	2.888	0.104	0.150	1.005	230	
810	49 944	B6 Vn	5.58	−0.44	−0.43	2.688	0.008	0.088	0.495	385	SB
817	48 927	A1 Vn	7.46	0.113	0.07	2.866	0.071	0.149	0.998	270	
831	47 835	B9 V	7.36	0.007	−0.12	2.828	0.021	0.126	0.831	135	
835	49 945	B3 V	4.66	−0.098	−0.54	2.678	−0.022	0.084	0.373	190	
868	48 933	A1 IVn	7.28	0.092	0.01	2.858	0.060	0.147	0.930	180	
875	47 840	A0 Vn	7.66	0.103	0.06	2.858	0.068	0.137	1.008	250	Emission at H_α
904	47 844	B8 V	5.82	−0.040	−0.30	2.745	0.002	0.101	0.683	380	Shell star
955	47 846	B8.5 V	6.75	−0.019	−0.25	2.743	0.014	0.109	0.718	215	Be
965	48 943	B8 V	6.62	−0.028	−0.30	2.747	0.019	0.096	0.662	225	
985	47 847	B8 III	5.46	−0.104	−0.54	2.695	−0.038	0.109	0.369	50	
1082	48 949	B9 V	7.34	0.027	−0.10	2.829	0.034	0.126	0.847	205	
1153	46 773	(B8 V)	6.89	−0.020	−0.29	2.766	0.014	0.106	0.648	25	
1259	47 865	(A0 V)	7.45	0.004	−0.08	2.850	0.016	0.142	0.873	45	

Table II–3. Effects of rotation for α-Persei B stars

		from β, c_1		from β,(u-b)		from β (b-y)	
No	$V sin\ i$	$\Delta\beta$	Δc_1	$\Delta\beta$	Δ(u-b)	$\Delta\beta$	Δ (b-y)
167	20	.026	−.051	.023	−.080	.022	−.007
212	280	−.020	.052	−.015	.063	−.015	.014
285	35	−.022	.074	–	–	–	–
333	230	.005	−.014	−.004	.006	−.035	.024
383	145	.006	−.026	.000	−.015	−.070	.019
401	320	−.018	.076	−.022	−.094	−.066	.012
423	280	−.028	.056	−.006	.040	.016	−.003
557	250	.001	.059	–	–	–	–
575	85	.015	−.030	.020	−.066	.019	−.005
581	200	.003	−.008	.006	−.033	.027	−.011
625	25	.027	−.014	–	–	–	–
675	70	.023	−.089	.021	−.120	.034	−.025
692	340	.006	.032	–	−.084	–	–
729	225	−.001	.002	.003	.006	−.006	.012
735	375	−.035	.105	−.029	.117	−.010	.005
774	65	.012	−.041	–	–	–	–
775	200	.007	−.018	−.003	.007	−.036	.026
780	230	−.004	.007	−.007	.062	−.019	.022
810	385	−.021	.147	–	–	–	–
817	270	−.022	.043	−.013	.078	.005	.004
831	135	.014	−.037	.015	−.073	.047	−.022
835	190	−.003	.012	−.001	−.007	−.024	−.007
868	180	.004	−.008	−.001	.018	.014	−.001
875	250	−.035	.070	−.017	.092	.002	.007
904	380	−.017	.074	–	–	–	–
955	215	−.010	.116	–	–	–	–
965	225	−.029	.036	−.016	.058	−.030	.014
985	50	.015	−.062	.013	−.076	.024	−.027
1082	205	.009	−.024	.007	−.035	.026	−.010
1153	25	.013	−.042	.004	−.034	−.003	.001
1259	45	.020	−.048	.024	−.103	.078	−.040

2.2. The effect on (u-b) and β in the β, (u-b) plane

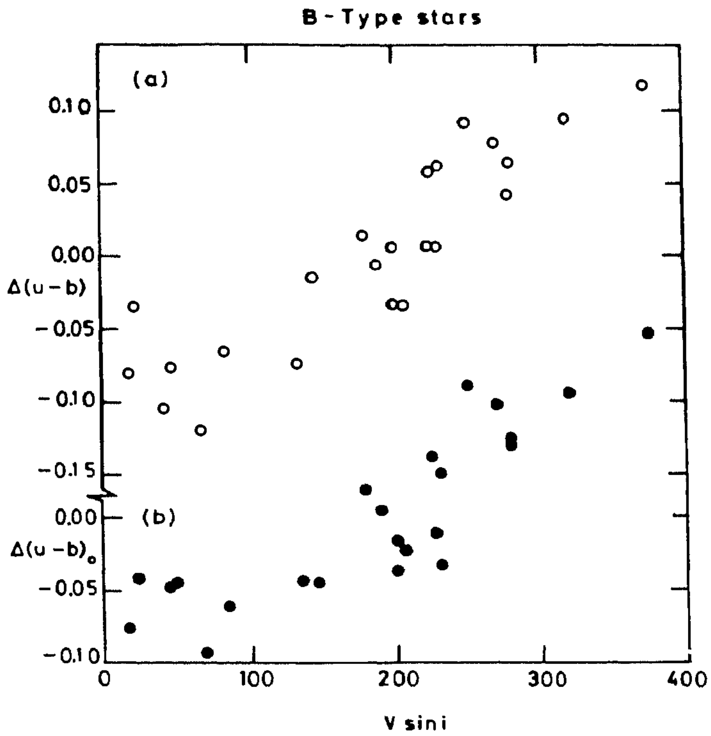

Fig II–3 : *Same as figure II–2 for reddened and dereddened indices of (u-b) in the β, (u-b) plane for α-Persei B-stars.*

From a second order polynomial fit to the β, (u-b) data for the same 23 B stars in α-Persei we derived the residuals Δ(u-b) and $\Delta\beta$. Δ(u-b) is plotted against $Vsin\ i$ in Fig II–3a. A linear fit to the derived residual gives

$$\Delta(u-b) = 0.618(\pm 0.046) \times 10^{-3} Vsin\ i - 0.114(\pm 0.009), \quad (5)$$

$$\Delta\beta = -0.134(\pm 0.010) \times 10^{-3} Vsin\ i + 0.025(\pm 0.002). \quad (6)$$

Similarly from the dereddened data we derive

$$\Delta(u-b)_o = 0.528(\pm 0.045) \times 10^{-3} Vsin\ i - 0.097(\pm 0.009), \quad (7)$$

$$\Delta\beta = -0.125(\pm 0.011) \times 10^{-3} Vsin\ i + 0.023(\pm 0.002). \quad (8)$$

Δ(u-b)$_o$ values are plotted against $Vsin\ i$ in Fig II–3b.

2.3. The effect on (b-y) and β in the β, (b-y) plane

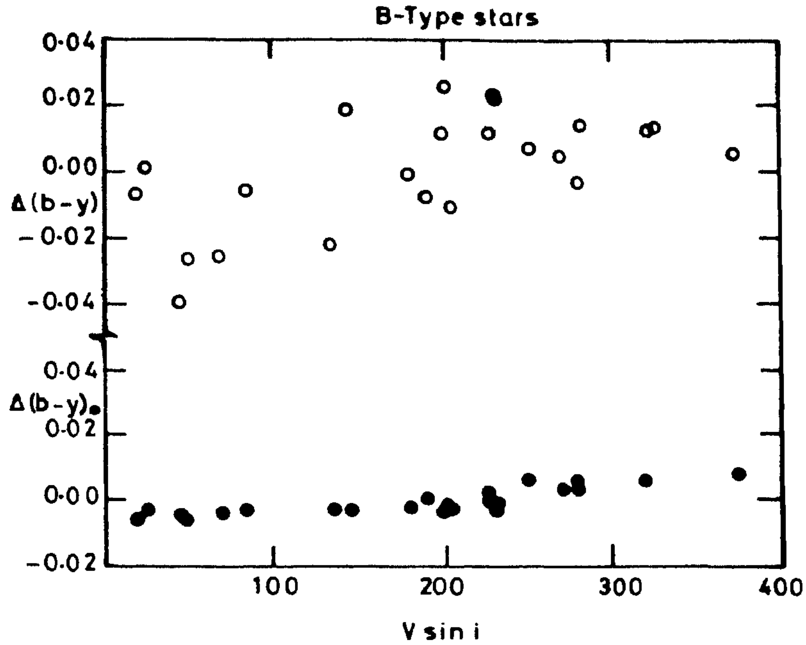

Fig II–4 : *The deviations derived for the reddened (open circles) and dereddened (filled circles) from the observed mean relation in the β, (b-y) plane for α-Persei B-stars.*

From a second order polynomial fit to the β,(b-y) data we derived the residuals Δ(b-y) and $\Delta\beta$. Δ(b-y) is plotted against $Vsin\ i$ in Fig II–4a. A straight line fit gives

$$\Delta(b-y) = 0.103(\pm 0.022) \times 10^{-3} Vsin\ i - 0.019(\pm 0.005) \tag{9}$$

$$\Delta\beta = -0.174(\pm 0.046) \times 10^{-3} Vsin\ i + 0.032(\pm 0.010) \tag{10}$$

From indices dereddened for interstellar extinction we derive

$$\Delta(b-y)_o = 0.043(\pm 0.003) \times 10^{-3} Vsin\ i - 0.008(\pm 0.001), \tag{11}$$

$$\Delta\beta = -0.162(\pm 0.014) \times 10^{-3} Vsin\ i + 0.029(\pm 0.003). \tag{12}$$

Δ(b-y)$_o$ are plotted against $Vsin\ i$ in Fig II–4b.

The residuals in colours in different planes for the B stars in α-Persei are given in Table II–3.

3. Alpha-Persei : A stars

3.1. The effect on c_1 & β in the β, c_1 plane

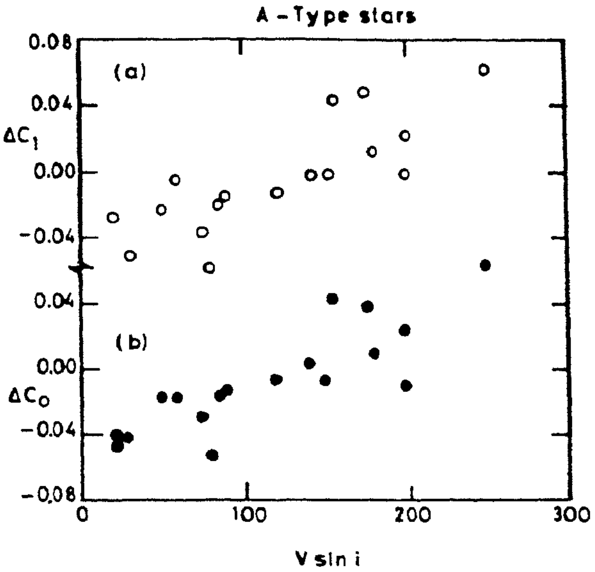

Fig II–5 : *The deviations derived for the reddened (open circles) and dereddened (filled circles) from the observed mean relation in the β, c_1, and β, c_o plane for α-Persei A stars*

In most of the colour-colour plots the 19 A type stars are scattered around two positions and therefore the actual relationship between them could not be defined. Therefore early F stars which are 14 are combined with the 19 A stars to derive the mean relationship between sets of different indices.

Table II–4 lists the data for all 19 A type stars and 14 F-type stars in α-Persei. Remarks column indicates the other possible causes that can contribute to the observed colours of the member stars. From a second order polynomial fit to the data we derive Δc_1 and $\Delta\beta$. A linear fit excluding star Nos. 314 & 1218 yields

$$\Delta c_1 = 0.344(\pm 0.054) \times 10^{-3} V sin\ i - 0.040(\pm 0.007), \tag{13}$$

$$\Delta\beta = -0.133(\pm 0.034) \times 10^{-3} V sin\ i + 0.016(\pm 0.005). \tag{14}$$

Similarly from the dereddened indices we derive

$$\Delta c_o = 0.305(\pm 0.052) \times 10^{-3} V sin\ i - 0.035(\pm 0.007), \quad (15)$$

$$\Delta \beta = -0.121(\pm 0.033) \times 10^{-3} V sin\ i + 0.014(\pm 0.004). \quad (16)$$

Δ c_1 and Δ c_o are plotted against $V sin\ i$ in Fig II–5.

3.2. The effect on β and (u-b) in the β, (u-b) plane

Similar analysis in the β, (u-b) plane lead to

$$\Delta(u - b) = 0.432(\pm 0.082) \times 10^{-3} V sin\ i - 0.062(\pm 0.010), \quad (17)$$

$$\Delta \beta = 0.118(\pm 0.139) \times 10^{-3} V sin\ i + 0.006(\pm 0.017). \quad (18)$$

Δ (u-b) against $V sin\ i$ are plotted in Fig II–15a. Four stars nos. 651, 609, 1050 and 1218 are found to deviate in Δ(u-b) vs $V sin\ i$ diagram. Nos 651, 1050 and 1218 are Am stars. These were excluded in deriving the slopes.

3.3. The effect on c_1 and (b-y) in the c_1, (b-y) plane

From c_1 (b-y) relation we derived Δ (b-y) and Δc_1. Δ (b-y) Vs $V sin\ i$ are plotted in Fig II–14a.

$$\Delta(b - y) = 0.188(\pm 0.057) \times 10^{-3} V sin\ i - 0.022(\pm 0.007), \quad (19)$$

$$\Delta c_1 = 0.633(\pm 0.116) \times 10^{-3} V sin\ i - 0.068(\pm 0.015). \quad (20)$$

3.4. The effect on m_1 and β in the β, m_1 plane

Among the 19 A and 14 F stars three A-type stars (Nos 228, 958 & 1218) are found to deviate considerably from the mean relationship between Δm_1 and $V sin\ i$. No 1218 is a possible Am star (Crawford & Barnes 1974). No 958 is a suspected binary. From the rest of the 16 A stars and 14 F stars we derive

$$\Delta m_1 = -0.155(\pm 0.021) \times 10^{-3} Vsin\ i + 0.019(\pm 0.003), \quad (21)$$

$$\Delta\beta = 0.677(\pm 0.055) \times 10^{-3} Vsin\ i - 0.071(\pm 0.007). \quad (22)$$

Δm_1 values are plotted against $Vsin\ i$ in Fig II–6.

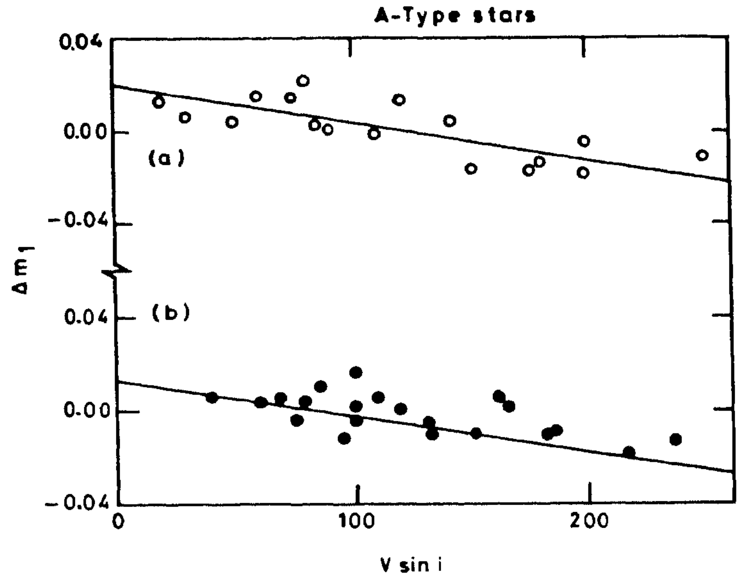

Fig II–6 : *The deviations in m_1 derived from the β, m_1, relation are plotted against $Vsin\ i$ for A stars of α-Persei (open circles) and Pleiades (filled circles).*

The residuals in colours for A stars in α-Persei are given in Table II–5.

We find that both reddened and dereddened indices in general lead to similar results. This is as expected since a uniform extinction leads only to a shift of the entire sequence and any small non-uniformity in extinction can be expected to be random. But it appears that in the case of the B-stars, dereddening reduces the scatter and also the values of the slope derived for rotation effects in different planes. However, for highly non-uniform extinction, the use of dereddened indices especially for A-stars, may not be appropriate (Gray & Garrison 1989). Therefore, for the rest of the clusters, we have used the observed indices excepting for the upper scorpius B-stars. For clusters analysed by both procedures, the differences were only marginal. One tends to get slightly larger effects if the indices are not corrected for extinction especially in the (u-b) index for B stars.

Table II–4. Data for α-Persei A&F-type stars

No	BD	MK	V	β	(b-y)	m_1	c_1	$V sin\ i$	Remarks
151	47°780	F0 Vn	8.97	2.765	0.213	0.166	0.763	140	
220	48 865	A9 IV	9.14	2.792	0.209	0.180	0.805	85	
228		F0 V	9.95	2.759	0.313	0.140	0.727		
314	50 728	F2 V	9.25	2.736	0.274	0.163	0.754	110	SB
481	47 808	F1 IV:n	9.16	2.763	0.249	0.157	0.772	180	
501	48 894	F0 IV	9.14	2.770	0.212	0.189	0.741	75	
522	51 723	A7 Vn	9.13	2.868	0.192	0.172	0.936	200	
606	48 905	A8 V	8.98	2.775	0.207	0.178	0.765	50	Am
609	49 918	F1 Vn	9.22	2.755	0.284	0.151	0.789	175	
635	49 921	A8 V	9.05	2.758	0.215	0.182	0.721	20	
651	48 909	A5 V:n	8.42	2.862	0.108	0.178	0.993	250	
721	47 825	F2 Vn	9.66	2.730	0.333	0.158	0.686		
885	48 934	A7 IV	8.79	2.856	0.156	0.210	0.867	80	Am
906	47 842	A6 Vn	8.78	2.872	0.167	0.174	0.939	150	
921	49 953	A6 Vn	8.59	2.880	0.114	0.187	0.970	200	
958	49 858	F1 V	9.20	2.739	0.247	0.172	0.741	155	SB?
970	48 944	A5 V?	8.19	2.886	0.098	0.208	0.938	120	
1050	49 967	A6m F2	9.48	2.834	0.250	0.202	0.893	60	Am
1218	46 780	F3 IV	9.17	2.729	0.262	0.184	0.733	120	
135	49 868	F5 V	9.71	2.683	0.328	0.143	0.472	20	
270	48 871	F7 V	10.11	2.660	0.342	0.143	0.426		
309	49 889	F5 V	9.96	2.656	0.336	0.141	0.426		
361	49 896	F4 V	9.68	2.686	0.292	0.158	0.478	30	
365	49 897	F6 V	9.90	2.657	0.345	0.133	0.435		
421	48 885	F2 V	9.23	2.713	0.292	0.158	0.606	90	
490	48 892	F3 IV-V	9.51	2.696	0.294	0.151	0.533		
588	49 914	F5 V	9.99	2.664	0.379	0.138	0.450		
621	47 816	F4 V	9.86	2.672	0.327	0.137	0.463		
632	46 745	F4 V	9.71	2.674	0.312	0.157	0.469		
715		F4 V	9.72	2.663	0.321	0.140	0.477		
733	48 916	F6 V	9.94	2.666	0.344	0.137	0.463		
833		F6 V	10.03	2.660	0.338	0.157	0.423		
799	48 923	F4 V	9.66	2.673	0.312	0.139	0.472	20	

Table II–5. Effects of rotation for α Persei A stars.

		from β, c_1		from β,(u-b)		from c_1 (b-y)		from β,m_1		from c_1, m_1	
No	*Vsin i*	$\Delta\beta$	Δc_1	$\Delta\beta$	Δ(u-b)	Δc_1	Δ (b-y)	$\Delta\beta$	Δm_1	Δc_1	Δm_1
151	140	−.002	−.003	.000	−.051	−.043	−.019	.008	−.005	.056	−.008
220	85	.005	−.021	−.004	−.010	−.009	−.004	−.008	.003	.001	.003
228	–	.008	−.024	−.054	.068	–	–	–	–	–	–
314	110	−.027	.064	–	–	.106	.038	−.011	−.001	.071	−.010
481	180	−.008	.011	−.034	−.014	.053	.021	−.036	.014	.141	−.017
501	75	.013	−.037	−.008	−.033	−.067	−.029	−.054	.017	−.111	.017
522	200	.008	−.002	.049	.064	.088	.046	.092	−.018	.184	−.013
606	50	.007	−.024	.002	−.046	−.053	−.024	−.019	.005	−.026	.004
609	175	−.024	−.048	–	–	.171	.063	.049	−.018	.214	−.025
635	20	.010	−.028	−.004	−.049	−.080	−.034	−.047	.013	−.094	.012
651	250	−.034	.061	–	–	.032	−.005	.068	−.011	.202	−.010
721	–	−.004	.014	−.089	.139	−.041	−.027	.000	−.005	–	–
885	80	.036	−.059	−.054	−.005	.048	.022	−.018	.022	−.055	.029
906	150	.010	−.002	.063	.023	.014	−.013	.090	−.017	.174	−.011
921	200	−.001	.022	.088	−.021	.017	.006	.061	−.005	.128	.000
958	155	−.018	.043	−.056	.038	−.030	−.047	–	–	−.011	.000
970	120	.025	−.014	.105	−.040	.050	.018	.016	.015	.020	.023
1050	60	.000	−.005	–	–	–	–	−.023	.017	–	–
1218	120	−.024	.064	–	–	–	–	–	–	−.093	.013
135	20	.013	−.047	–	–	.004	.005	.007	−.007	−.020	−.005
270	–	−.002	−.006	−.007	.003	.011	.010	−.016	.000	−.066	.000
309	–	−.006	.010	.005	−.003	−.012	.004	−.012	−.001	−.044	−.002
361	30	.015	−.052	.037	−.073	−.115	−.030	−.044	.007	−.162	.010
365	–	−.006	.015	−.005	.005	.032	.015	.020	−.009	.058	−.011
421	90	.008	−.015	−.043	.004	.013	.003	−.017	.000	−.034	−.003
490	–	.012	−.031	.004	−.048	−.053	−.016	−.010	−.003	−.042	−.003
588	–	−.002	.003	−.077	.081	–	–	.007	−.007	–	–
621	–	.004	−.015	.010	−.030	−.009	.002	.019	−.010	.039	−.010
632	–	.004	−.017	−.004	−.019	−.057	−.012	−.053	.010	−.162	.010
715	–	−.008	.035	−.007	−.001	−.017	−.001	−.001	−.004	.018	−.008
733	–	−.002	.008	−.028	.018	.056	.019	.013	−.008	.039	−.010
833	–	−.001	−.009	−.023	.020	−.008	.006	−.067	.014	−.208	.014
799	20	.003	−.010	.028	−.049	−.054	−.011	–	–	.024	−.009

4. The Pleiades : B stars

Main sequence B stars are 19 and they are listed in Table II–6. Identification numbers for the stars are from Hertzsprung (1947). Among them, the majority belong to the category of variable radial velocity and emission-lined objects. If we drop double-lined binaries and close visual pairs with $\Delta m < 2.0$ magnitudes, we are left with only 8 stars which can be considered as normal main-sequence objects whose colours are free from effects other than that due to rotation. Not withstanding the fact that this sample is too small to warrant a separate analysis, we derived the residuals in β, c_1, (u-b) and (b-y) in different planes and they are listed in Table II–7.

From a second-order polynomial fit to β, c_1 values, the residuals Δc_1 and $\Delta\beta$ are derived. The residuals in c_1 for Pleiades B stars are superposed (Fig II–7b) over those derived for the members of the α-Persei cluster. Similarly $\Delta\beta$ for B stars in Pleiades are superposed (in Fig II–8b) over those derived for the members of the α-Persei cluster.

Similarly Δ (u-b) & $\Delta\beta$ are derived from β, (u-b) relation and superposed over those for α-Persei in Fig II–9b and II–10b respectively. The Δ (b-y) derived from β, (b-y) are superposed over the data for α-Persei in Fig II–11b. In all the above diagrams filled circles represent Pleiades members. From the diagrams it is clear that the reddening due to rotation of Pleiades B stars is similar to that of α-Persei B stars.

5. The Pleiades : A stars

In Pleiades, as in α-Persei, we have added the nine F stars earlier than spectral type F3 to the twenty three A type stars for data analysis. The data for the above 32 stars are given in Table II–8 and the derived residuals in Table II–9. Excluding star No 146 (Am) and 742 (binary) and following similar procedures, we derive from the rest of the 30 stars,

$$\Delta c_1 = 0.387(\pm 0.038) \times 10^{-3} V sin\ i - 0.044(\pm 0.005), \tag{23}$$

$$\Delta\beta = -0.169(\pm 0.019) \times 10^{-3} V sin\ i + 0.019(\pm 0.002). \tag{24}$$

In Δ (u-b), $V sin\ i$ plot six stars are found to deviate considerably. They are

HD 23157, HD 23194, HD 23375, HD 23567, HD 23664 and HD 23247. A least square fit excluding the 6 stars gives

$$\Delta(u-b) = 0.184(\pm 0.055) \times 10^{-3} V sin\ i - 0.027(\pm 0.008), \tag{25}$$
$$\Delta\beta = -0.150(\pm 0.071) \times 10^{-3} V sin\ i + 0.023(\pm 0.010). \tag{26}$$

In Δ (b-y) vs $V sin\ i$ diagram, the stars that deviate considerably are HD 23155, HD 23194 HD 23246, HD 23247, HD 23289 and HD 23607. Excluding them we derive

$$\Delta(b-y) = 0.075(\pm 0.046) \times 10^{-3} V sin\ i - 0.010(\pm 0.007), \tag{27}$$
$$\Delta c_1 = 0.231(\pm 0.103) \times 10^{-3} V sin\ i - 0.029(\pm 0.014). \tag{28}$$

From the above 24 stars from β, m_1 relationship we derive

$$\Delta m_1 = -0.109(\pm 0.018) \times 10^{-3} V sin\ i + 0.013(\pm 0.003), \tag{29}$$
$$\Delta\beta = 0.412(\pm 0.047) \times 10^{-3} V sin\ i - 0.051(\pm 0.007). \tag{30}$$

For the same 24 stars from c_1, m_1 relationship we derive

$$\Delta m_1 = -0.144(\pm 0.022) \times 10^{-3} V sin\ i + 0.017(\pm 0.003), \tag{31}$$
$$\Delta c_1 = 1.247(\pm 0.112) \times 10^{-3} V sin\ i - 0.153(\pm 0.016). \tag{32}$$

We derive from (b-y), m_1 relationship for the 24 stars

$$\Delta m_1 = -0.133(\pm 0.017) \times 10^{-3} V sin\ i + 0.016(\pm 0.002), \tag{33}$$
$$\Delta(b-y) = -0.477(\pm 0.049) \times 10^{-3} V sin\ i + 0.058(\pm 0.007). \tag{34}$$

The results for A stars in Pleiades are displayed in Figs II–12 to II–16. For comparison we also show in these figures the expected theoretical result (See Chapter 3) from Collins & Sonneborn (1977). The residuals in different colours for the Pleiades A stars are listed in Table II–9.

Table II–6. Data for Pleiades B-type stars

Hz	HD	MK	V	β	(b-y)	m_1	c_1	*Vsin i*	Remarks
117	23288	B7 IV	5.46	2.750	0.002	0.108	0.637	260	VB
150	23324	B8 V	5.65	2.746	−0.022	0.109	0.637	245	SB2
156	23338	B6 V	4.31	2.702	−0.034	0.094	0.553	135	SB1, VB
216	23387	A1 V	7.18	2.869	0.116	0.132	0.941	15	VB
255	23432	B8 V	5.76	2.793	−0.001	0.112	0.768	220	
265	23441	B9 V	6.43	2.823	0.000	0.127	0.860	250	VB
323	23480	B6 V	4.18	2.642	0.004	0.078	0.596	275	Be
436	23568	B9.5V	6.82	2.849	0.031	0.122	0.917	260	
540	23642	A0 V	6.81	2.879	0.040	0.164	0.930	40	SB2
722	23753	B8 V	5.45	2.736	−0.020	0.104	0.717	270	
878	23862	B8 Pe	5.09	2.579	−0.020	0.094	0.557	340	Be
910	23873	B9.5 V	6.60	2.852	−0.013	0.147	0.904	90	
977	23923	B9 V	6.17	2.794	−0.012	0.117	0.843	310	
1003	23964	A0 V	6.74	2.844	0.051	0.129	0.887	15	Ap
1129	24076	A2 V	6.93	2.867	0.064	0.150	0.926	155	
248	23410	A0 V	6.85	2.899	0.023	0.158	0.979	190	SB2
508	23629	A0 V	6.29	2.901	0.000	0.165	0.968	160	
510	23632	A1 V	6.99	2.899	0.013	0.166	1.009	235	
520	23631	A2 V	7.26	2.891	0.048	0.162	0.945	10	SB2, VB

Table II–7. Effects of rotation for Pleiades B stars

		from β, c_1		from β,(u-b)		from β (b-y)	
HD	*Vsin i*	$\Delta\beta$	Δc_1	$\Delta\beta$	Δ(u-b)	$\Delta\beta$	Δ (b-y)
23432	220	.021	−.041	.010	−.052	−.049	−.004
23568	260	−.007	.015	−.011	.016	−.043	.014
23753	270	−.008	.003	−.001	.017	−.038	.007
23873	120	.003	−.003	.006	−.044	.050	−.030
23923	310	−.021	.033	−.013	.008	−.012	−.015
24076	155	.006	−.007	−.022	.095	.011	.046
23629	160	.016	−.022	.023	−.057	.056	−.016
23632	235	−.009	.022	.008	.017	.025	−.003

Table II–8. Data for Pleiades A&F-type stars

Hz	HD	MK	V	β	(b-y)	m_1	c_1	$V sin\ i$	Remarks
27	23157	A9	7.90	2.790	0.213	0.182	0.739	100	
28	23156	A7	8.23	2.839	0.149	0.204	0.826	70	
43	23194	A5	8.06	2.882	0.118	0.197	0.908	20	SB
92	23246	A8	8.17	2.772	0.171	0.185	0.760	200	
146	23325	Am?	8.58	2.974	0.219	0.182	0.777	75	Am?
187	23361	A3	8.04	2.875	0.126	0.192	0.955	235	
206	23375	A9	8.60	2.765	0.227	0.176	0.705	75	
313	23479	A7	7.96	2.756	0.208	0.168	0.710	150	VB
447	23567	A9	8.28	2.788	0.229	0.173	0.734	95	VB
457	23585	A9	8.37	2.783	0.186	0.186	0.714	100	
501	23607	A7	8.25	2.841	0.153	0.188	0.816	12	
513	23628	A4	7.66	2.856	0.125	0.183	0.910	215	
534	23643	A3	7.77	2.862	0.090	0.194	0.942	185	
693	23733	A9	8.27	2.736	0.234	0.161	0.686	180	
742	23763	A1	6.95	2.875	0.071	0.177	0.952	105	SB
792	23791	A8	8.37	2.811	0.175	0.201	0.768	85	
885	23863	A7	8.12	2.826	0.128	0.201	0.861	160	SB
924	23886	A3	7.97	2.880	0.093	0.208	0.921	165	
975	23924	A7	8.10	2.852	0.116	0.218	0.855	100	
Tr 47	23155			2.882	0.073	0.197	0.967	106	
S 84	23430			2.859	0.115	0.204	0.887	118	
S 108	23610			2.826	0.143	0.216	0.826	0	
S 115	23664			2.840	0.151	0.202	0.871	61	
88	23247	F2	9.07	2.704	0.307	0.150	0.533	40	
123	23289	F3	8.95	2.699	0.263	0.158	0.525	40	
145	23326	F2	8.95	2.691	0.250	0.164	0.514	40	
169	23351	F3	8.99	2.695	0.292	0.164	0.510	80	
484	23608	F3	8.69	2.674	0.296	0.159	0.492	110	
948	23912	F3	9.10	2.671	0.290	0.147	0.487	130	
1184	24132	F2	8.83	2.689	0.254	0.147	0.592	230	
S 151 x	023975			2.646	0.337	0.142	0.419		
R 60	024302			2.648	0.314	0.152	0.410		

Table II–9. Effects of rotation for Pleiades A stars.

		from β, c_1		from β,(u-b)		from c_1 (b-y)		from β,m_1		from c_1, m_1		from (b-y), m_1	
HD	$V \sin i$	$\Delta\beta$	Δc_1	$\Delta\beta$	Δ(u-b)	Δc_1	Δ (b-y)	$\Delta\beta$	Δm_1	Δc_1	Δm_1	Δ (b-y)	Δm_1
23157	100	.006	−.017	–	–	.036	.018	−.008	−.004	−.033	−.002	.029	.004
23156	70	.015	−.030	−.008	.013	−.012	−.007	−.006	.006	−.038	.011	.017	.009
23194	20	.020	−.030	–	–	–	–	–	–	–	–	–	–
23246	200	−.021	.043	−.011	−.002	–	–	–	–	–	–	–	–
23361	235	−.010	.030	−.037	.055	.075	.033	.051	−.014	.131	−.014	−.032	−.009
23375	75	−.004	.003	–	–	.034	.017	−.015	−.003	−.028	−.004	.026	.002
23479	150	−.015	.028	−.016	.002	−.005	.000	.005	−.009	−.039	−.013	−.019	−.011
23567	95	.006	−.018	–	–	.068	.032	.019	−.012	.023	−.010	.018	.000
23585	100	.010	−.027	.015	−.024	−.049	−.020	−.026	.002	−.081	.005	.013	.001
23607	12	.022	−.044	.030	−.022	–	–	–	–	–	–	–	–
23628	215	−.007	.021	.015	−.002	.028	.010	.055	−.019	.132	−.019	−.056	−.018
23643	185	−.017	.041	.038	−.021	.002	−.009	.034	−.009	.109	−.011	−.063	−.015
23733	180	−.024	.049	−.051	.033	.032	.016	.014	−.010	.078	−.017	−.018	−.011
23791	85	.014	−.032	−.023	.018	−.018	−.007	−.030	.010	−.088	.014	.037	.013
23863	160	−.014	.031	−.007	.008	−.016	−.011	−.015	.006	.005	.004	−.010	.001
23886	165	.011	−.013	.042	−.015	−.015	−.017	.030	.001	.049	.005	−.032	.000
23924	100	.015	−.026	.014	−.003	−.043	−.026	−.006	.017	−.024	.022	.006	.015
23155	106	−.009	.029	.062	−.032	–	–	–		–	–	–	–
23430	118	.007	−.008	.019	−.004	−.012	−.012	.014	.002	.023	.005	−.017	.001
23610	–	.002	−.004	−.034	.033	−.023	−.013	−.031	.021	−.053	.023	.030	.020
23664	61	−.005	.013	–	–	.037	.017	−.002	.004	.012	.004	.015	.008
23247	40	.010	−.029	–	–	–	–	–	–	–	–	–	–
23289	40	.008	−.025	.026	−.039	–	–	–	–	–	–	–	–
23326	40	.005	−.017	.043	−.055	−.101	−.035	−.044	.006	−.122	.007	.009	−.003
23351	80	.010	−.030	−.035	.020	.006	.006	−.040	.005	−.126	.007	.051	.010
23608	110	−.003	.003	−.035	.024	−.001	.003	−.039	.006	−.096	.005	.036	.006
23912	130	−.004	.005	.004	−.014	−.023	−.005	.017	−.005	.031	−.007	−.018	−.008
24132	230	−.030	.066	−.012	−.001	−.013	−.002	.035	−.010	.136	−.020	−.054	−.019
23975	–	−.002	.001	−.038	.033	.044	.019	.019	−.002	.026	−.003	.007	.002
24302	–	.004	−.013	.000	−.005	−.033	−.006	−.032	.007	−.104	.008	.027	.005

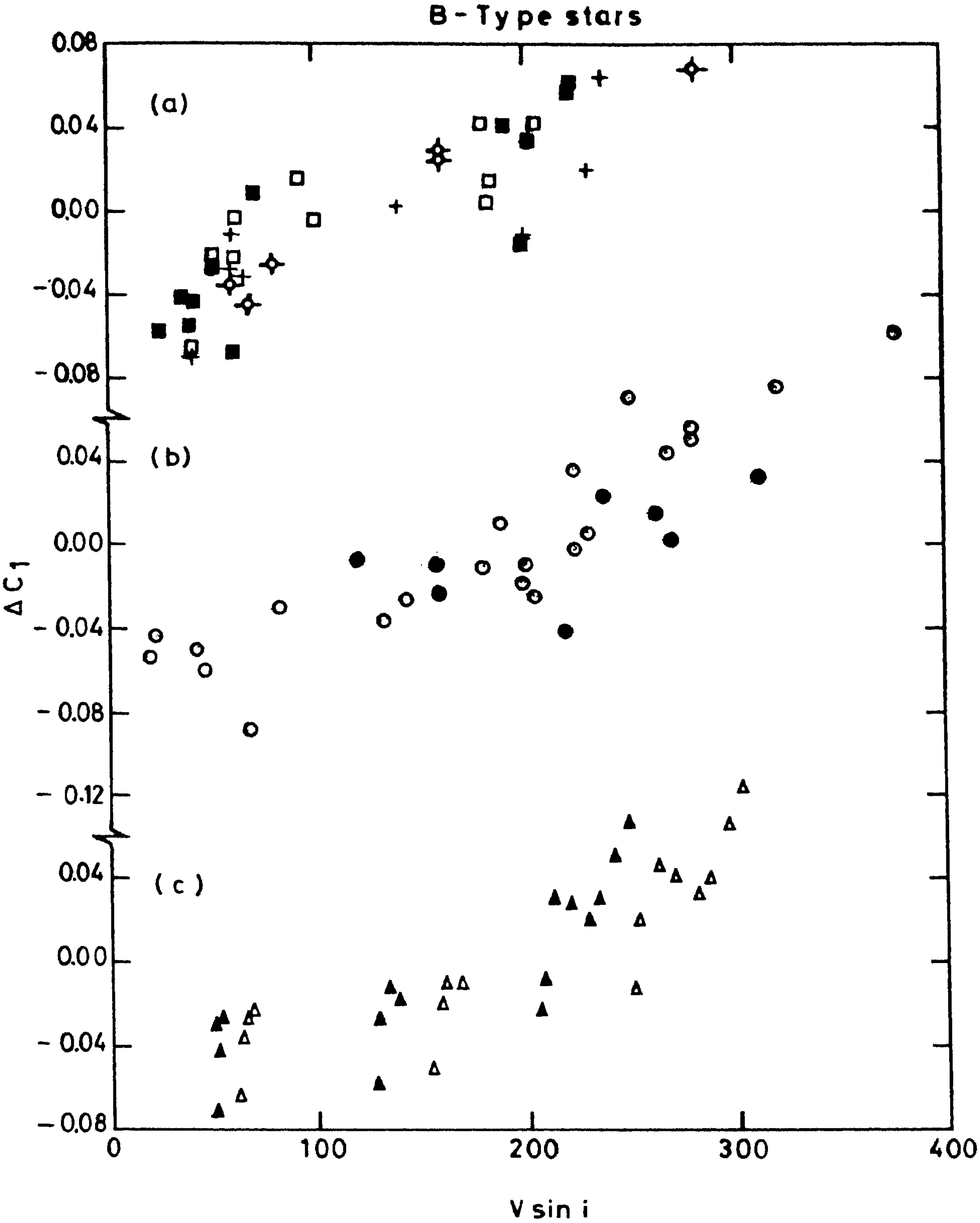

Fig II–7 : *(a) Residuals in c_1, derived from the observed mean relationship in the β, c_1 plane for B-stars are plotted against Vsin i for (a) IC 2391 (squares), IC 4665 (filled squares), NGC 2264 (circles with cross bars) and NGC 2422 (plus); (b) Pleiades (filled circles) and α-Persei (open circles); (c) Residuals derived from theoretical predictions by Collins and Sonneborn (1977) for B5-B9 stars for $i=45^o$ (filled triangles) and $i=60^o$ (open triangles) are shown for comparison.*

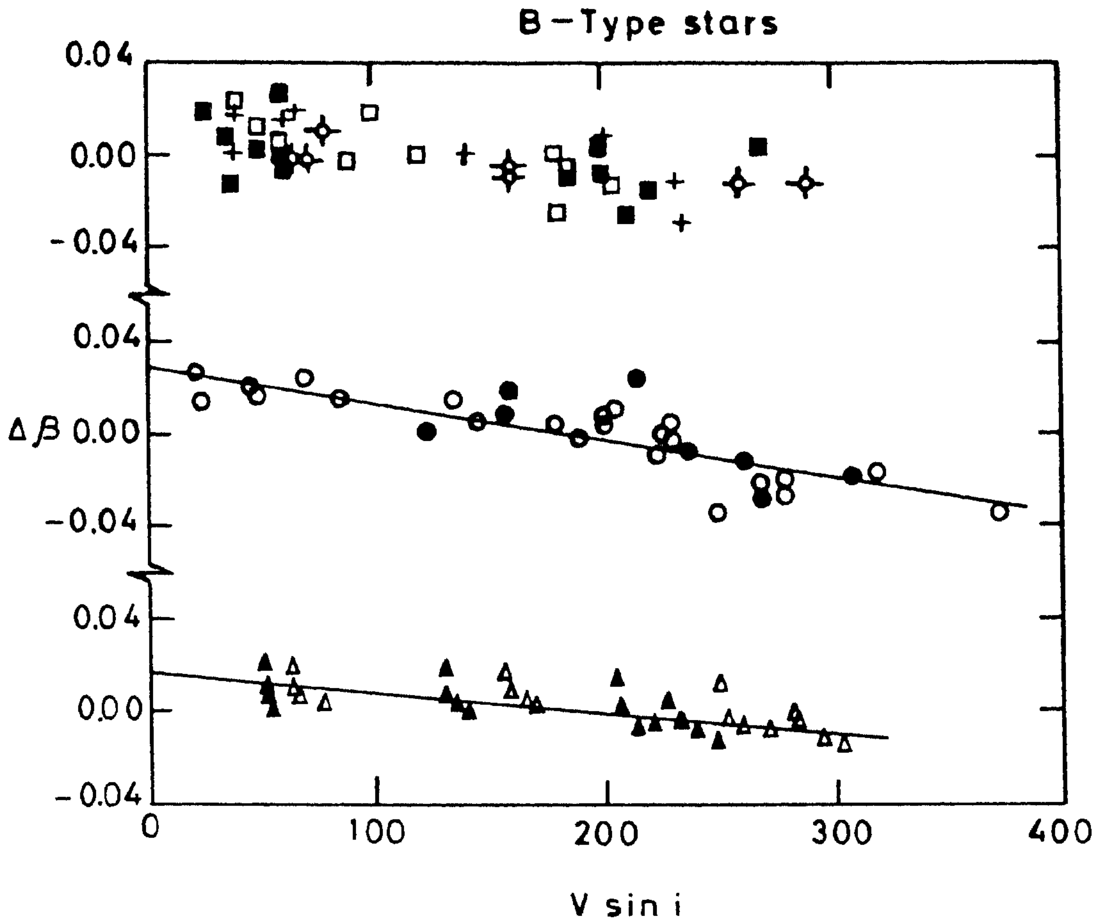

Fig II–8 : *The residuals Δβ derived for B-stars from the β, c relationship is plotted against V sin i. Symbols have same meaning as figure II–7.*

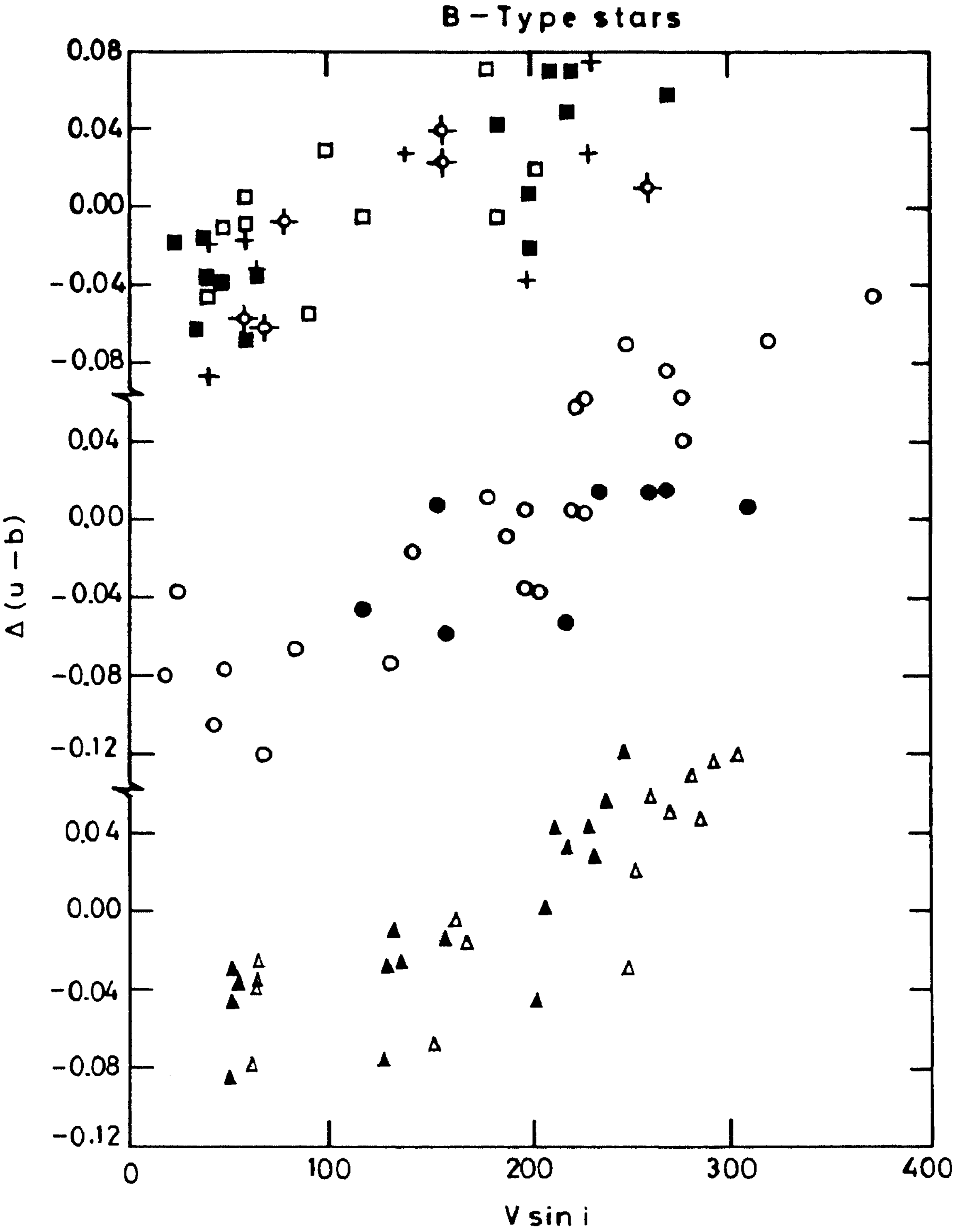

Fig II–9 : *Δ(u-b) Vs Vsin i diagram derived for B-stars from the β, (u-b) relation. Symbols have the same meaning as figure II–7.*

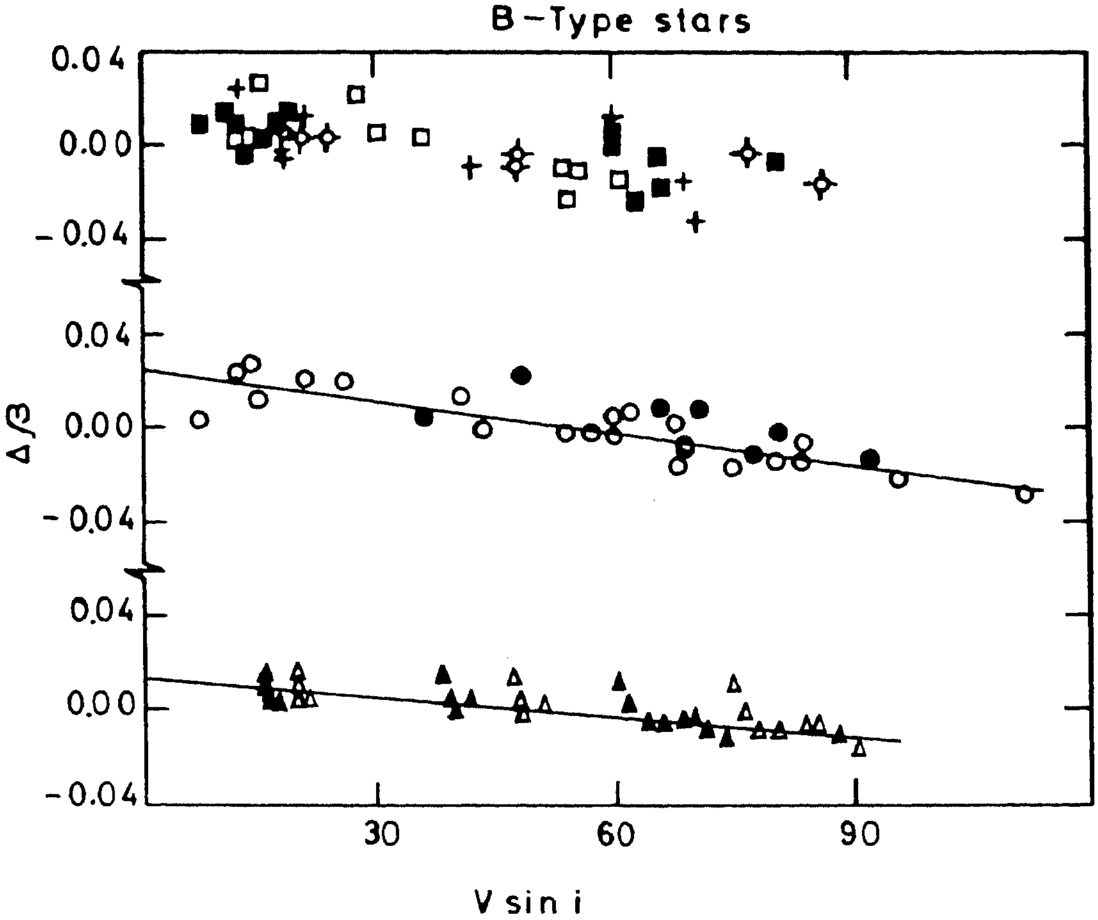

Fig II–10 : *Δβ Vs V sin i diagram derived for B stars from the β, (u-b) relation. Symbols have the same meaning as figure II-7.*

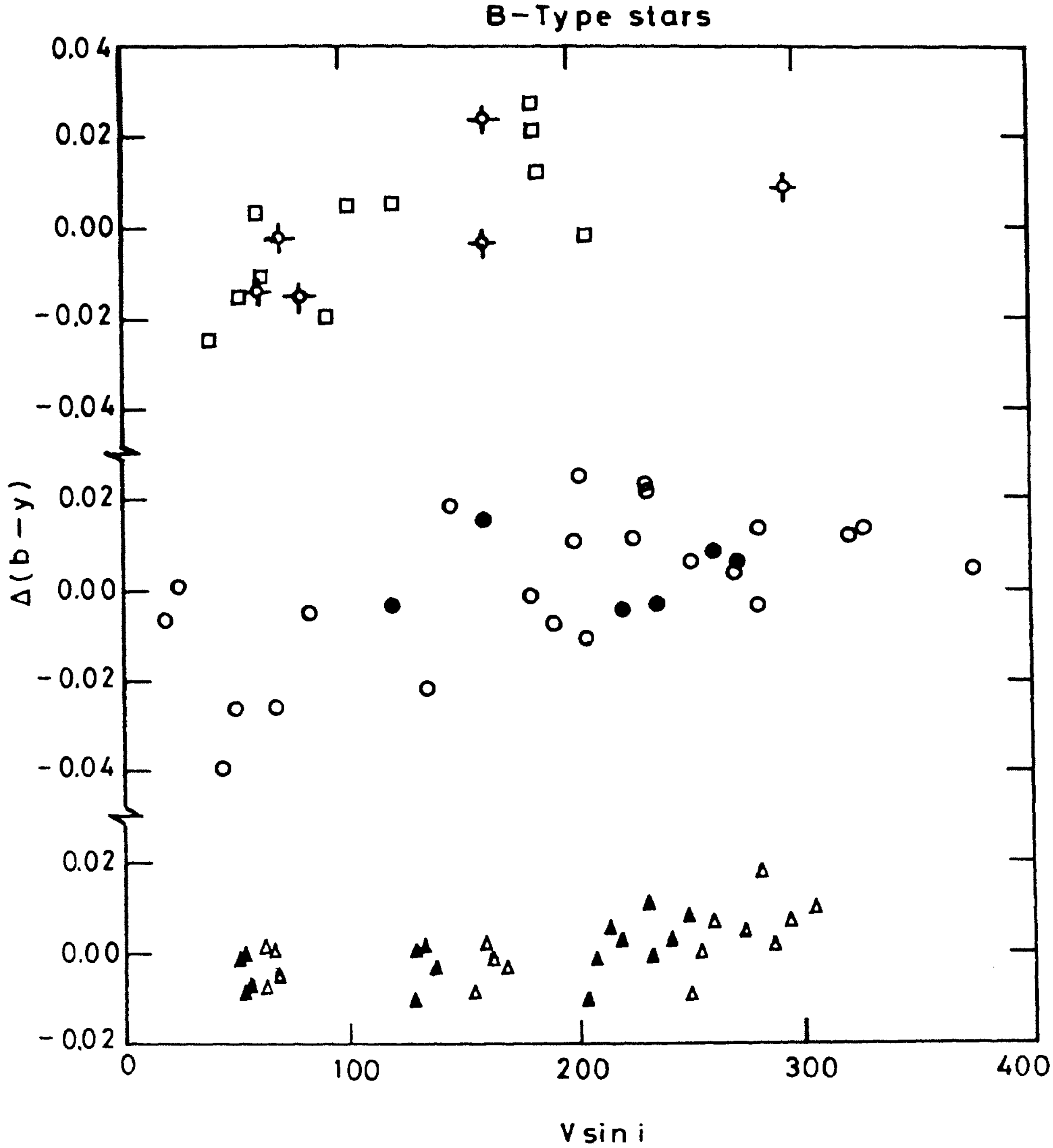

Fig II–11 : *The residuals Δ (b-y) for B-stars from the β, (b-y) relation is plotted against Vsin i. Symbols have the same meaning as figure II–7.*

6. The Hyades

Main-sequence members, earlier than spectral type F3 ($\beta > 2.71$) are 31, and are listed in Table II–10. The last column indicates the objects whose colours are likely to be affected for reasons other than rotation such as binary nature and chemical peculiarity. As the colours of only the double-lined spectroscopic binaries and close visual pairs with $\Delta m < 2.0$ magnitudes are likely to be affected seriously, we include the rest of the main sequence members to determine the effects of rotation. The β, c_1 values of Ams that are not SB2's or close VB's are also included. They are VB nos 38, 45, 83, 107, 112, 130 and 131.

6.1. The effect on c_1 and β in the β, c_1 plane

A second-order polynomial fit was derived for 23 out of the 31 stars listed in Table 2 (excluding the 8 stars which have an unfavourable remark). For each star, a calculated c_1 value was derived using the polynomial coefficients for its observed β.

Δc_1, the observed minus computed value of c_1 for its observed value of β, are given in Table II–11 and are plotted against $Vsin\ i$ in Fig II–12(d). A least square fit to the residuals in c_1 gives,

$$\Delta c_1 = 0.371(\pm 0.058) \times 10^{-3} Vsin\ i - 0.032(\pm 0.006). \tag{35}$$

The deviations in β are given in Table II–11 and are plotted against $Vsin\ i$ in Fig II–13(d). A linear fit to the data points yields,

$$\Delta\beta = -0.150(\pm 0.023) \times 10^{-3} Vsin\ i + 0.013(\pm 0.002). \tag{36}$$

6.2. The effect on c_1, (b-y) in the c_1,(b-y) plane

The c_1, (b-y) relation for the same 23 stars was also represented by a second order polynomial.

The deviations in (b-y) and c_1 are given in Table II–11. They are found to be related to $Vsin\ i$.

$$\Delta(b-y) = 0.130(\pm0.025) \times 10^{-3} V sin\ i - 0.011(\pm0.006), \quad (37)$$
$$\Delta c_1 = 0.283(\pm0.055) \times 10^{-3} V sin\ i - 0.025(\pm0.006). \quad (38)$$

Δ (b-y) is plotted against $V sin\ i$ in Fig II–14(d).

6.3. The effect on (u-b), β in the β, (u-b) plane

In β, (u-b) diagram, the Am stars were found to deviate considerably from the mean relation. Hence they were not included in the analysis. A second order polynomial was fitted for the rest of the stars and Δ (u-b) and $\Delta\beta$ computed are given in Table II–11. Δ (u-b) values are plotted against $V sin\ i$ in Fig II–15c.

A linear fit yields

$$\Delta(u-b) = 0.258(\pm0.058) \times 10^{-3} V sin\ i - 0.029(\pm0.007), \quad (39)$$
$$\Delta\beta = -0.215(\pm0.053) \times 10^{-3} V sin\ i + 0.024(\pm0.006). \quad (40)$$

Table II–10. Data for Hyades A-type stars

VB	HD	MK	V	β	(b-y)	m_1	c_1	$V \sin i$	Remarks
6	24357	(d F1)	5.97	2.712	0.221	0.166	0.610	50	
24	27176	(d A8)	5.65	2.768	0.175	0.186	0.787	125	SB, VB
30	27397	F0 V	5.59	2.767	0.170	0.198	0.770	100	SB1
33	27459	A9 V	5.26	2.812	0.126	0.208	0.868	35	SB1
38	27628	Am	5.72	2.757	0.196	0.204	0.719	15	A3m
45	27749	Am	5.64	2.783	0.180	0.237	0.738	12	SB1, Am
47	27819	A7.5 V	4.80	2.857	0.081	0.210	0.981	35	
54	27934	A7 V	4.22	2.864	0.070	0.200	1.054	90	SB?, VB
55	27946	(A5 n)	5.28	2.784	0.149	0.193	0.840	210	VB
56	27962	A3 V	4.30	2.889	0.021	0.191	1.046	30	
60	28024	A8 Vn	4.29	2.753	0.165	0.175	0.947	215	SB1, VB
67	28226	Am	5.72	2.775	0.164	0.213	0.770	130	SB2
68	28294	F0 V	5.90	2.747	0.206	0.170	0.701	135	
74	28355	(A5)	5.03	2.831	0.104	0.225	0.912	140	
80	28485	(A6 n)	5.58	2.740	0.196	0.197	0.716	150	
82	28527	A6 Vn	4.78	2.856	0.088	0.217	0.965	100	SB, VB
83	28546	Am	5.48	2.809	0.142	0.233	0.795	30	
84	28556	F0 Vn	5.40	2.797	0.154	0.201	0.814	140	
89	28677	F2 Vn	6.02	2.725	0.215	0.175	0.658	100	
95	28910	A8 Vn	4.66	2.797	0.144	0.205	0.823	95	SB2
103	29375	F0 V	5.79	2.754	0.191	0.188	0.740	155	
104	29388	A6 Vn	4.27	2.870	0.067	0.197	1.048	115	SB1
107	29499	(A5 V)	5.39	2.811	0.150	0.222	0.827	70	
108	29488	A5 Vn	4.68	2.852	0.088	0.193	1.014	160	
111	30034	(dA6)	5.40	2.791	0.149	0.195	0.814	75	
112	30210	(Am)	5.37	2.844	0.091	0.253	0.955	30	
123	30780	(dA5)	5.10	2.813	0.122	0.207	0.900	155	
126	31236	(dF0)	6.37	2.739	0.178	0.190	0.739	110	
129	32301	(A7 V)	4.64	2.847	0.079	0.204	1.030	126	VB
130	33254	(Am)	5.43	2.796	0.138	0.245	0.820	30	
131	33204	(Am)	6.01	2.796	0.149	0.245	0.803	30	

Table II–11. Effects of rotation for Hyades A stars.

		from β, c_1		from β,(u-b)		from c_1 (b-y)		from β,m_1	
HD	$V sin\ i$	$\Delta\beta$	Δc_1	$\Delta\beta$	Δ(u-b)	Δc_1	Δ (b-y)	$\Delta\beta$	Δm_1
24357	50	.006	−.031	.002	−.029	−.025	−.009	−.006	−.002
27176	125	−.014	.032	−.007	.006	.026	.012	.008	−.011
27397	100	−.008	.017	−.005	.004	−.004	.000	−.012	.001
27628	15	.003	−.012	–	–	.014	.006	−.029	.012
27749	12	.021	−.051	–	–	−.010	−.002	−.024	.003
27819	35	.003	−.002	.026	−.015	.006	.000	–	–
27962	30	.014	−.033	–	–	−.034	−.030	–	–
28294	135	.001	−.008	.012	−.020	.024	.009	.019	−.017
28355	140	.002	.002	−.008	.006	−.016	−.007	.028	.002
28485	150	−.013	.021	−.029	.040	.011	.005	−.037	.014
28546	30	.024	−.058	–	–	−.048	−.018	.003	.018
28556	140	.004	−.009	.008	−.012	.000	.002	.014	−.009
28677	100	−.002	−.007	−.002	.001	.006	.002	−.014	.000
29375	155	−.009	.016	−.012	.014	.021	.009	−.009	−.003
29388	115	−.006	.027	.023	−.006	.046	.016	–	–
29499	70	.013	−.031	–	–	.003	.003	.009	.006
29488	160	−.013	.045	.005	.000	.053	.022	–	–
30034	75	−.002	.006	.022	−.028	−.012	−.003	.017	−.013
30210	30	−.001	.009	–	–	.000	−.001	–	–
30780	155	−.012	.037	−.012	.007	.011	.006	.023	−.010
31236	110	−.023	.046	−.009	.014	−.014	−.004	−.028	.007
33254	30	.001	.000	–	–	−.032	−.012	–	–
33204	30	.008	−.017	–	–	−.023	−.008	–	–

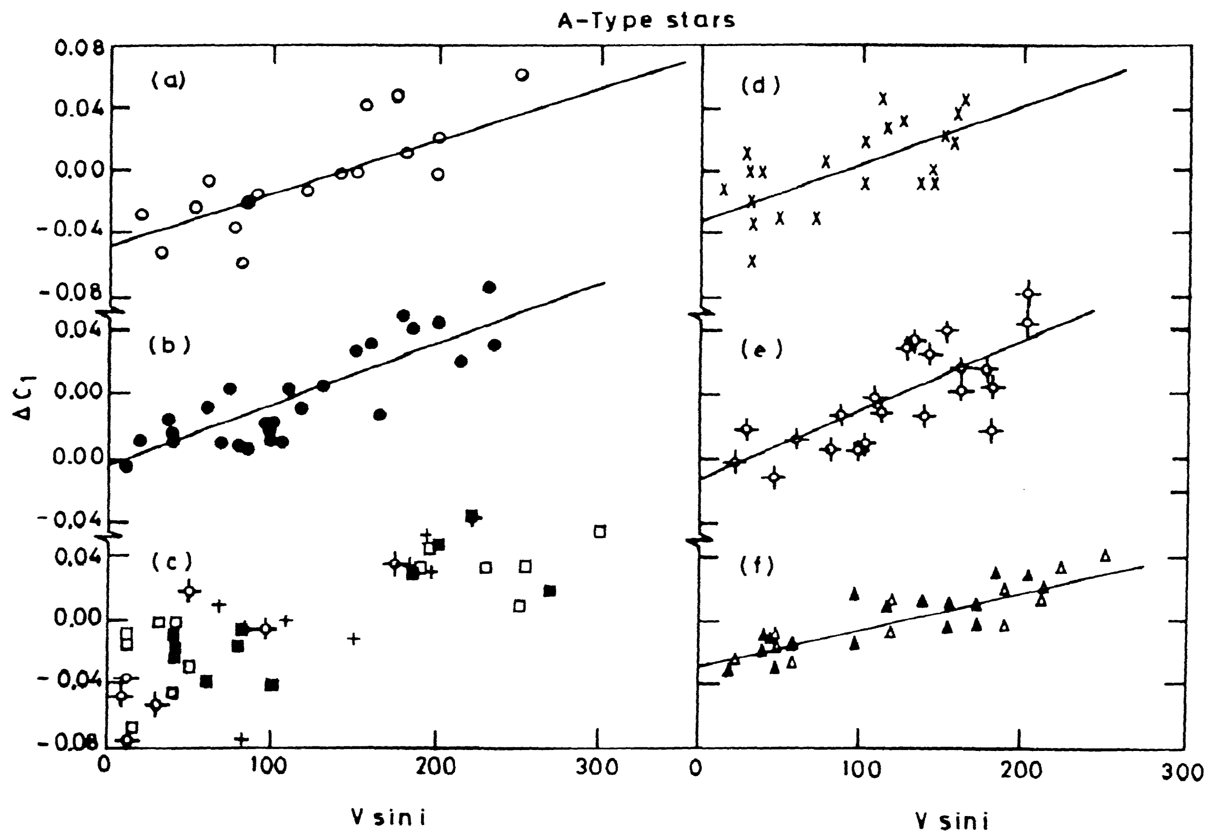

Fig II–12 : *Δc_1 versus $V sin\ i$ diagram derived from the β, c_1 plane for A stars in various clusters (a) ○ - α-Persei (b) ● - Pleiades (c) ■ - IC 4665. -◇- - Coma, + - IC4756, □ - NGC 2516 (d) × - Hyades (e) -◇- - Praesepe (f) ▲ - i=45° and △ - i=60° derived from theoretical predictions.*

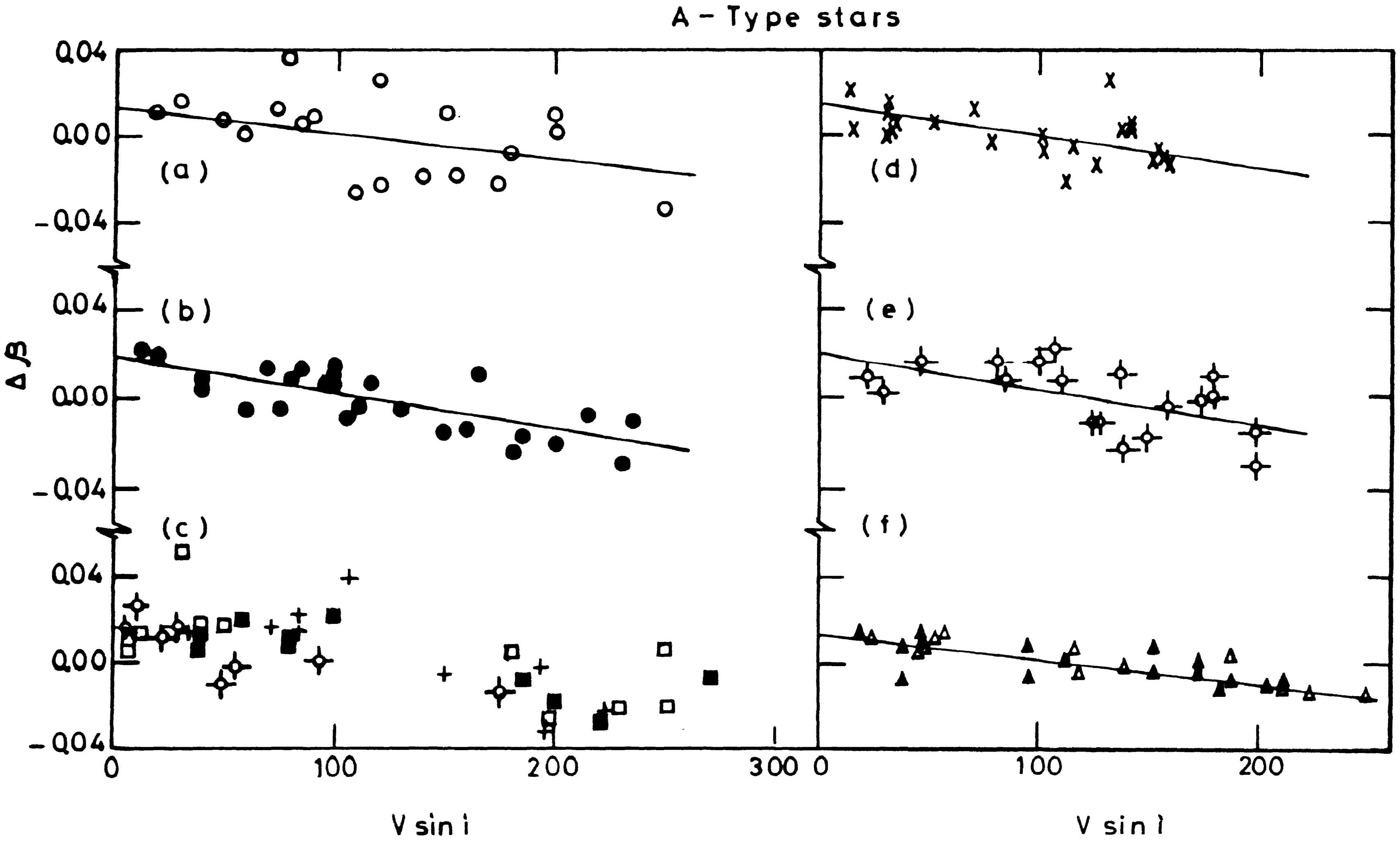

Fig II–13 : *The $\Delta\beta$ Versus $V sin\ i$ diagram derived from β, c_1 plane for A-stars in various clusters. Symbols have the same meaning as figure II–12.*

7. Praesepe

Only main-sequence earlier than F2($\beta > 2.71$) are considered. These 38 stars are listed in Table II–12 and the remarks column indicates the other possible causes that can contribute to the observed colours of the member stars.

The mean relationship between β and c_1 was derived for the 22 apparently normal stars and the deviations in c_1 from the mean relationship were derived. A least square fit of the deviations in c_1 plotted in Fig II–12(e) and that of β plotted in Fig II-13(e) gives

$$\Delta c_1 = 0.432(\pm 0.059) \times 10^{-3} V sin\ i - 0.053(\pm 0.008), \tag{41}$$

$$\Delta \beta = -0.172(\pm 0.024) \times 10^{-3} V sin\ i + 0.021(\pm 0.003). \tag{42}$$

Among the 22 stars, excluding the 3 stars which deviate in β (u-b), we derive

$$\Delta(u - b) = 0.219(\pm 0.032) \times 10^{-3} V sin\ i - 0.029(\pm 0.004), \tag{43}$$

$$\Delta \beta = -0.190(\pm 0.034) \times 10^{-3} V sin\ i + 0.029(\pm 0.005). \tag{44}$$

In c_1, (b-y) plane the Am stars are found to deviate. Therefore excluding the 5 Ams, star Nos. 40, 45, 154, 286 and 340, we derive

$$\Delta(b - y) = 0.147(\pm 0.022) \times 10^{-3} V sin\ i - 0.019, (\pm 0.003) \tag{45}$$

$$\Delta c_1 = 0.347(\pm 0.049) \times 10^{-3} V sin\ i - 0.044(\pm 0.007). \tag{46}$$

From β, (b-y) relationship of the 20 apparent normal stars excluding Nos 375 and 429 we derive,

$$\Delta(b - y) = -0.172(\pm 0.018) \times 10^{-3} V sin\ i + 0.020(\pm 0.002), \tag{47}$$

$$\Delta \beta = -0.183(\pm 0.019) \times 10^{-3} V sin\ i + 0.021(\pm 0.002). \tag{48}$$

The results for the Praesepe stars are shown in Fig II-12 to II-16 and these residuals are listed in Table II–13.

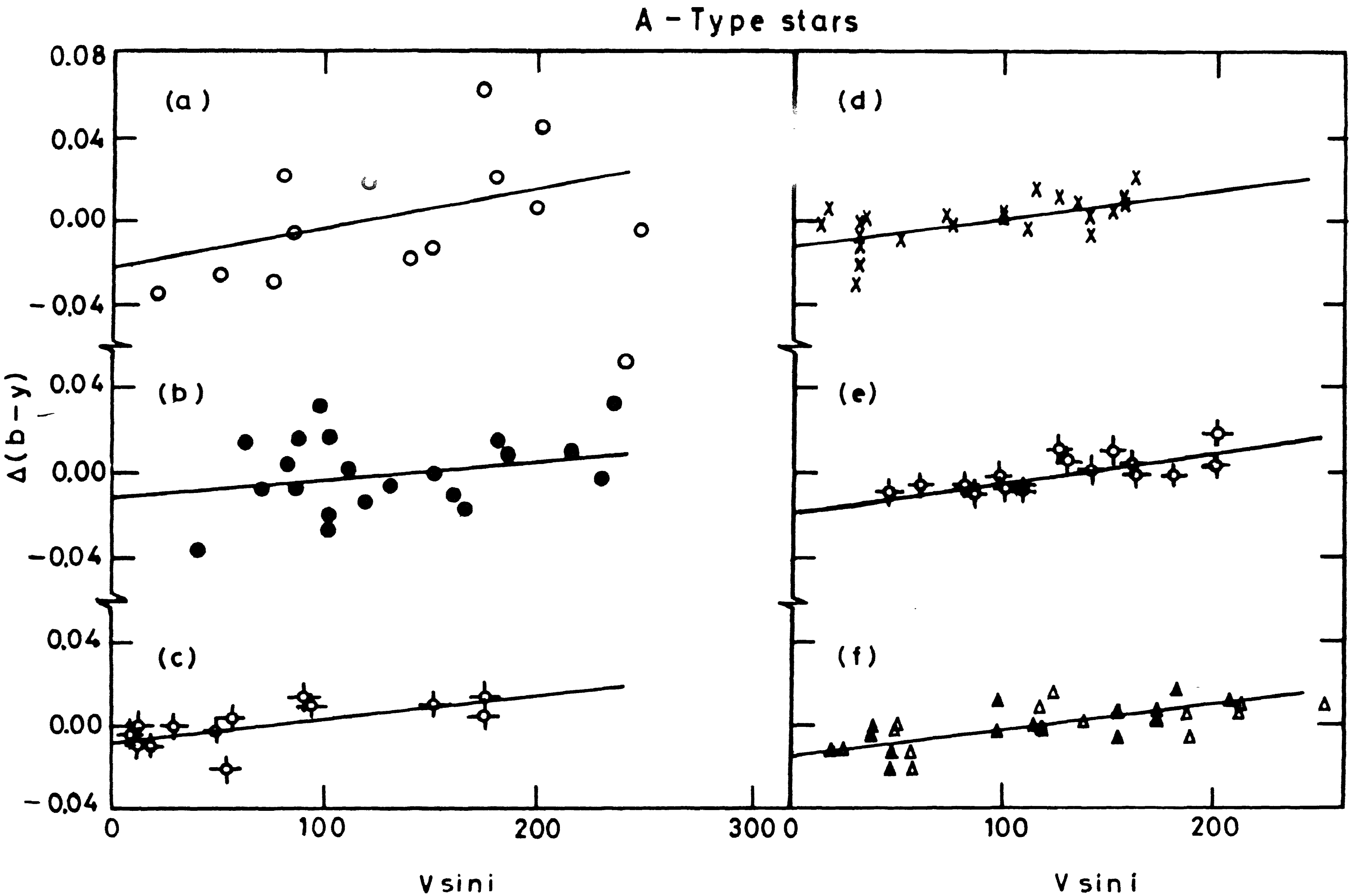

Fig II–14 : Δ *(b-y) Versus Vsin i diagram derived from* c_1, *(b-y) plane for A stars in various clusters. Symbols have the same meaning as figure II-12.*

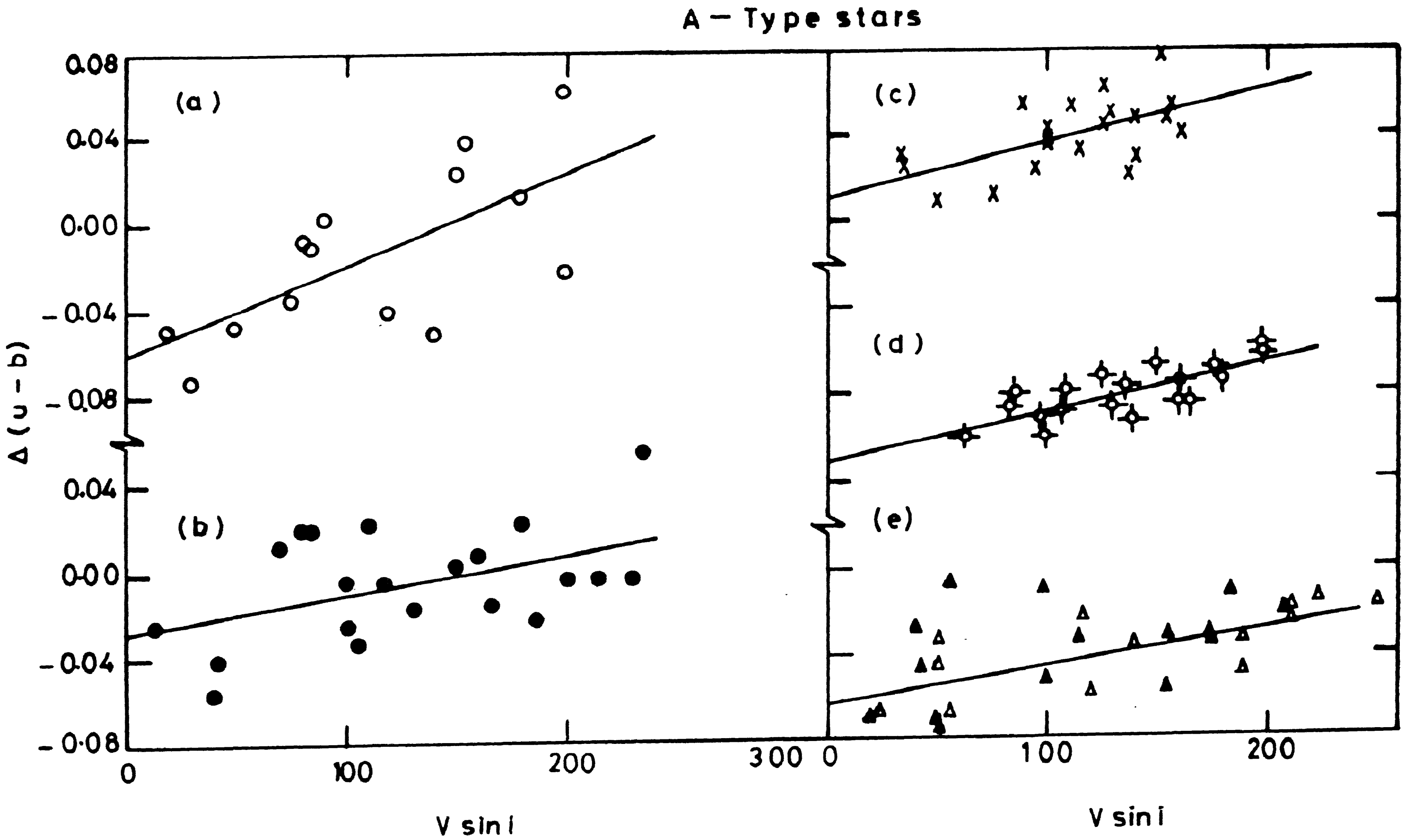

Fig II–15 : Δ *(u-b) Vsin i diagram derived from the β, (u-b) relationship for (a) α-Persei (b) Pleiades (c) Hyades (d) Praesepe and (e) theoretical predictions for $i=45^o$ and $i=60^o$.*

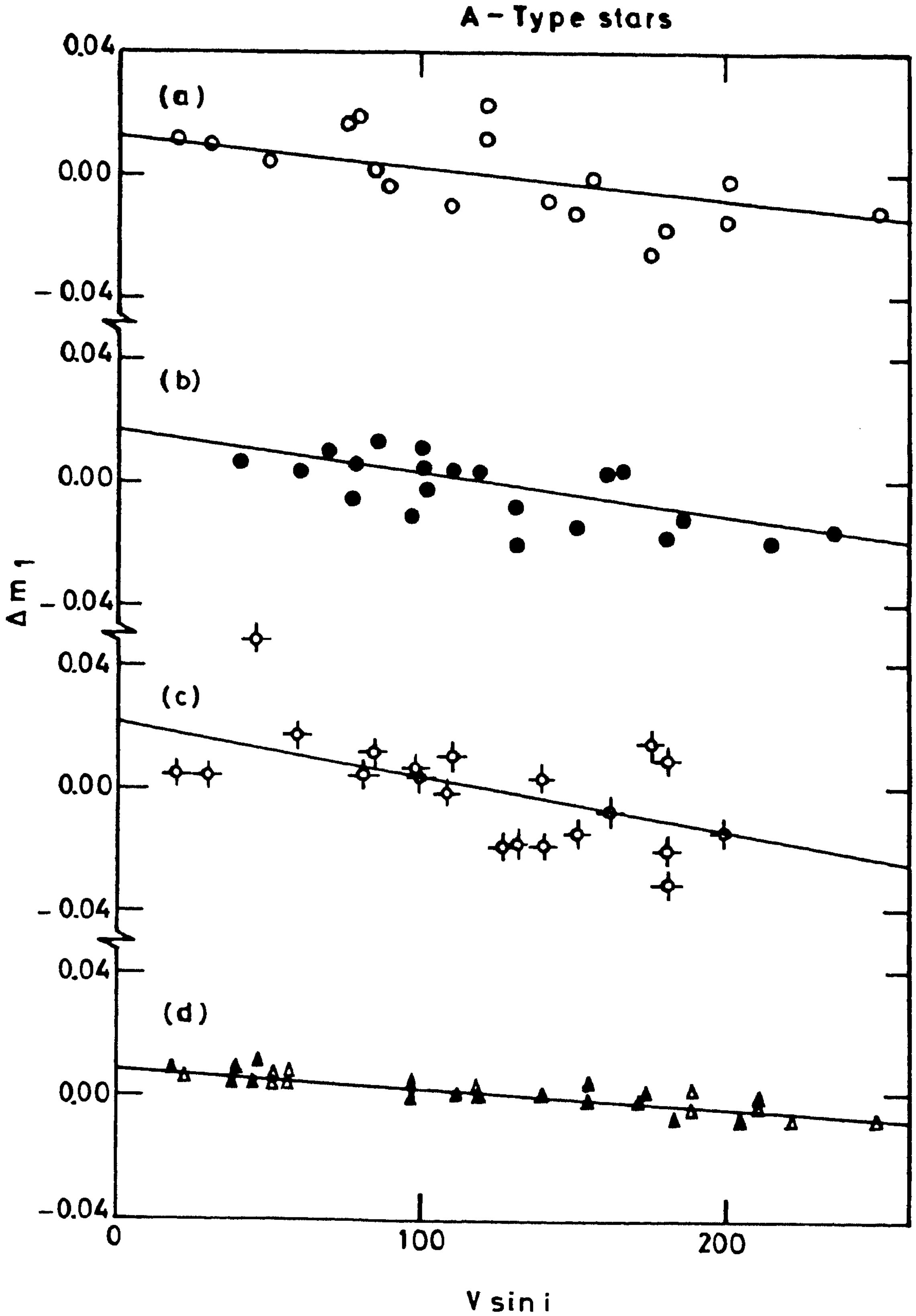

Fig II–16 : *Δm_1 Versus V sin i diagram derived from the c_1, m_1 relationship for (a) α-Persei (b) Pleiades (c) Praesepe and (d) theoretical predictions for $i = 45^o$ and 60^o.*

Table II–12. Data for Praesepe A-type stars

HD	KW	ST	V	β	(b-y)	m_1	c_1	$V sin\ i$	Remarks
73174	40	A4m		2.844	0.112	0.215	0.951	20	
73210	50		6.75	2.810	0.120	0.169	1.022	80	
73430	143	A9	8.31	2.813	0.127	0.210	0.876	82	
73449	150	A9n	7.45	2.759	0.157	0.181	0.942	235	
73450	154			2.770	0.149	0.197	0.793	138	
73574	203		7.73	2.801	0.126	0.204	0.879	108	
73576	207	A7n	2.67	2.812	0.104	0.199	0.969	200	
73618	224	A4m	7.32	2.845	0.104	0.230	0.964	70	SB2, Am
73619	229	A4m	7.54	2.824	0.143	0.237	0.828	135	SB2, Am
73666	265		11.98	2.868	0.005	0.159	1.095	40	
73711	276	A3m	7.54	2.858	0.075	0.234	1.004	60	Am
73709	279	A3m	7.70	2.843	0.099	0.260	0.937	45	Am
73712	284	A9	6.78	2.756	0.161	0.180	0.937	40	VB
73730	286	A3m	8.02	2.838	0.113	0.216	0.954	30	Am
73731	300	A5m	6.30	2.839	0.091	0.219	1.037	100	SB2, Am
73763	323	A9	7.80	2.796	0.130	0.189	0.900	130	
73819	348		6.78	2.818	0.091	0.195	1.075	152	
73818	350	A7m	8.71	2.749	0.190	0.222	0.752	85	SB2, Am
73872	375		8.33	2.812	0.129	0.176	0.885	180	
73890	385	A7n	7.92	2.791	0.144	0.196	0.855	165	SB2
74028	445	A7	7.95	2.812	0.120	0.201	0.911	160	
74050	449	A7n		2.812	0.115	0.197	0.947	150	
72942	534			2.850	0.060	0.202	1.039	62	
73045	538	A4m		2.799	0.208	0.200	0.763	20	Am
72846				2.845	0.076	0.198	1.019	140	
73161	038	F0n		2.741	0.188	0.183	0.760	160	
73175	045	F0n	8.25	2.790	0.131	0.213	0.858	180	
73345	114	F0	8.14	2.815	0.122	0.211	0.881	98	
73397	124	F4	9.00	2.730	0.208	0.181	0.688	100	
73616	226	F2	8.89	2.721	0.209	0.167	0.731	125	
	271	F2	8.81	2.735	0.192	0.194	0.719	85	
73729	292	F2n	8.18	2.742	0.198	0.172	0.809	160	SB2
73746	318	F0	8.65	2.748	0.181	0.197	0.749	110	
73798	340	F0n	8.48	2.764	0.147	0.213	0.809	175	
73993	429	F2n	8.53	2.738	0.194	0.173	0.780	200	

Table II–13. Effects of rotation for Praesepe A stars.

		from β, c_1		from β,(u-b)		from c_1 (b-y)		from β,m_1	
KW	$V sin\ i$	$\Delta\beta$	Δc_1	$\Delta\beta$	Δ(u-b)	Δc_1	Δ (b-y)	$\Delta\beta$	Δm_1
40	20	.011	−.040	–	–	–	–	.039	.004
143	82	.016	−.033	.010	−.006	−.014	−.007	−.024	.006
154	138	.011	−.013	–	–	–	–	−.069	.003
203	108	.002	.000	.016	−.008	−.013	−.007	−.004	−.001
207	200	−.030	.062	−.028	.019	.025	.009	.101	−.014
276	60	−.002	−.026	–	–	−.011	−.005	.059	.019
279	45	.017	−.051	–	–	−.018	−.010	−.019	.050
286	30	.003	−.020	–	–	–	–	.040	.004
323	130	−.012	.033	.013	−.006	.017	.006	.066	−.018
375	180	.011	−.022	–	–	.000	−.002	.105	−.029
445	160	−.002	.004	.004	−.003	.005	.000	.037	−.007
449	150	−.019	.040	−.022	.015	.029	.011	.085	−.014
72846	140	−.023	.026	−.008	−.012	.006	.002	.154	−.018
38	160	−.004	.017	−.002	.006	.006	.004	−.050	−.006
45	180	.001	.005	−.006	.007	–	–	−.049	.011
114	98	.016	−.033	.018	−.011	−.020	−.010	−.021	.006
124	100	.016	−.031	.018	−.019	−.024	−.006	−.114	.004
226	125	−.011	.030	−.005	.008	.021	.013	−.006	−.018
271	85	.008	−.011	.003	.001	−.026	−.009	−.133	.011
318	110	.008	−.009	.003	.002	−.020	−.007	−.113	.010
340	175	−.002	.016	−.008	.012	–	–	−.098	.017
429	200	−.016	.044	−.017	.021	.039	.019	.014	−.019
385	165	–	–	.012	−.005	–	–	–	–
534	62	–	–	.016	−.019	–	–	–	–
370	137	–	–	−.002	.003	–	–	–	–

8. Scorpio-Centaurus Association

The existence of different subgroups in this association and the fact that the upper Scorpius subgroup is younger than the other two subgroups was pointed out by Blaauw (1959, 1964). If the sample does not confirm to a homogeneous coeval group this would introduce a spread in the observed colour-magnitude diagrams. This is illustrated in Figs II–17 and II–18. A second-order common polynomial fit was determined for the β versus c_o relation for the stars in the upper Centaurus and upper Scorpius regions and the colour excess Δc_o was determined. Fig II–17 is a plot of Δc_o versus $Vsin\ i$. Only the two subgroups—upper Centaurus and upper Scorpius— are plotted. Upper Centaurus stars are represented by open squares and upper Scorpius stars by crosses. Similarly in Fig. II–18 Δ(u-b)$_o$ is plotted against $Vsin\ i$. It is clear from these figures that the upper Scorpius stars which are younger, lie below the upper Centaurus stars. This would appear as a scatter in the diagram if all the points are plotted with the same symbol. In order to take into account such evolutionary effects even on the main sequence, the data analysis was carried out independently for the lower Centaurus, upper Centaurus and upper Scorpius subgroups. Removing the binaries, peculiar and emission-lined stars, whose colours may be affected due to reasons other than rotation, we are left with 10 stars out of the 13 possible stars of luminosity classes IV and V in the lower Centaurus subgroup and 27 stars out of the possible 42 in the upper Centaurus subgroup listed in Table 3 of Glaspey (1971). We have analyzed them separately and the colour excesses were calculated in c_o, (u-b)$_o$, β and (b-y)$_o$. $\Delta\beta$ was calculated from both β, c_o and β(u-b)$_o$ relations. A detailed description of the analysis of this association is given in paper II (Mathew & Rajamohan 1990).

The scatter in upper scorpius is caused by the inclusion of the whole range of B0-B9 stars and the added effect due to high variable reddening of the upper scorpius members. We illustrate this by the rotation effect in B2, B3 stars for upper Centaurus members listed in Table II–14. From a second order polynomial fit in β, c_o and β, (u-b)$_o$ planes we derive

$$\Delta c_0 = 0.169(\pm 0.056) \times 10^{-3} Vsin\ i - 0.031(\pm 0.011), \qquad (49)$$

$$\Delta\beta = -0.054(\pm 0.017) \times 10^{-3} Vsin\ i + 0.010(\pm 0.003), \qquad (50)$$

$$\Delta(u-b)_o = 0.278(\pm 0.057) \times 10^{-3} Vsin\ i - 0.052(\pm 0.011), \qquad (51)$$

$$\Delta\beta = -0.058(\pm 0.012) \times 10^{-3} Vsin\ i - 0.058(\pm 0.012). \qquad (52)$$

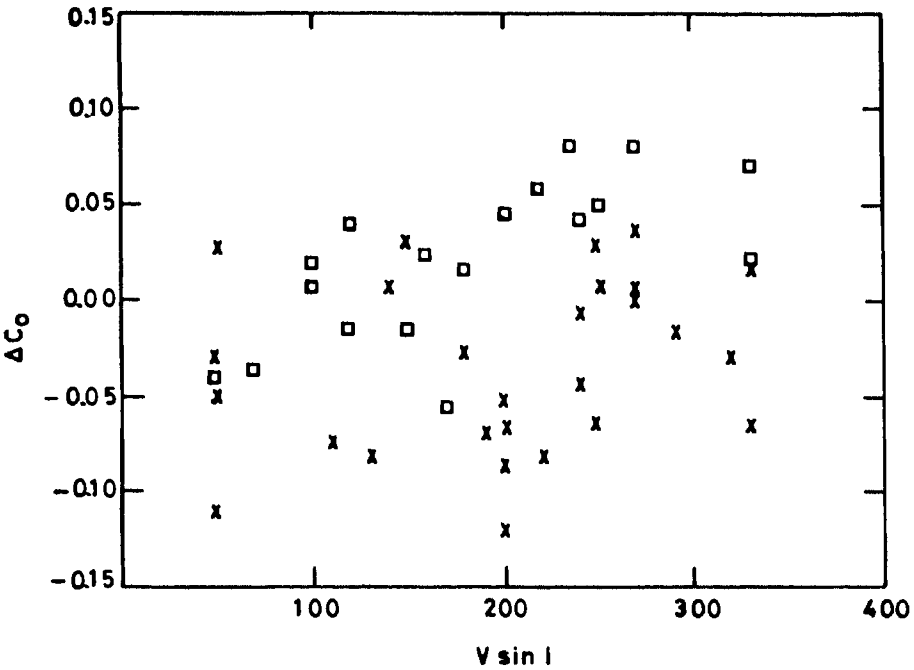

Fig II–17 : *The deviations in c_0 derived, from the observed β, c_0 for the members of the two large sub-groups of the Scorpio-Centaurus association are plotted against $V sin\ i$. Notice the different distribution of upper centaurus (open squares) and upper scorpius (crosses) members due to age differences (evolutionary effect) between the two sub groups.*

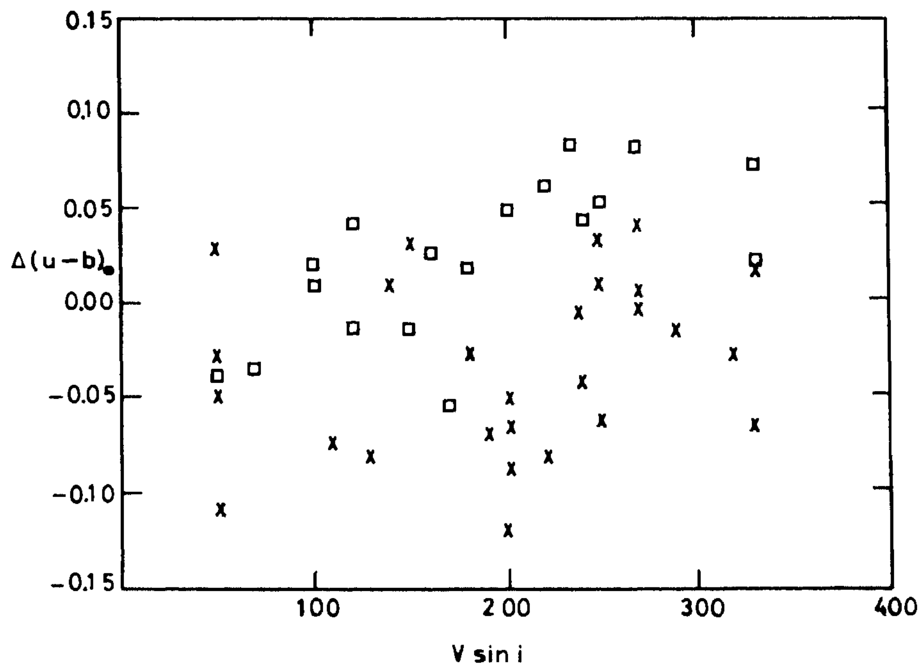

Fig II–18 : *$\Delta(u\text{-}b)_0$ versus $V sin\ i$ diagram derived from $\beta(u\text{-}b)_0$ relation for upper centaurus (open squares) and upper scorpius (crosses) members. Note the different distribution due to evolutionary effects.*

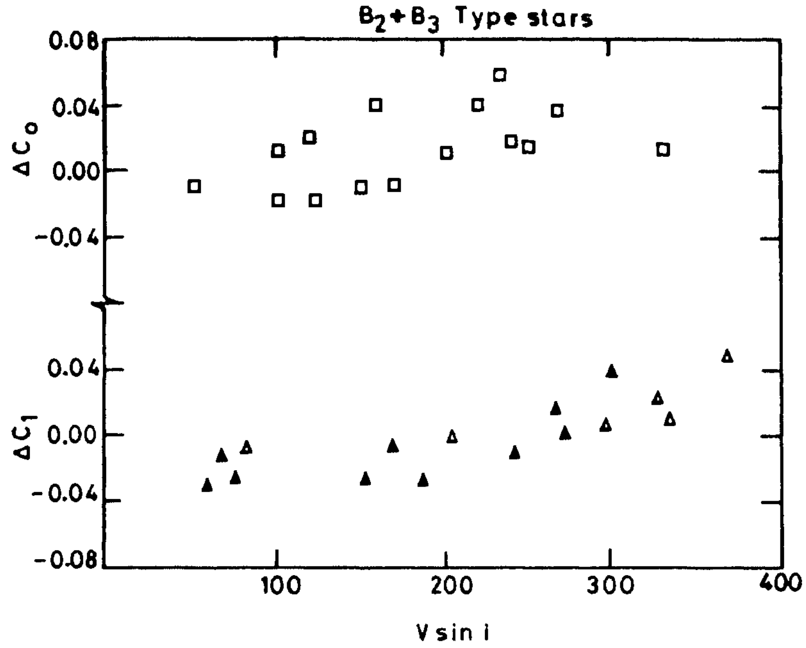

Fig II–19 : *The deviations in c_o derived from β, c_o of B2, B3 stars (a) upper centaurus and lower centaurus (b) residuals derived from theoretical predictions by Collins and Sonneborn (1977) for similar mass range stars for $i=45^o$ (filled triangles) and $i=60^o$ (open triangles) are shown for comparison.*

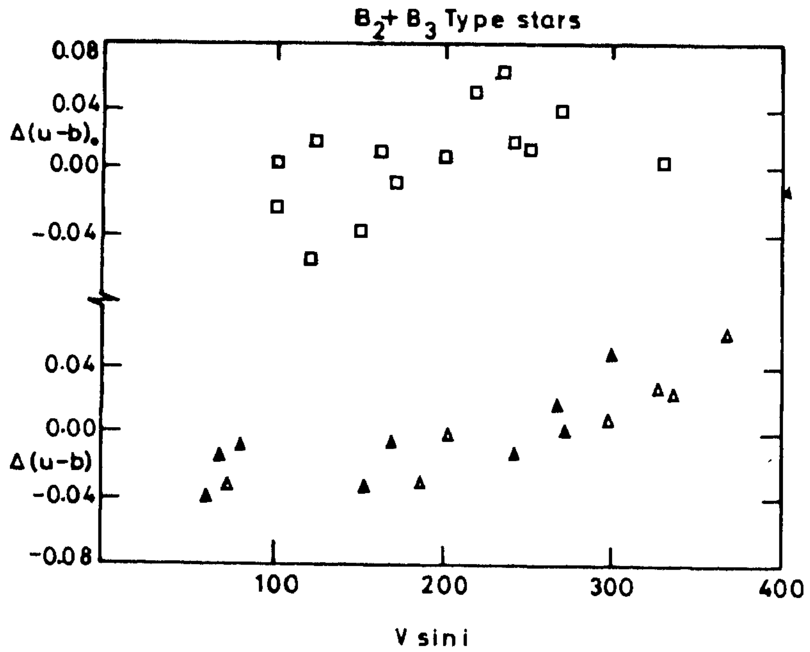

Fig II–20 : *The same as II-18 for $\Delta(u\text{-}b)_o$ derived from β, $(u\text{-}b)_o$ relationship.*

Table II–14. Data for Lower-Cen + Upper-Cen stars

HD	MK	V_o	β	$(b-y)_o$	m_o	c_o	$V\sin i$	Remarks
				Lower Cen				
105435	B2 IV ne	2.07	2.467	−0.119	0.079	−0.031	200	
105937	B3 V	3.94	2.707	−0.087	0.114	0.326	210	
106490	B2 IV	2.78	2.619	−0.113	0.086	0.043	120	
106983	B2.5 V	4.04	2.680	−0.019	0.106	0.259	140	
108483	B2 V	3.86	2.654	−0.101	0.096	0.155	220	
109658	B2 IV-V	2.69	2.649	−0.105	0.093	0.112	190	
110956	B3 V	4.57	2.701	−0.037	0.101	0.298		
112092	B2 IV-V	3.99	2.664	−0.099	0.098	0.176		
116087	B3 V	4.52	2.700	−0.082	0.111	0.347	300	
				Upper Cen				
120307	B2 IV	3.37	2.626	−0.108	0.078	0.083	100	SB
120324	B2 Ve	3.12	2.478	−0.120	0.075	0.043	210	Be
121743	B2 IV	3.81	2.646	−0.105	0.082	0.145	120	
121790	B2 V	3.85	2.642	−0.101	0.090	0.162	200	
122980	B2 V	4.34	2.651	−0.090	0.090	0.175	50	
125238	B2.5 IV	3.50	2.656	−0.091	0.085	0.256		
125823	B3:p	4.36	2.656	−o.096	0.083	0.209	100	CP
129116	B2.5 V	3.90	2.675	−0.092	0.093	0.248	170	
132058	B2 IV	2.68	2.618	−0.106	0.066	0.097	110	SB
132200	B2 V	3.14	2.639	−0.097	0.080	0.191	80	
132955	B3 V	5.24	2.705	−0.093	0.108	0.336	50	
133955	B3 V	4.02	2.698	−0.089	0.101	0.278	180	
136298	B2 IV	3.17	2.616	−0.108	0.070	0.083	240	
136664	B3 V	4.47	2.684	−0.084	0.097	0.324	220	
137432	B3 V	5.42	2.707	−0.078	0.095	0.391	160	SB?
138690	B2 V	2.79	2.634	−0.102	0.083	0.141	250	
138769	B3 IVp	4.53	2.684	−0.090	0.097	0.271	150	CP
143118	B2 V	3.41	2.619	−0.105	0.078	0.113	270	
144294	B2.5 V	5.89	2.671	−0.091	0.090	0.260	330	

Table II–15. Effects of rotation for Lower-Cen + Upper-Cen B2, B3 stars

		from β, c_1		from β,(u-b)		from β (b-y)	
HD	$V sin\ i$	$\Delta\beta$	Δc	$\Delta\beta$	Δ(u-b)	$\Delta\beta$	Δ (b-y)
105937	210	.012	−.026			.040	−.020
106490	120	.005	−.034	.006	−.038	.009	−.009
106983	140	.005	−.012	.005	−.017	.016	−.008
108483	220	.010	−.036	.004	−.022	−.010	.003
109668	190	.016	−.063			.016	−.010
110956	75	.015	−.036	.012	−.044	.009	.000
116087	300	−.002	.016	−.004	.031	.007	.002
120307	100	.001	−.018	.003	−.025	−.011	.000
121743	120	.004	−.020	.010	−.055	.016	−.010
121790	200	−.004	.009	−.002	.005	.003	−.004
125238	235	−.018	.059	−.013	.062	−.020	.009
125823	100	−.004	.012	−.001	.003	−.013	.005
129116	170	.004	−.008	.003	−.009	−.007	.005
132955	50	.007	−.010			−.006	.022
136298	240	−.009	.016	−.005	.016	−.032	.008
136504	120	−.006	.018	−.004	.017	−.008	.002
136664	220	−.010	.041	−.009	.052	−.009	.010
137432	160	−.008	.039	.001	.010	.015	−.003
138690	250	−.007	.014	−.005	−.015	−.014	.003
138769	150	.006	−.012	.009	−.039	.019	−.009
143118	270	−.014	.036	−.010	.038	−.018	.002
144294	330	−.004	.016	.000	.003	−.001	.001

The derived residuals are listed in Table II–15. The residuals in c_o and (u-b)$_o$ for the upper Centaurus stars are plotted respectively in Fig II–19 and II–20 are compared with theoretical predictions (Chapter 3) for B2 to B3 stars. This excellent agreement demonstrates the dependence of rotation on the masses of stars; smaller for B0-B3 ranges and higher for the B5-B9 ranges.

9. Other clusters

We analysed the data of most of the clusters for which a statistically significant sample of single main sequence members was present. The colour excesses due to rotation for NGC 2422, NGC 2516, NGC 2264. IC 4665, Coma, and IC 4756 are plotted against $V sin\ i$ in Figs II–7 to II–11 with different symbols. A summary of the results of all the clusters analysed is given in Table II–16.

The slopes of the colour excess versus $V sin\ i$ per 100 km s^{-1} of $V sin\ i$ for the selected clusters in all possible planes are given in Table II–17.

Table II–16. Observed reddening due to rotation for 100 km s^{-1} of V sin i

	from β, c_1		from β(u-b)	
Cluster	$\Delta\beta$	Δc_1	$\Delta\beta$	Δ(u-b)
Hyades	−.015	.037	−.022	.026
	±.002	±.006	±.005	±.006
Praesepe	−.015	.037	−.028	.022
	±.003	±.006	±.004	±.004
Pleiades	−.017	.039	−.015	.018
A stars	±.002	±.004	±.007	±.006
α-Persei	−.014	.030	.012	.043
A stars	±.004	±.006	±.006	±.008
α-Persei	−.015	.045	−.013	.062
B stars	±.001	±.003	±.001	±.005
IC 4665	−.016	.033		
A stars	±.003	±.006		
IC 4665	−.013	.043	−.010	.045
B stars	±.002	±.007	±.002	±.005
NGC 2264	−.008	.038	−.007	.052
	±.001	±.006	±.001	±.001
IC 2391	−.016	.038	−.019	.066
	±.003	±.007	±.003	±.016
IC 2602	−.013	.036	−.012	.057
	±.004	±.011	±.004	±.015
NGC 2422	−.013	.032	−.013	.036
	±.003	±.008	±.004	±.011
NGC 4755	−.011	.032	−.008	.031
	±.002	±.005	±.002	±.007
Scorpio-Centaurus	−.007	.028	−.006	.033
	±.001	±.003	±.001	±.004
NGC 2287	−.006	.020	−.026	.064
	±.004	±.024	±.007	±.016
NGC 1976	−.007	.032	−.002	.013
	±.003	±.011	±.002	±.011

Table II–17. Observed reddening due to rotation for 100 km s^{-1} of V sin i

	from β, c_1		from β,(b-y)		from β, (u-b)		from β,m_1		from c_1, (b-y)	
Cluster	$\Delta\beta$	Δc_1	$\Delta\beta$	Δ(b-y)	$\Delta\beta$	Δ(u-b)	$\Delta\beta$	Δm_1	Δc_1	Δ(b-y)
Upper-Cen+	−.005	.017	−.004	.000	−.006	.028	−.002	.001	−.002	−.001
Lower-cen	±.002	±.006	±.003	±.002	±.001	±.006	±.003	±.001	±.009	±.001
B2, B3 stars										
α-Persei	−.015	.045	−.017	.010	−.013	.062	.007	−.002	−.013	.002
B stars	±.001	±.003	±.005	±.002	±.001	±.005	±.005	±.002	±.015	±.002
α-Persei	−.014	.030	−.013	.007	.012	.043	.068	−.016	.065	.019
A stars	±.004	±.006	±.005	±.005	±.014	±.008	±.006	±.002	±.012	±.006
Pleiades	−.017	.039	−.012	−.013	−.015	.018	.041	−.011	.023	.008
A stars	±.002	±.004	±.004	±.004	±.007	±.006	±.002	±.002	±.010	±.005
Hyades	−.015	.037	−.004	−.003	−.022	.026	−.002	.003	.028	.013
	±.002	±.006	±.003	±.003	±.005	±.006	±.002	±.003	±.006	±.003
Praesepe	−.015	.037	−.018	−.017	−.028	.022	.003	−.004	.035	.015
	±.003	±.006	±.002	±.002	±.004	±.004	±.003	±.002	±.005	±.002

	from c_1, (u-b)		from c_1,m_1		from (b-y), (u-b)		from (b-y), m_1		from (u-b) m_1	
Cluster	Δc_1	Δ(u-b)	Δc_1	Δm_1	Δ(b-y)	Δ(u-b)	Δ(b-y)	Δm_1	Δ(u-b)	Δm_1
Upper-Cen	.000	−.000	.010	−.001	−.002	−.001	−.002	.000	.006	−.001
Lower-cen	±.003	±.004	±.013	±.001	±.001	±.011	±.003	±.002	±.017	±.001
B2, B3 stars										
α-Persei	.005	−.009	.072	−.007	.003	−.024	.012	−.006	.096	−.006
B stars	±.002	±.004	±.015	±.001	±.002	±.019	±.004	±.002	±.022	±.001
α-Persei	.038	.018	.145	−.010	−.013	.050	−.040	−.007	.065	−.006
A stars	±.020	±.009	±.016	±.003	±.012	±.012	±.007	±.002	±.013	±.003
Pleiades	.059	−.014	.125	−.014	−.021	−.004	−.048	−.013	.029	−.008
A stars	±.018	±.009	±.011	±.002	±.012	±.011	±.005	±.002	±.010	±.003
Hyades	.021	−.009	.017	−.007	−.016	−.029	.004	−.025	.021	−.014
	±.041	±.005	±.025	±.003	±.006	±.008	±.013	±.003	±.007	±.003
Praesepe	.066	−.030	.025	−.013	−.016	.000	−.011	−.016	−.002	−.003
	±.014	±.006	±.023	±.003	±.005	±.005	±.008	±.004	±.008	±.003

III. COMPARISON WITH THEORY

1. Theoretical Predictions : The B-Stars

Collins & Sonneborn (1977) have calculated theoretical values of (b-y), c_1, m_1, and β for rigidly rotating model stars for the mass range 14.5 $M_\odot$ to 1.2 $M_\odot$. Plots are made with β and the different predicted colour indices at each value of i, the inclination between the line of sight and the rotation axis for various values of fractional angular velocity ω. Fig.III–1 is a plot shown as an example between β and c_1 for $i = 60°$ and $\omega = 0.2$, 0.5, 0.8 and 0.9 for B0 to B9 stars. The points corresponding to different ω values are marked with different symbols and joined by dotted lines for each spectral class. The shift Δc along the x-axis for each value of ω for a given spectral type was determined from Fig.III–1. Similarly the shift $\Delta\beta$ along the y-axis was determined for each value of ω. This was repeated for each value of i and the deviation in c_1 and β from the relation for $\omega = 0.2$ is given in Table III–1. We chose to derive the reddening due to rotation relative to $\omega = 0.2$ for the following reason. Observationally one derives only the projected rotational velocity and the value of i is unknown. We do not know whether a really nonrotating, single, normal, main-sequence star exists (Rajamohan 1978). Also for comparison of observations with theory, it is sufficient if we derive the slope of the reddening effect due to rotation for different mass ranges. This would be independent of calibration errors.

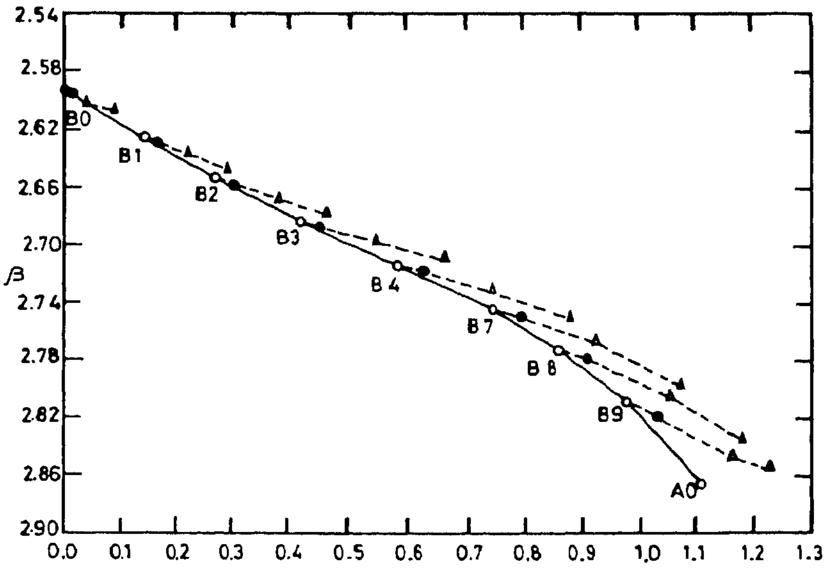

Fig III–1 : *β versus c_1 plot, Collins and Sonneborn (1977), for i=60° and ω=0.2 (open circles),ω=0.5 (filled circles), ω=0.8 (open triangles) and ω=0.9 (filled triangles).*

In (u-b) also a similar analysis was done for various values of i and different values of ω and for different mass ranges. These deviations are given in Table III–2. As an example we have plotted in Figs III–2 and III–3 the deviations in Δc_1 and Δ(u-b) in Tables III–1 and III–2 aginst V sin i for a representative value of $i = 60^o$ and ω=0.2 to 0.9 for B0 to B9 stars. It is evident that the slope of the predicted effect is a function of the mass: low for B0 stars and high for B9 stars.

In order to compare these predictions from theoretical models of Collins and Sonneborn (1977) we have analysed the theoretical u, v, b, y and H_β indices in a similar way as we did for the cluster data. For this we have arranged the B stars into two groups B0 to B3 and B5 to B9. For each group at a given value of i and different values of ω, a second order polynomial fit was determined for each of the various pairs of colours and colour indices like β versus c_1, β versus (u-b), β versus (b-y) etc. relations and the deviations in all colours and colour indices like $\Delta\beta$, Δc_1, Δ (u-b), Δ (b-y) etc were determined. This was done for i = 30°, 45°, 60° and 90°. The slopes of the relation between $V sin\ i$ and the colour excess derived

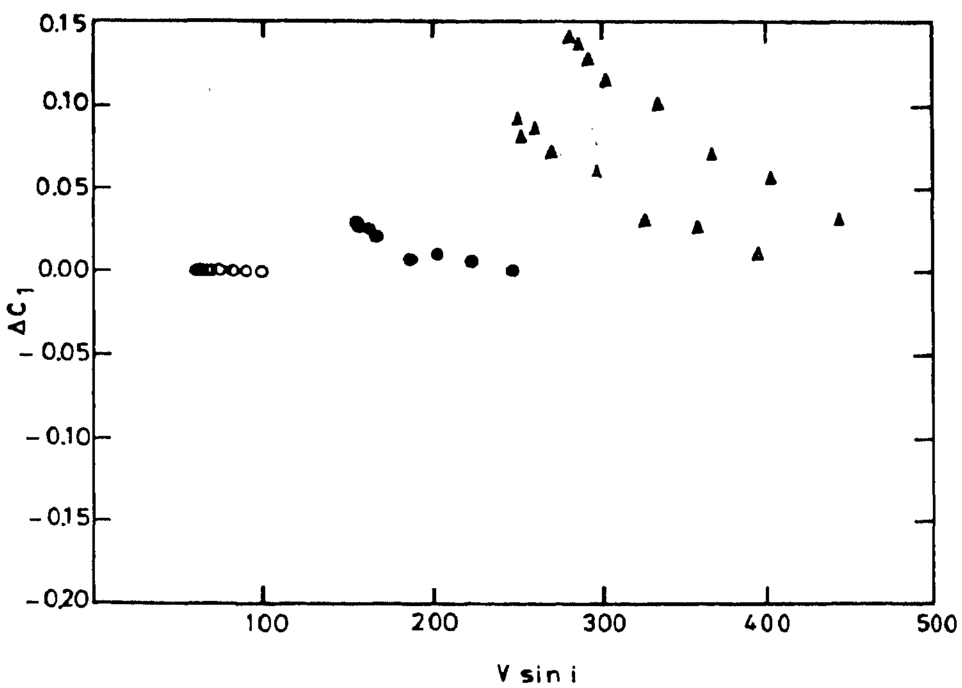

Fig III–2 : *The deviations in c_1 from figure III–1 are plotted against Vsin i for ω=0.2 (open circles),ω=0.5 (filled circles), ω=0.8 (open triangles) and ω=0.9 (filled triangles). The deviations at any given ω increases from B0 to B9.*

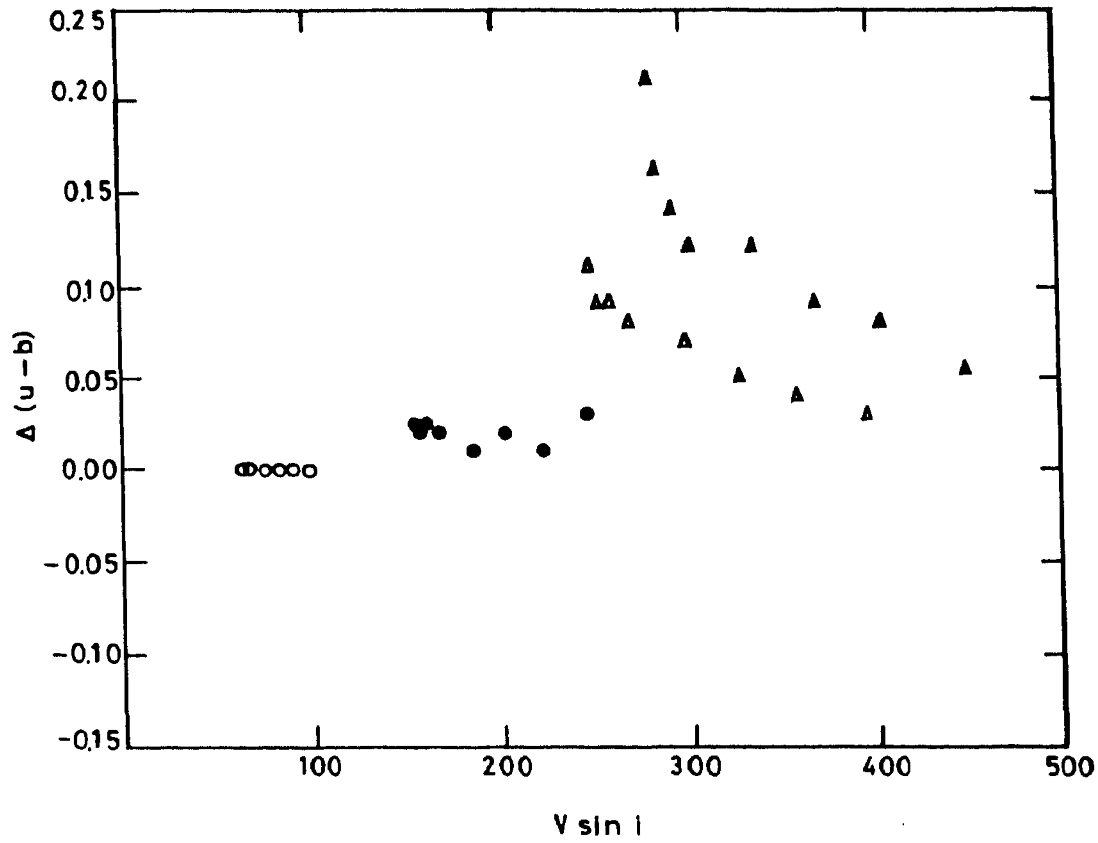

Fig III–3 : *Deviations in (u-b) derived from the theoretical predictions for β, (u-b) are plotted against V sin i. Symbols have the same meaning as in figure III-2. Note that the slope of the rotation effect is a function of the spectral type in figure III-2 and III-3.*

for different values of i for B5 to B9 stars are given in Table III–3 and for B0 to B3 stars are given in Table III–4. These were derived in the following manner. Four values of ω were assigned to each spectral type. There are four spectral subclasses between B0 and B3 and B5 and B9 for which predicted values of β and various colour indices are available.Hence for each group at a given value of i we have sixteen values of various colour indices. These sixteen values were analysed the same way as we did the cluster stars. This was repeated for the next value of i. This simple approach was taken as we really do not know whether cluster members have inclination axis randomly distributed or they have a preferred orientation. In either case we expect that the theoretical values for i=30^o & 90^o to straddle the observational slope.

Table III–1. Theoretical effects of rotation

Sp	ω	i = 30 $\Delta\beta$	i = 30 Δc_1	i = 60 $\Delta\beta$	i = 60 Δc_1	i = 90 $\Delta\beta$	i = 90 Δc_1
B0	0.2	0.000	0.000	0.000	0.000	0.000	0.000
	0.5	0.010	0.070	0.000	0.000	0.010	0.070
	0.8	0.010	0.070	0.002	0.010	0.010	0.070
	0.9	0.010	0.070	0.008	0.030	0.012	0.090
B1	0.2	0.000	0.000	0.000	0.000	0.000	0.000
	0.5	0.003	0.015	0.002	0.005	0.001	0.005
	0.8	0.008	0.035	0.006	0.025	0.006	0.035
	0.9	0.009	0.050	0.012	0.055	0.014	0.080
B2	0.2	0.000	0.000	0.000	0.000	0.000	0.000
	0.5	0.003	0.015	0.007	0.010	0.002	0.015
	0.8	0.005	0.025	0.017	0.030	0.007	0.040
	0.9	0.010	0.050	0.014	0.070	0.016	0.080
B3	0.2	0.000	0.000	0.000	0.000	0.000	0.000
	0.5	0.003	0.015	0.005	0.007	0.002	0.015
	0.8	0.005	0.025	0.010	0.060	0.013	0.060
	0.9	0.010	0.050	0.020	0.100	0.020	0.100
B5	0.2	0.000	0.000	0.000	0.000	0.000	0.000
	0.5	0.003	0.025	0.004	0.020	0.004	0.020
	0.8	0.012	0.060	0.014	0.070	0.016	0.080
	0.9	0.018	0.090	0.030	0.115	0.030	0.120
B7	0.2	0.000	0.000	0.000	0.000	0.000	0.000
	0.5	0.003	0.015	0.006	0.025	0.005	0.030
	0.8	0.020	0.060	0.026	0.085	0.023	0.080
	0.9	0.040	0.110	0.040	0.125	0.047	0.130
B8	0.2	0.000	0.000	0.000	0.000	0.000	0.000
	0.5	0.005	0.020	0.008	0.025	0.006	0.025
	0.8	0.027	0.070	0.031	0.080	0.038	0.090
	0.9	-	0.130	-	0.135	-	0.150
B9	0.2	0.000	0.000	0.000	0.000	0.000	0.000
	0.5	0.010	0.030	0.012	0.030	-	0.030
	0.8	-	0.085	-	0.090	-	0.100
	0.9	-	0.130	-	0.140	-	0.160

Table III–2. Theoretical effects of rotation

Sp	ω	i = 30 $\Delta\beta$	i = 30 Δ(u-b)	i = 60 $\Delta\beta$	i = 60 Δ(u-b)	i = 90 $\Delta\beta$	i = 90 Δ(u-b)
B0	0.2	0.000	0.000	0.000	0.000	0.000	0.000
	0.5	0.001	0.004	0.003	0.030	0.001	0.010
	0.8	0.003	0.020	0.004	0.030	0.002	0.020
	0.9	0.006	0.040	0.008	0.055	0.009	0.070
B1	0.2	0.000	0.000	0.000	0.000	0.000	0.000
	0.5	0.001	0.010	0.002	0.010	0.001	0.010
	0.8	0.005	0.035	0.006	0.040	0.006	0.040
	0.9	0.008	0.050	0.012	0.080	0.013	0.090
B2	0.2	0.000	0.000	0.000	0.000	0.000	0.000
	0.5	0.001	0.010	0.003	0.020	0.002	0.010
	0.8	0.004	0.030	0.008	0.050	0.007	0.050
	0.9	0.008	0.060	0.012	0.090	0.015	0.100
B3	0.2	0.000	0.000	0.000	0.000	0.000	0.000
	0.5	0.002	0.010	0.002	0.010	0.002	0.020
	0.8	0.006	0.045	0.009	0.070	0.010	0.080
	0.9	0.012	0.080	0.017	0.120	0.020	0.120
B5	0.2	0.000	0.000	0.000	0.000	0.000	0.000
	0.5	0.002	0.015	0.003	0.020	0.002	0.020
	0.8	0.009	0.060	0.010	0.080	0.014	0.090
	0.9	0.016	0.100	0.020	0.120	0.020	0.140
B7	0.2	0.000	0.000	0.000	0.000	0.000	0.000
	0.5	0.002	0.020	0.005	0.025	0.006	0.025
	0.8	0.015	0.070	0.018	0.090	0.025	0.110
	0.9	0.030	0.120	0.033	0.140	0.024	0.160
B8	0.2	0.000	0.000	0.000	0.000	0.000	0.000
	0.5	0.004	0.020	0.005	0.020	0.006	0.030
	0.8	0.020	0.080	0.022	0.090	0.024	0.100
	0.9	-	0.140	-	0.160	-	0.180
B9	0.2	0.000	0.000	0.000	0.000	0.000	0.000
	0.5	0.005	0.020	0.006	0.025	0.010	0.030
	0.8	-	0.090	-	0.110	-	0.120
	0.9	-	0.180	-	0.210	-	0.250

In figures III–4 and III–5 the theoretical slopes of the relation between $V sin\ i$ and the colour excess derived from the different planes for B5 to B9 spectral types are plotted against 'i'. These figures show how the rotation effect varies with 'i'. The probable errors are also shown in the figures. Figures III–6 and III–7 are similar to the above for B0 to B3 stars. For the early B-stars, only in the c_1, m_1 and u-b, m_1 planes are the slopes sensitive to i while for the late B stars the slopes derived in the β, c_1 plane are also found to be sensitive to i. No sensitivity to i exists in other combinations.

In each of the colour excess verses $V sin\ i$ diagrams (Chapter II) showing rotation effects for clusters, the computed colour excess for i=45° and 60° (32 values each set) are also shown. The i = 45 is represented by closed triangles and i = 60° by open triangles.

2. A Stars

For A type stars, we followed a similar procedure and analysed the theoretical data the same way as we did for cluster data. We chose the theoretical indices for A3 to F0 type stars since the α-Persei and Pleiades cluster A-type groups that we analysed contained mainly A3 to F0 type stars. For each value of i and different values of ω a second order polynomial fit was determined for different colours and colour indices etc. β, c_1; c_1,(b-y); β,(b-y) and the deviations in all colours and colour indices $\Delta\beta$, Δc and Δ(b-y) were determined. This was done for i = 30°, 45°, 60° and 90°. The slopes of the relation between $V sin\ i$ and the colour excess derived for different values of i are given in Table III–5.

In figures III–8 and III–9 the theoretical slopes of the relation between $V sin\ i$ and the colour excess derived from the different planes for A3 to F0 stars together with the associated probable errors are plotted against 'i'. It can be noticed that for the A-stars, almost in all planes, the derived slopes are sensitive to i. In figures II–12 to II–16 the colour excesses for i=45 and i=60 (32 values each set) are plotted.

From the theoretical indices of Collins and Sonneborn corresponding to ω=0.9 and 0.2 for i=60°, the changes in different indices per 100 km s^{-1} of $V sin\ i$ were calculated. I have chosen i=60, since for a Maxwellian distribution this is the most representative value. This was repeated for all the spectral types.

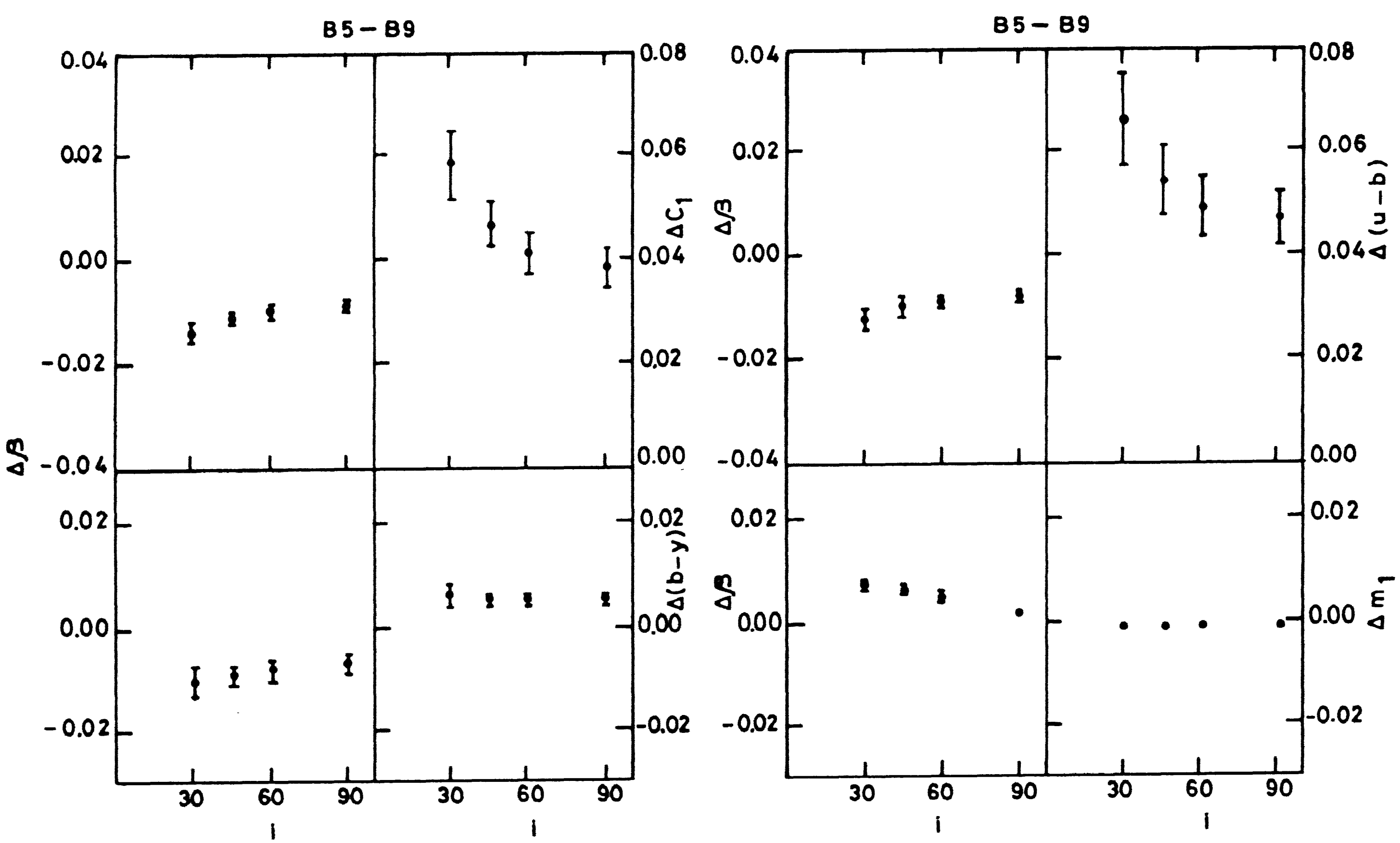

Fig III–4 : *The theoretical deviations for B5-B9 stars.* Δ_β *and* Δc_1 *from the* β, c_1 *plane (top left panel);* Δ_β, Δ*(b-y) from the* β, *(b-y) plane (bottom left panel);* Δ_β, Δ *(u-b) from the* β, *(u-b) plane (top right panel); and* Δ_β, Δm_1 *from the* β, m_1 *plane (bottom right panel). These slopes for 100 km* s^{-1} *of* $V \sin i$ *are shown as a function of* i.

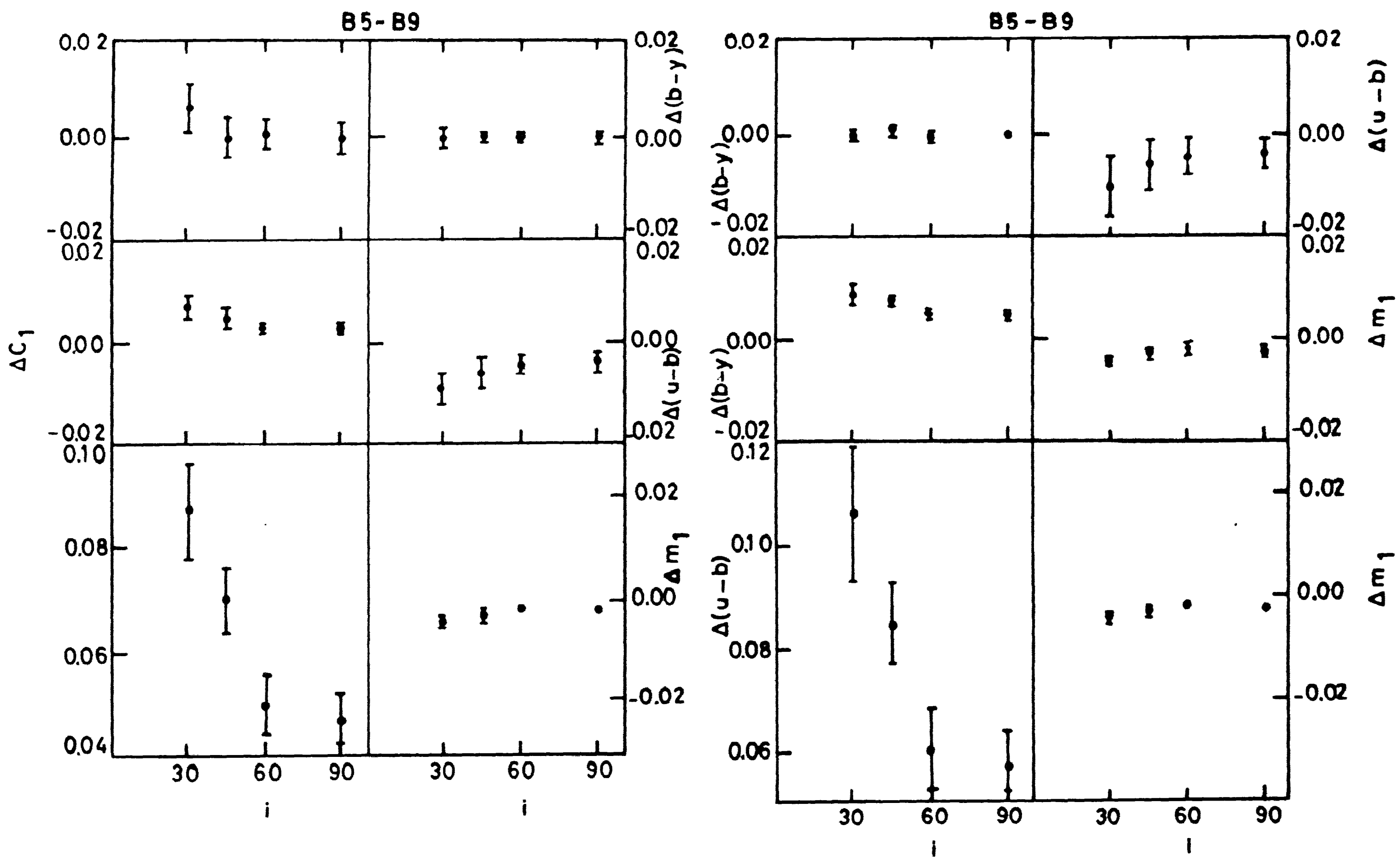

Fig III–5 : *Same as figure III-4 for c_1, (b-y); c_1, (u-b) and c_1, m_1 planes (left panel) and (b-y), (u-b); (b-y), m_1 and (u-b), m_1 planes (right panel). The derived slopes for 100 km s^{-1} from theoretical predictions are plotted against 'i'.*

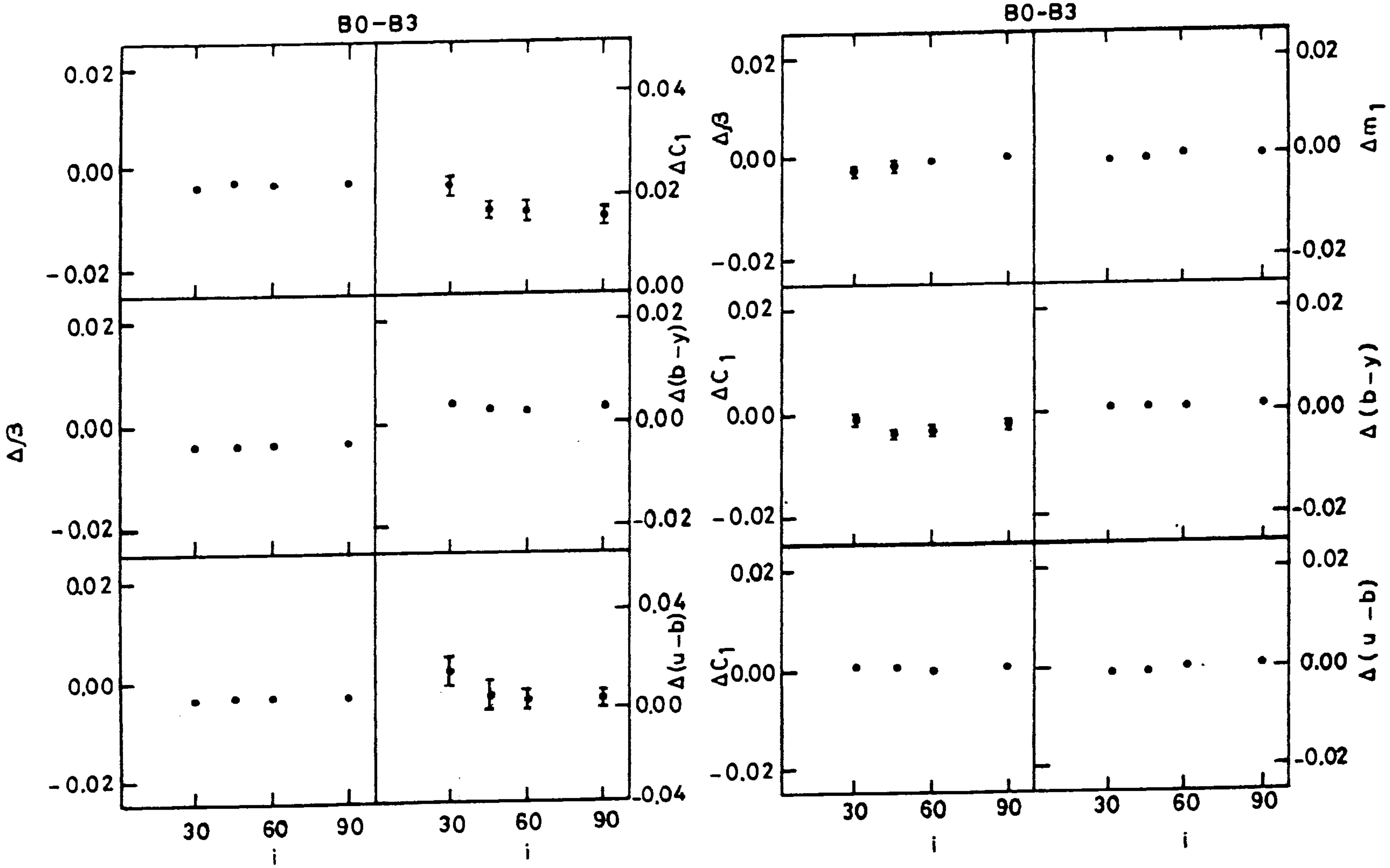

Fig III–6 : *Same as III–4 and III–5 for B0-B3 Stars*

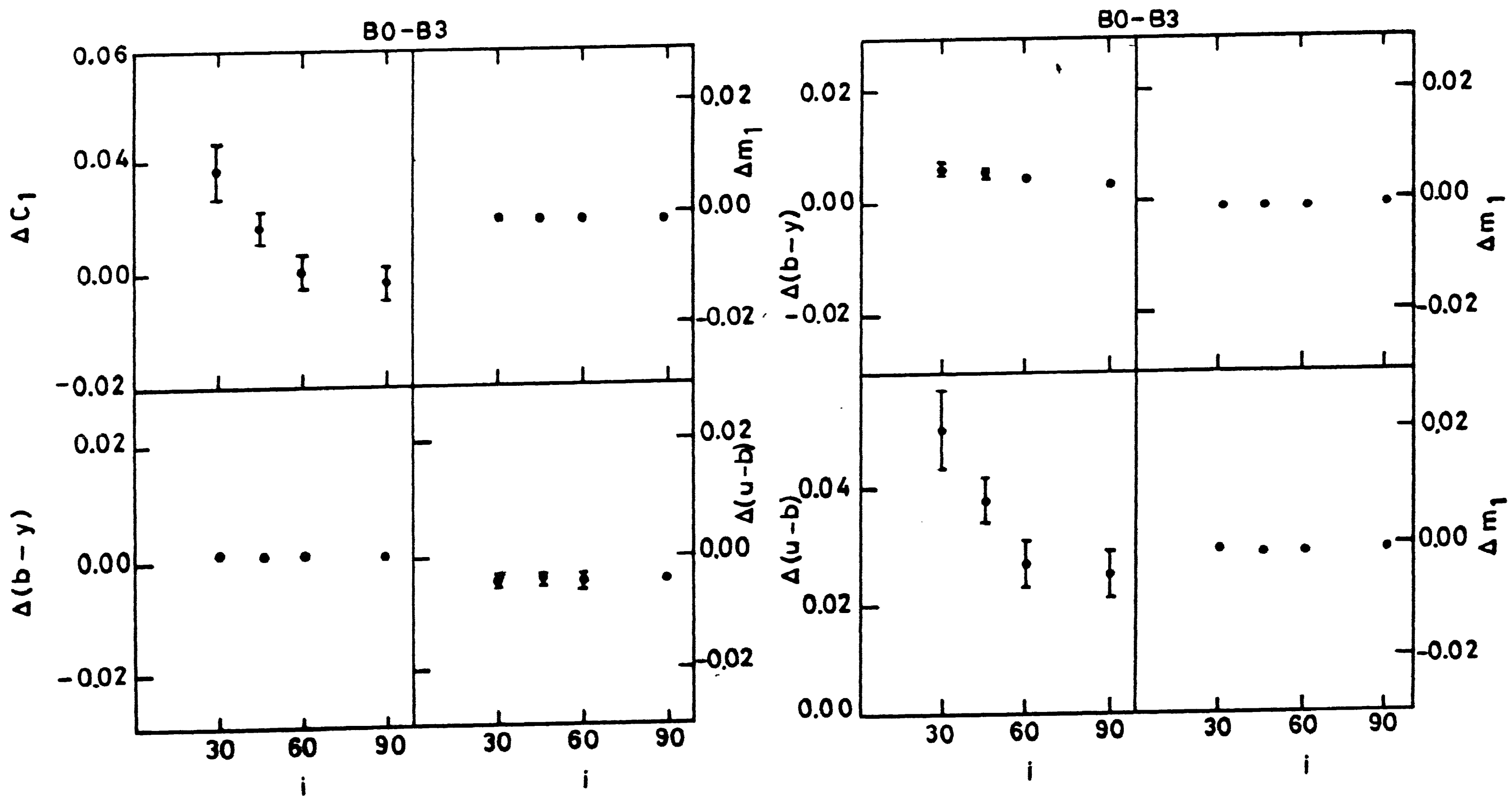

Fig III–7 : *Same as figures III–4 to III–6 for B0 to B3 Stars.*

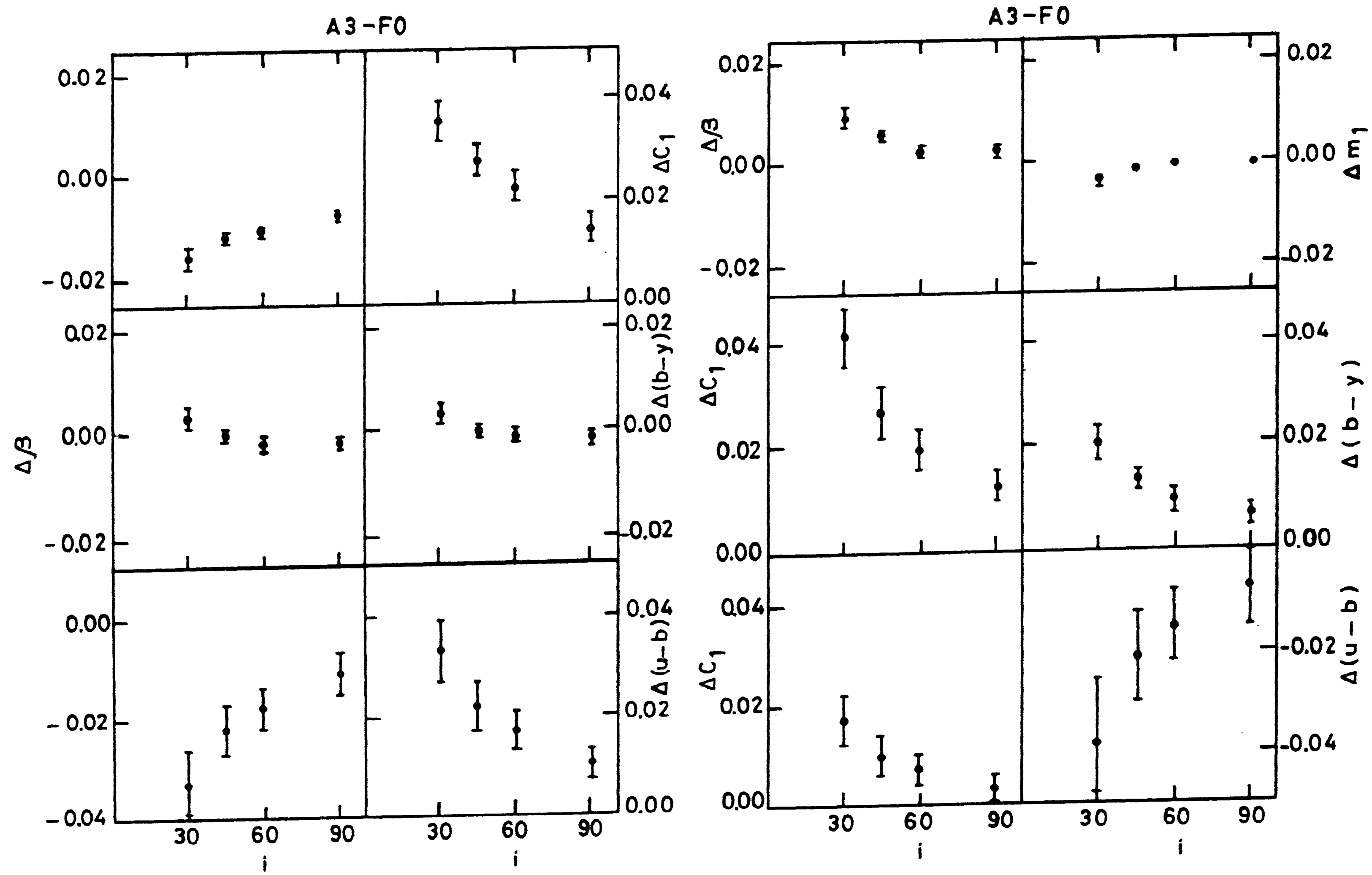

Fig III–8 : *Same as figures III–4 to III–7 for A3-F0 Stars.*

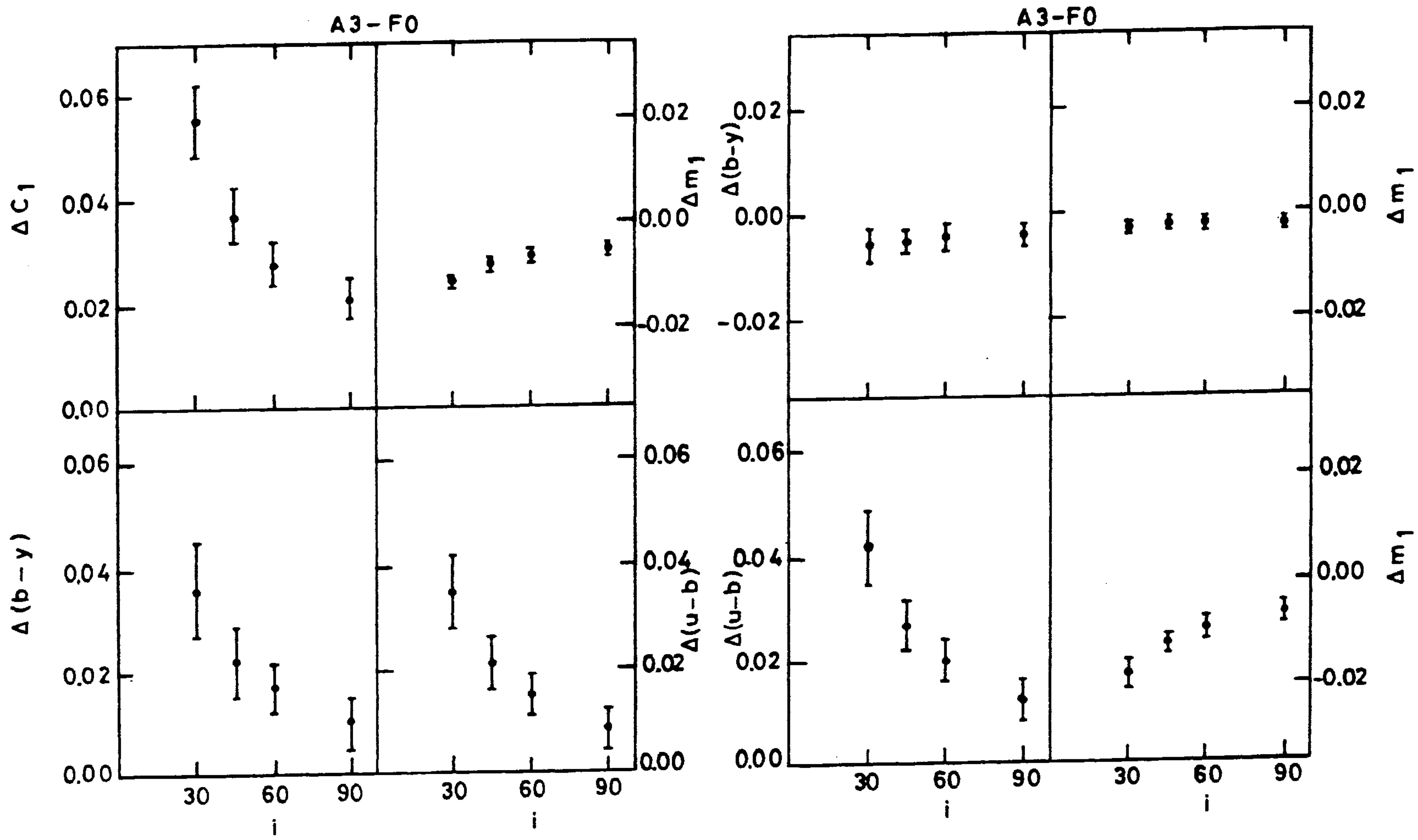

Fig III–9 : *Same as figures III–4 to III–8 for A3-F0 Stars.*

3. Discussion

3.1. The B-type Stars

Before analysing the available observational data for determining rotation effects, we first had to choose a homogeneous group of stars, at a common stage of evolution, with colours unaffected due to reasons other than rotation. However, the sample of such a group available is small in each cluster and further division by spectral type is not possible at this stage. Therefore a comparison with theoretical predictions at each spectral type is impossible except for B2 and B3 stars in Upper-Centaurus and Lower-Centaurus. Further, only projected rotational velocities can be derived from observations and 'i' remains unknown. Therefore B and A-type stars were analysed separately. However, we found that the predicted slope of rotation effect for various colour indices is strongly dependent on the mass of the star. The slope increases as we go from B0 to B9. Therefore, it was decided to subdivide the B-stars into two subgroups, namely B0 to B3 and B5 to B9.

For comparison with theoretical predictions for B5 to B9 stars, α-Persei Cluster is the best, as this cluster has the maximum number of B5 – B9 stars with known $V sin\ i$ values with least variable extinction. In α-Persei cluster out of the total 23 apparently normal main-sequence stars, 14 are in the spectral type range B5 to B9, 2 stars in the range B0 to B3 and 7 in the range A0 to A2. For comparison with theory the slopes of the relation between colour excess and $V sin\ i$ are tabulated for all the colours in all possible planes for different 'i' values together with the results for α-Persei B-type stars, in table III–3. These derived rotation effects are relative as both indices in any plane are affected by rotation. In β, c_1 plane the observed slope for α-Persei B stars for Δc_1 and $\Delta\beta$ are 0.045 $\pm$ 0.003 and -0.015 ± 0.001 magnitudes per 100 km s^{-1} of $V sin\ i$, respectively. This can be compared with the expected theoretical value for B5 to B9 stars. The slope for Δc_1 ranges from 0.038 $\pm$ 0.004 for i=90^o to 0.058 $\pm$ 0.007 for i=30^o and $\Delta\beta$ ranges from -0.009 ± 0.001 for i=90^o to -0.014 ± 0.002 for i=30^o. We have no specific reason to believe that the rotation axes in clusters are randomly distributed (Rajamohan 1978). Therefore, the observed value of 0.045 for the slope of Δc_1 and -0.015 for $\Delta\beta$, in the β, c plane can be deemed to be in excellent agreement with theoretical predictions of Collins & Sonneborn (1977). Similarly from β,(u-b) relation, in (u-b) and β the observed effects of 0.062 $\pm$ 0.005 and -0.013 ± 0.001 per 100 km s^{-1} of $V sin\ i$ are in agreement with the predicted values 0.047 $\pm$ 0.005 for i = 90^o and 0.066 $\pm$ 0.009 for i=30^o in (u-b) and -0.008 ± 0.001 for i=90^o and -0.012 ± 0.002 for i=30^o in β. Figs II–7 to II–11 also

Table III–3. Theoretical reddening due to rotation for 100 km s^{-1} of $V sin\ i$ for B5 to B9 stars

i	from β, c_1		from β,(b-y)		from β, (u-b)		from β,m_1		from c_1, (b-y)	
	$\Delta\beta$	Δc_1	$\Delta\beta$	Δ(b-y)	$\Delta\beta$	Δ(u-b)	$\Delta\beta$	Δm_1	Δc_1	Δ(b-y)
30	−.014	.058	−.010	.006	−.012	.066	.007	−.001	.006	.000
	±.002	±.007	±.003	±.002	±.002	±.009	±.001	±.000	±.005	±.002
45	−.011	.046	−.009	.005	−.010	.054	.006	−.001	.000	.000
	±.001	±.005	±.002	±.001	±.002	±.007	±.001	±.000	±.004	±.001
60	−.010	.041	−.008	.005	−.009	.049	.005	−.001	.001	.000
	±.001	±.004	±.002	±.001	±.001	±.006	±.001	±.000	±.003	±.001
90	−.009	.038	−.007	.005	−.008	.047	.002	−.000	.000	.000
	±.001	±.004	±.002	±.001	±.001	±.005	±.000	±.000	±.003	±.001
Observed reddening due to rotation for 100 km s^{-1} of $V sin\ i$ for α-Persei B stars										
α-Persei	−.015	.045	−.017	.010	−.013	.062	.007	−.002	−.013	.002
B stars	±.001	±.003	±.005	±.002	±.001	±.005	±.005	±.002	±.015	±.002

Theoretical reddening due to rotation for 100 km s^{-1} of $V sin\ i$ for B5 to B9 stars

i	from c_1, (u-b)		from c_1,m_1		from (b-y), (u-b)		from (b-y), m_1		from (u-b), m_1	
	Δc_1	Δ(u-b)	Δc_1	Δm_1	Δ(b-y)	Δ(u-b)	Δ(b-y)	Δm_1	Δ(u-b)	Δm_1
30	.007	−.009	.087	−.004	.000	−.010	.009	−.004	.106	−.004
	±.002	±.003	±.009	±.001	±.001	±.006	±.002	±.001	±.013	±.001
45	.005	−.006	.070	−.003	.001	−.006	.008	−.003	.085	−.003
	±.002	±.003	±.006	±.001	±.001	±.005	±.001	±.001	±.008	±.001
60	.003	−.004	.050	−.002	.000	−.004	.005	−.002	.060	−.002
	±.001	±.002	±.006	±.000	±.001	±.004	±.001	±.001	±.008	±.000
90	.003	−.004	.047	−.002	.000	−.004	.005	−.002	.057	−.002
	±.001	±.002	±.005	±.000	±.000	±.003	±.001	±.001	±.007	±.000
Observed reddening due to rotation for 100 km s^{-1} of $V sin\ i$ for B stars										
α-Persei	.005	−.009	.072	−.007	.003	−.024	.012	−.006	.096	−.006
B stars	±.002	±.004	±.015	±.001	±.002	±.019	±.004	±.002	±.022	±.001

Table III–4. Theoretical reddening due to rotation for 100 km s^{-1} of $V sin\ i$ for B0 to B3 stars

i	from β, c_1		from β,(b-y)		from β, (u-b)		from β,m_1		from c_1, (b-y)	
	$\Delta\beta$	Δc_1	$\Delta\beta$	Δ(b-y)	$\Delta\beta$	Δ(u-b)	$\Delta\beta$	Δm_1	Δc_1	Δ(b-y)
30	−.004 ±.000	.021 ±.002	−.004 ±.000	.004 ±.000	−.004 ±.000	.027 ±.003	.003 ±.001	−.001 ±.000	−.001 ±.001	.001 ±.000
45	−.003 ±.000	.016 ±.002	−.004 ±.000	.003 ±.000	−.003 ±.000	.022 ±.003	.002 ±.001	−.001 ±.000	−.004 ±.001	.001 ±.000
60	−.003 ±.000	.016 ±.002	−.004 ±.000	.003 ±.000	−.003 ±.000	.021 ±.002	.001 ±.000	.000 ±.000	−.003 ±.001	.001 ±.000
90	−.003 ±.000	.015 ±.002	−.003 ±.000	.003 ±.000	−.003 ±.000	.021 ±.002	.001 ±.000	−.000 ±.000	−002 ±.001	.001 ±.000
	Observed reddening due to rotation for 100 km s^{-1} of $V sin\ i$ for B0, B3 stars									
Upper-Cen+ Lower-cen B2, B3 stars	−.005 ±.002	.017 ±.006	−.004 ±.003	.000 ±.002	−.006 ±.001	.028 ±.006	−.002 ±.003	.001 ±.001	−.002 ±.009	−.001 ±.001

Theoretical reddening due to rotation for 100 km s^{-1} of $V sin\ i$ for B0, B3 stars

i	from c_1, (u-b)		from c_1,m_1		from (b-y), (u-b)		from (b-y), m_1		from (u-b) m_1	
	Δc_1	Δ(u-b)	Δc_1	Δm_1	Δ(b-y)	Δ(u-b)	Δ(b-y)	Δm_1	Δ(u-b)	Δm_1
30	.001 ±.000	−.001 ±.001	.038 ±.005	−.001 ±.000	.001 ±.000	−.004 ±.001	.006 ±.001	−.001 ±.000	.050 ±.007	−.001 ±.000
45	.001 ±.000	−.001 ±.001	.028 ±.003	−.001 ±.000	.001 ±.000	−.004 ±.001	.005 ±.001	−.001 ±.000	.038 ±.004	−.001 ±.000
60	.000 ±.000	.000 ±.000	.020 ±.003	.001 ±.000	.001 ±.000	−.004 ±.001	.004 ±.001	−.001 ±.000	.027 ±.004	−.001 ±.000
90	.000 ±.000	.000 ±.000	.018 ±.003	−.001 ±.000	.001 ±.000	−.004 ±.000	.003 ±.000	−.001 ±.001	.025 ±.004	−.001 ±.000
	Observed reddening due to rotation for 100 km s^{-1} of $V sin\ i$ for B2, B3 stars									
Upper-Cen Lower-cen B2, B3 stars	.000 ±.003	−.000 ±.004	.010 ±.013	−.001 ±.001	−.002 ±.001	−.001 ±.011	−.002 ±.003	.000 ±.002	.006 ±.017	−.001 ±.001

Table III–5. Theoretical reddening due to rotation for 100 km s^{-1} of $V sin\ i$ for A3 to F0 stars

i	from β, c_1 $\Delta\beta$	Δc_1	from β,(b-y) $\Delta\beta$	Δ(b-y)	from β, (u-b) $\Delta\beta$	Δ(u-b)	from β,m_1 $\Delta\beta$	Δm_1	from c_1, (b-y) Δc_1	Δ(b-y)
30	−.016	.035	.003	.003	−.003	.033	.009	−.004	.041	.020
	±.002	±.004	±.002	±.002	±.007	±.006	±.002	±.001	±.006	±.003
45	−.012	.027	.000	.000	−.022	.022	.005	−.002	.026	.013
	±.001	±.003	±.001	±.001	±.005	±.005	±.001	±.000	±.005	±.002
60	−.011	.022	−.002	−.001	−.018	.017	.003	−.001	.019	.009
	±.001	±.003	±.001	±.001	±.004	±.004	±.001	±.000	±.004	±.002
90	−.008	.016	−.002	−.002	−.011	.010	.002	−.001	.012	.006
	±.001	±.003	±.001	±.001	±.004	±.003	±.001	±.000	±.003	±.002

Observed reddeniinig due to rotation for 100 km s^{-1} of $V sin\ i$ for A-type stars

α-Persei	−.014	.030	−.013	.007	.012	.043	.068	−.016	.065	.019
	±.004	±.006	±.005	±.005	±.014	±.008	±.006	±.002	±.012	±.006
Pleiades	−.017	.039	−.012	−.013	−.015	.018	.041	−.011	.023	.008
	±.002	±.004	±.004	±.004	±.007	±.006	±.002	±.002	±.010	±.005
Hyades	−.015	.037	−.004	−.003	−.022	.026	.003	−.002	.028	.013
	±.002	±.006	±.003	±.003	±.005	±.006	±.003	±.002	±.006	±.003
Praesepe	−.015	.037	−.018	−.017	−.028	.022	.003	−.004	.035	.015
	±.003	±.006	±.002	±.002	±.004	±.004	±.003	±.002	±.005	±.002

Table III–5. (Continued). Theoretical reddening for 100 km s^{-1} of $V sin\ i$ for A3 to F0 stars

i	from c_1, (u-b) Δc_1	Δ(u-b)	from c_1,m_1 Δc_1	Δm_1	from (b-y), (u-b) Δ(b-y)	Δ(u-b)	from (b-y), m_1 Δ(b-y)	Δm_1	from (u-b) m_1 Δ(u-b)	Δm_1
30	−.038	.017	.055	−.011	.036	.035	−.006	−.003	.042	−.018
	±.013	±.005	±.007	±.001	±.009	±.007	±.003	±.001	±.007	±.003
45	−.021	.010	.037	−.008	.022	.021	−.005	−.002	.027	−.012
	±.009	±.004	±.005	±.001	±.007	±.005	±.002	±.001	±.005	±.002
60	−.015	.007	.028	−.006	.017	.015	−.004	−.002	.020	−.009
	±.007	±.003	±.004	±.001	±.005	±.004	±.002	±.001	±.004	±.002
90	−.007	.003	.021	−.005	.010	.008	− .004	−.002	.012	−.006
	±.007	±.003	±.004	±.001	±.005	±.004	±.002	±.001	±.004	±.002
	Observed reddening due to rotation for 100 km s^{-1} for A-type stars									
α-Persei	.038	.018	.145	−.010	−.013	.050	−.040	−.007	.065	−.006
	±.020	±.009	±.016	±.003	±.012	±.012	±.007	±.002	±.013	±.003
Pleiades	.059	−.014	.125	−.014	−.021	−.004	−.048	−.013	.029	−.008
	±.018	±.009	±.011	±.002	±.012	±.011	±.005	±.002	±.010	±.003
Hyades	.021	−.009	.017	−.007	−.016	−.029	.004	−.025	.021	−.014
	±.041	±.005	±.025	±.003	±.006	±.008	±.013	±.003	±.007	±.003
Praesepe	.066	−.030	.025	−.013	−.016	.000	−.011	−.016	−.002	−.003
	±.014	±.006	±.023	±.003	±.005	±.005	±.008	±.004	±.008	±.003

illustrate the agreement between observed and theoretical rotation effects in c_1, β,(u-b) and (b-y) for α-Persei B stars with theoretical predictions of Collins and Sonneborn.

To compare the observed results with the theoretical predictions for early B-type stars we have analysed the B2, B3 stars in Upper-Centaurus and Lower-Centaurus. Table III-4 gives the theoretical slopes of the relation between colour excess and $V sin\ i$ for all the colours in all possible planes for the different 'i' values for the B0 to B3 spectral types together with the observed results for B2, B3 stars in upper-Centaurus and lower-Centaurus. The observed slopes in Δc_1 is 0.017 $\pm$ 0.006 and in $\Delta\beta$ is -0.005 ± 0.002 in the β, c_1 plane. This is in good agreement with those predicted by theory for B0 to B3 stars. The values derived from Collins & Sonneborn (1977) predicted colour indices for B0 to B3 spectral types lead to a value for Δc_1 of 0.015 ± 0.002 for i=90^o and 0.021 $\pm$0.002 for i=30^o and for $\Delta\beta$ of -0.003 ± 0.000 for i=90^o and -0.004 ± 0.000 for i=30^o. Figs II–19 and II–20 also illustrate this. In general the observed results in all the colours from the different possible planes are in good agreement with predictions made from theory for B0 to B3 stars.

Rotation also affects the observed spectral types at a given mass. However, this effect is considerable only when the stars rotate close to their break-up speeds. Such objects have already been eliminated as most of them would appear as emission-lined objects. Only a few stars rotate near break-up limits (see also Collins & Sonneborn 1977). For the large majority of the stars in Table II–2 to II–15 this effect would not be more than one or two spectral subdivisions. The results in Table III–4 and III–5 should be highly representative for the observed spectral type groups given.

3.2. A-type Stars

The reddening for various colour indices derived for α-Persei, Pleiades, Hyades and Praesepe A-type stars together with that derived from theoretical colour indices predicted by Collins and Sonneborn (1977) are given in table III–5. In general the agreement between observation and theory is good. The figures II–12 to II–16 in Chapter II also illustrate the good agreement between observed results and theoretical predictions of Collins and Sonneborn, in c_1, β, (u-b), (b-y) and m_1 from β, c_1, β, (u-b), c_1, (b-y) and c_1, m_1 relationships. For A-type stars in c_1, (u-b); (b-y), m_1 and (u-b), (b-y) planes, the analysis following the procedures set up here was difficult. This is because of the problems in the non monotonic variation of (u-b) near the balmer maximum. In fact it is a bit surprising that in spite of the various uncertainties the agreement is excellent between observations and predictions of Collins & Sonneborn (1977) for rigidly rotating stars. We believe that this became possible because we eliminated all the scatter in the diagrams that would have been introduced by including double-lined binaries, emission-lined objects and highly peculiar objects. Further, by analysing each cluster separately we were able to eliminate most of the uncertainties that would have otherwise been introduced.

Gray & Garrison (1989) derived a higher slope for the effect in c_o for field F-type stars. They suggested that field F stars may be rotating differentially but that no firm conclusion can be drawn and that the different slopes derived may also be due to evolutionary effects. We find that differences in the evolutionary stage of the stars even on the main sequence will introduce a large scatter in the observed effect. This is amply demonstrated by the Scorpio-Centaurus association where we find that the two subgroups, if analysed together, produces a large scatter in the Δc_o, $V sin\ i$ and Δ(u-b)$_o$, $V sin\ i$ diagrams. Even though F stars have much longer main sequence life time than B-stars, evolutionary effects may be important for field F-stars.

When this work was almost completed, Collins, Traux & Cranmer (1991) published the results of extensive model atmosphere calculations applicable to rotating early-type stars. These indices were also analysed the same way as we did for Collins and Sonneborn (1977) models, and the results are shown in Table III–6. On an average the predicted theoretical rotation effects of the two models does not differ appreciably.

Table III–6. Theoretical reddening due to rotation for 100 km s^{-1} of $V sin\ i$ for B5 to B9 stars. (Derived from Collins, Truax and Cranmer 1991)

i	from $H_\beta,(u-b)$		from $H_\beta,(b-y)$		from $(u-b),(b-y)$	
	ΔH_β	$\Delta(u-b)$	ΔH_β	$\Delta(b-y)$	$\Delta(u-b)$	$\Delta(b-y)$
30	−.518	.059	−.513	.004	.003	.000
	±.062	±.006	±.142	±.001	±.009	±.001
45	−.518	.059	−.680	.005	−.018	.001
	±.070	±.007	±.167	±.001	±.010	±.001
60	−.652	.075	−1.012	.008	−.042	.003
	±.072	±.0C7	±.126	±.001	±.008	±.000
90	−.788	.093	−1.240	.010	−.055	.004
	±.070	±.007	±.122	±.001	±.007	±.001

IV. THE ZERO ROTATION MAIN SEQUENCE (ZRMS) OF SELECTED STAR CLUSTERS

As the distance scale of the universe is literally based on the observations of the nearby Hyades cluster, we first discuss the determination of the Hyades ZRMS. The observed colour indices are of course free of interstellar extinction for this cluster. We took two approaches to the determination of the ZRMS values for each cluster.

1a. ZRMS from observed slopes of rotation effects

In this approach, the observed rotation effects in different planes listed in Table II–17 were utilised to derive the ZRMS values as a function of β. This table does not reflect the true effects due to rotation as the slopes determined are relative. In these determinations two photometric quantities, say X versus Y are plotted and a polynomial fit is derived. The residuals ΔX in X at the observed value of Y and ΔY in Y at the observed value of X are plotted against $V sin\ i$ to determine the rotation effects. The observed effects are therefore relative and the true effects cannot be determined unless one of the quantities X or Y is independant of rotation, such as the mass of the star.

However, we can use the slope of the relationship between ΔX and $V sin\ i$ or ΔY and $V sin\ i$ to determine where the non rotating sequence actually lies. This can be done by shifting the observed points either in X or Y by an amount corresponding to its observed $V sin\ i$ value. Even though the shifted value for each star does not correspond to the appropriate ZRMS value for its mass, the locus of the shifted positions of all stars would define the ZRMS in that plane. This method should work as long as the relationship between X and Y is not highly non linear and also that ΔX and ΔY are not highly non linear with $V sin\ i$. The analysis of B and A stars independantly should partially take care of such non linearity in the relationship between different quantities. Also for ω up to 0.9 (V $\leq$ 250 km s^{-1}), the residuals can be expected to be linear (see Fig 17 of Collins & Harrington 1966 and Fig 5 of Collins & Smith 1985).

This was the logic followed for deriving the ZRMS values of different indices for each cluster from observationally determined slopes.

1b. ZRMS from theoretical predictions

We have established in Chapter II that rotation effects derived from analysis of observations are in excellent agreement with theoretical predictions of Collins & Sonneborn (1977). Hence one can in principle utilise the predicted effects to correct the observed data for each star to derive its ZRMS value. However the value of i, the inclination between the rotation axis and the line of sight remains unknown. But we can derive the average ZRMS curve statistically based on the assumption that i is close to 60^o as we have done in Chapter III where we compare observations with theory.

Collins & Sonneborn (1977) list the effects as a function of mass for various values of V and i. They have also given the other indices like $(b\text{-}y)_o$ etc as a function of mass. Collins & Smith (1985) have also listed the Zero Rotation Zero Age values as a function of mass for the A-stars. As the values in the latter paper appear to be more consistent with observations, we have combined the two tables appropriately to derive the theoretical zero age values of $(b\text{-}y)_o$. m_o and c_o as a function of mass.

The calculations of rotation effects by Collins & Sonneborn (1977) for the mass range 14.5 $M_\odot$ to 1.5 $M_\odot$ for ω=0.2 and ω=0.9 and i=60^o were used to produce a table of average corrections in β, c_1, (b-y), (u-b) and m_1 for 100 km s^{-1} of $Vsin\ i$. This is given in Table IV-1. The results from Collins & Smith (1985) were appropriately combined with those of Collins & Sonneborn (1977) paper to get the corresponding values of $(b\text{-}y)_o$ etc for the entire mass range. The table for rotation corrections in different indices were listed as a function of $(b\text{-}y)_o$ as the masses of stars are unknown. For A-stars the observed $(b\text{-}y)_o$ value was used to get the first set of corrections in (b-y), c_1, (u-b), m_1 and β. The corrected (b-y) was used to derive a second set of corrections in (b-y), c_1 etc. The average of these two sets was used to correct each and every star for its observed value of $Vsin\ i$. For B-stars, we followed the same procedure using the observed $(u\text{-}b)_o$ index instead of the $(b\text{-}y)_o$ index.

2. The ZRMS of Hyades

2.1. The ZRMS values of β and c_1

The observed rotation effects listed in Table II–17 were used to correct, β and c_1 in the β, c_1 plane. We denote these corrected indices as β_{ZR} and c_{1ZR} respectively.

Table IV–1. Average change in indices per 100 km s^{-1} of $V sin\ i$ (ω=0.9; i=60°)

$M/M_\odot$	(u-b)	(b-y)	δ(b-y)	δM_v	δ(u-b)	δc	δm_1	$\delta\beta$
14.5	−.200	−.150	.007	0.17	.044	.028	.001	.004
11.0	.030	−.118	.008	−.010	.068	.050	.001	.006
8.3	.210	−.098	.009	−.018	.087	.067	.001	.009
6.3	.390	−.078	.010	−.031	.115	.092	.002	.010
4.9	.620	−.059	.012	−.043	.154	.126	.003	.016
3.9	.810	−.045	.013	−.031	.181	145	.005	.024
3.3	.959	−.034	.017	.009	.191	.144	.007	.029
2.8	1.228	−.015	.026	.106	.178	.115	.006	.022
2.5	1.358	.005	.045	.270	.145	.024	−.006	−.015
2.3	1.433	.026	.050	.311	.057	−.019	−.012	−.031
2.1	1.445	.082	.056	.332	.019	−.055	−.018	−.044
1.9	1.402	.152	.073	.400	−.030	−.118	−.029	−.070
1.8	1.375	.177	.084	.313	−.093	−.181	−.040	−.090
1.7	1.345	208	.086	.227	−.114	−.203	−.042	−.088
1.5	1.308	.259	.076	.242	−.121	−206	−.033	−.082

As mentioned in the previous section we plot β_{ZR} versus c_1 and c_{1ZR} versus β. The locus of these two plots should coincide. These are shown in Fig IV–1a. A least square fit to the data points in Fig IV–1a was derived to determine the β_{ZR}, c_{1ZR} relationship for Hyades. We list these ZRMS values (at equal intervals of β) in Table IV-2. β is chosen as an independant parameter following Crawford as it is free of interstellar extinction. The range in β for which the ZRMS values are listed corresponds to the observed range of β in Hyades.

Similarly, following method 1b, we use the theoretical corrections listed in Table IV–1 to correct the individual stars in β and c_o. The corrected positions and the least square fit to the data points are shown in Fig IV–1b. The derived ZRMS values are given in Table IV–2.

The observed values of β and c_1 for all stars together with the ZRMS given in Column 1 and 4 of Table IV–2 are shown in Fig IV–1c. The Am stars are shown as filled circles, and the apparent normal single stars are plotted as open circles and the SB2's and VB's with $\Delta m < 2.0$ magnitudes as crosses.

2.2. The ZRMS values of (b-y)

From Table II–17 we see that in the β, (b-y) plane, the rotation effects are negligible while in the c_1, (b-y) plane, they are discernible. The first set of $(b\text{-}y)_{ZR}$ values was derived from a least square fit between β and (b-y). A second set was derived by correcting for rotation effects in the c_1, (b-y) plane following procedures already described in case of β, c_1. Now the $(b\text{-}y)_{ZR}$ values that correspond to β_{ZR} and c_{ZR} listed in Columns 1 and 4 of Table IV–2 were calculated. The $(b\text{-}y)_{ZR}$ values from both these methods were found to agree very well. The average of the two values is listed in Column 2 of Table IV–2.

The same values derived by using method 1b are listed in Column 7 of Table IV–2. The observed positions of stars together with the ZRMS derived from observed slopes in the β, (b-y) plane are shown in Fig IV–2a.

2.3. The ZRMS values of (u-b)

Following procedures set up for c_1 and (b-y), the $(u\text{-}b)_{ZR}$ values derived from observed effects (method 1a) are listed in Column 5 of Table IV–2 and those derived from theoretical expectations (method 1b) are listed in Column 10 of Table IV–2.

The β,(u-b) ZRMS curve together with the observed β, u-b values of the Hyades members is shown in Fig IV–2b.

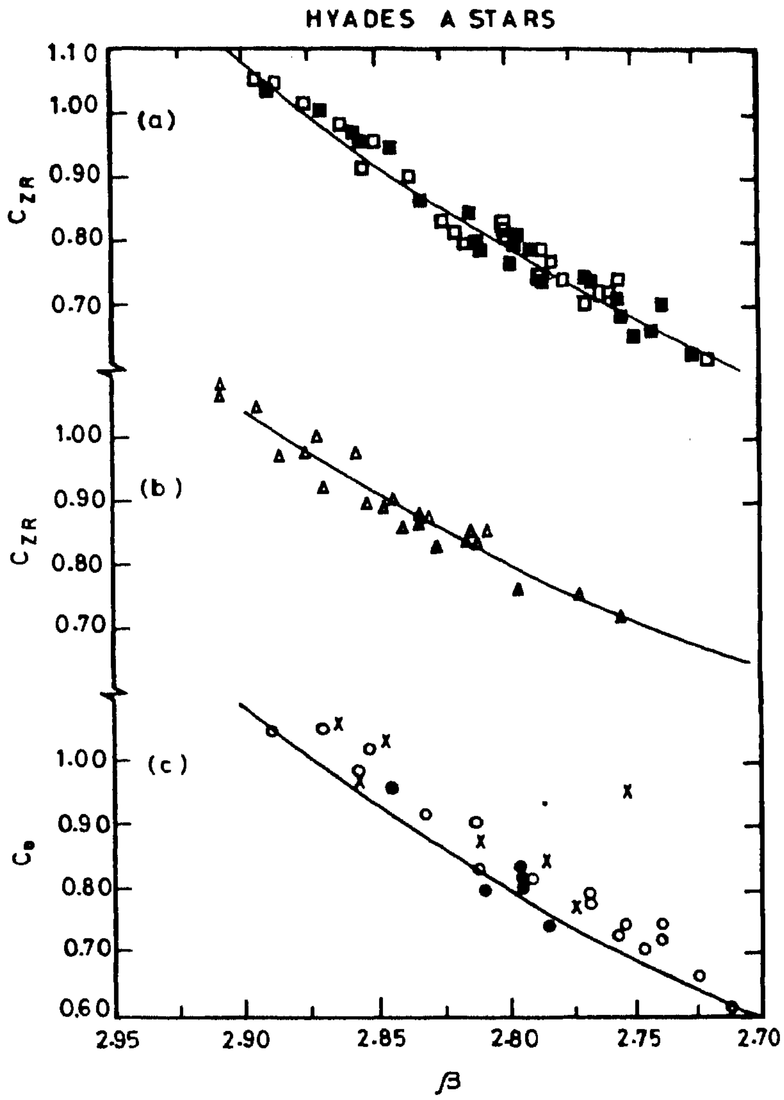

Fig IV–1 : *The ZRMS of Hyades cluster in the spectral type range A3-F0.*

(a) Corrected positions of stars in the c_1, β plane. Each star has been plotted twice; the observed c_1 value versus β corrected for rotation effect and the c_1 value corrected for rotation versus the observed β value have been plotted. The locus defined by the least-square fit to the data points which define the zero rotation values from observed slopes of rotation effects is shown by a continuous line.

(b) The c_o and β index independently corrected for rotation effects for each star is shown. The least-square fit is shown by the continuous line which defines the zero rotation values determined from theoretically derived slopes for $i=60^o$ from the work of Collins & Sonneborn (1977).

(c) The observed position of all stars have been plotted in the c_o, β plane. The continuous line is the ZRMS determined from (a).

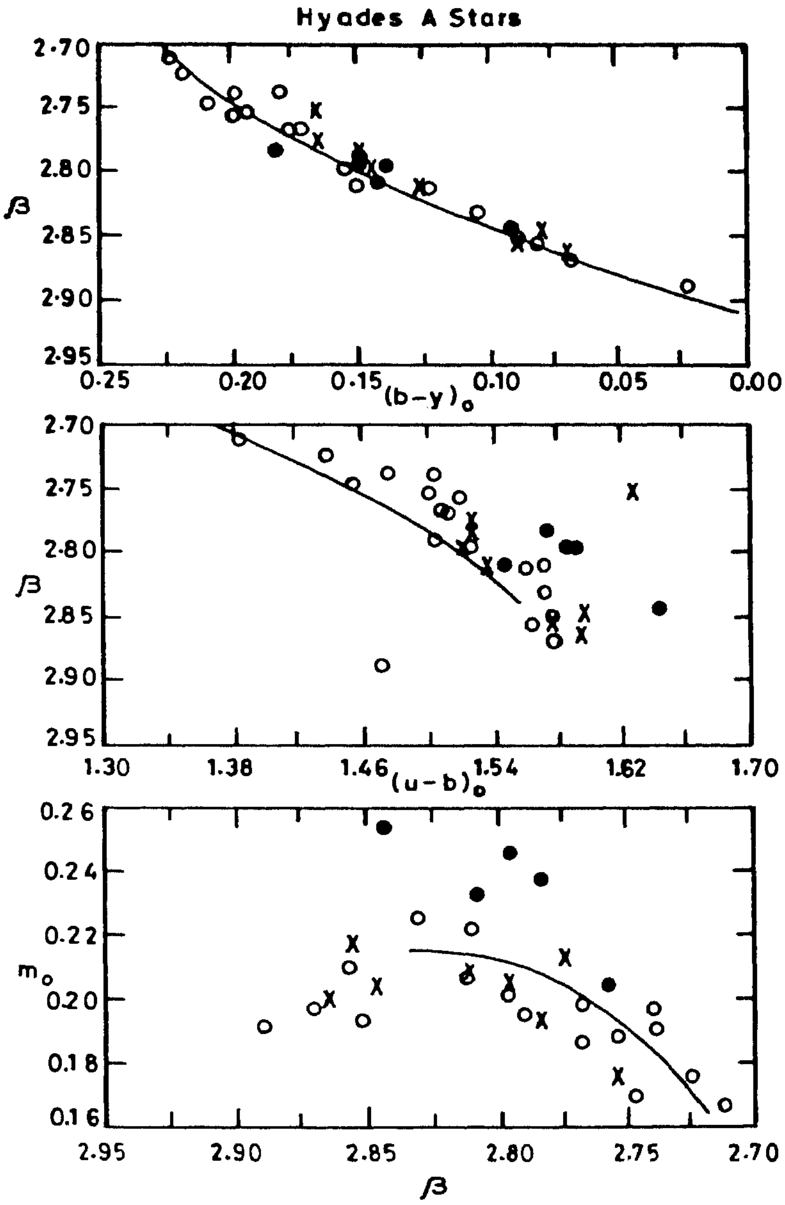

Fig IV–2 : *Same as Fig IV–c (a) The observed β, (b-y) values of Hyades stars are plotted. The ZRMS locus determined from observed slopes of rotation effects is shown as a continuous line. (b) & (c): Same as (a) in the β, (u-b) and β, m_1 planes.*

2.4. The ZRMS values of m_1

The ZRMS values of m_1 were calculated from the observed rotation effects in the β, m_1 plane and c_1, m_1 plane. The average value of m_{1ZR} thus derived was compared with the m_{1ZR} calculated from the c_{1ZR}, $(b\text{-}y)_{ZR}$ and $(u\text{-}b)_{ZR}$ derived in earlier sections. We find that for mid values of β in Table IV–2, the two agree while at the two ends of the β range, the differences were of the order of 0.02 magnitudes.

We also calculated m_1 using method 1b and found it agrees very well with m_1 calculated from (b-y), c_1, (u-b).

The observed values of β, m_1 and the observed β_{ZR}, m_{1ZR} relation for Hyades are shown in Fig IV–2c.

Table IV–2. Hyades

β	$(b\text{-}y)_o$	m_o	c_o	$(u\text{-}b)_o$	M_v	$(b\text{-}y)_o$	m_o	c_o	$(u\text{-}b)_o$
	Observational ZRMS					Theoretical ZRMS			
2.680	.236	.154	.552	1.332	5.518	.235	.099	.619	1.287
2.690	.231	.160	.569	1.351	5.595	.230	.111	.629	1.311
2.700	.226	.166	.586	1.370	5.659	.224	.123	.640	1.334
2.710	.221	.171	.603	1.387	5.710	.218	.134	.652	1.356
2.720	.215	.177	.622	1.406	5.748	.212	.144	.665	1.377
2.730	.208	.181	.641	1.419	5.773	.205	.154	.678	1.396
2.740	.201	.186	.661	1.435	5.785	.197	.164	.692	1.414
2.750	.194	.190	.682	1.450	5.784	.189	.172	.708	1.430
2.760	.186	.194	.703	1.463	5.770	.181	.180	.724	1.445
2.770	.177	.198	.726	1.476	5.744	.172	.187	.741	1.459
2.780	.168	.201	.749	1.487	5.704	.163	.193	.759	1.472
2.790	.159	.204	.772	1.498	5.651	.153	.200	.777	1.483
2.800	.149	.207	.797	1.509	5.586	.143	.204	.797	1.492
2.810	.138	.209	.822	1.516	5.508	.132	.210	.817	1.501
2.820	.127	.211	.848	1.524	5.416	.121	.214	.839	1.508
2.830	.115	.212	.875	1.529	5.312	.109	.217	.861	1.513
2.840	.103	.214	.902	1.536	5.195	.097	.220	.884	1.518
2.850	.090	.215	.930	1.540	5.065	.084	.222	.908	1.521
2.860	.077	.210	.959	1.533	4.922	.071	.223	.933	1.522
2.870	.062	.215	.989	1.543	4.766	.057	.225	.959	1.523
2.880	.048	.214	1.019	1.543	4.597	.043	.226	.985	1.522
2.890	.033	.213	1.050	1.542	4.415	.029	.224	1.013	1.519
2.900	.016	.212	1.082	1.538	4.221	.014	.223	1.041	1.515

3. The ZRMS of Praesepe

Procedures exactly similar to those followed for Hyades were used to determine the ZRMS of Praesepe. No interstellar extinction corrections are needed for this cluster either. The ZRMS derived from observed rotation effects (method 1a) is listed in Table IV–3. The ZRMS values derived from predicted effects from theory (method 1b) are also listed in Table IV–3 (columns 6 to 10). The ZRMS values derived from theory seem to give consistently larger values of all indices (at a given β) for the late A-stars. The different diagrams similar to those for Hyades, in the β, c_1 plane are displayed in Fig IV–3.

4. The ZRMS values of α-Persei and Pleiades

The B stars and A stars were treated separately for determining rotation effects. The methods followed are exactly similar to those for Hyades and Praesepe and we derived the ZRMS value from observed effects (method Ia) for B stars and A stars independently. The ZRMS values for the B stars in α-Persei are listed in Table IV–4 and for the A stars in Table IV–5. We had taken care always to check for the self consistency of the m_1 values derived.

The ZRMS values derived from predicted effects (method 1b) are listed in Table IV–4 for B stars and Table IV–5 for A stars. The ZRMS values derived from both the methods are found to agree very well with each other.

The ZRMS values are corrected for the average observed interstellar reddening. Extinction corrections are discussed in Section 6.1 where we discuss the derivation of the Zero Rotation Zero Age Main Sequence (ZRZAMS). In Figures IV–4 and IV–5 the different diagrams similar to those for Hyades in the β, c_1 plane are shown respectively for the B and A stars in α-Persei.

Procedures similar to those for α-Persei were followed for A-stars in Pleiades and the dereddened ZRMS values derived from observations (method 1a) and theory (method 1b) are listed in Table IV–6. Diagrams similar to those of α-Persei are displayed in Figs IV–6a,b,c for Pleiades A-stars. The theoretical ZRMS for the B stars in Pleiades are listed in Table IV–7. The ZRMS from observations (method Ia) was not calculated as pleiades contains a few single main sequence B-type stars.

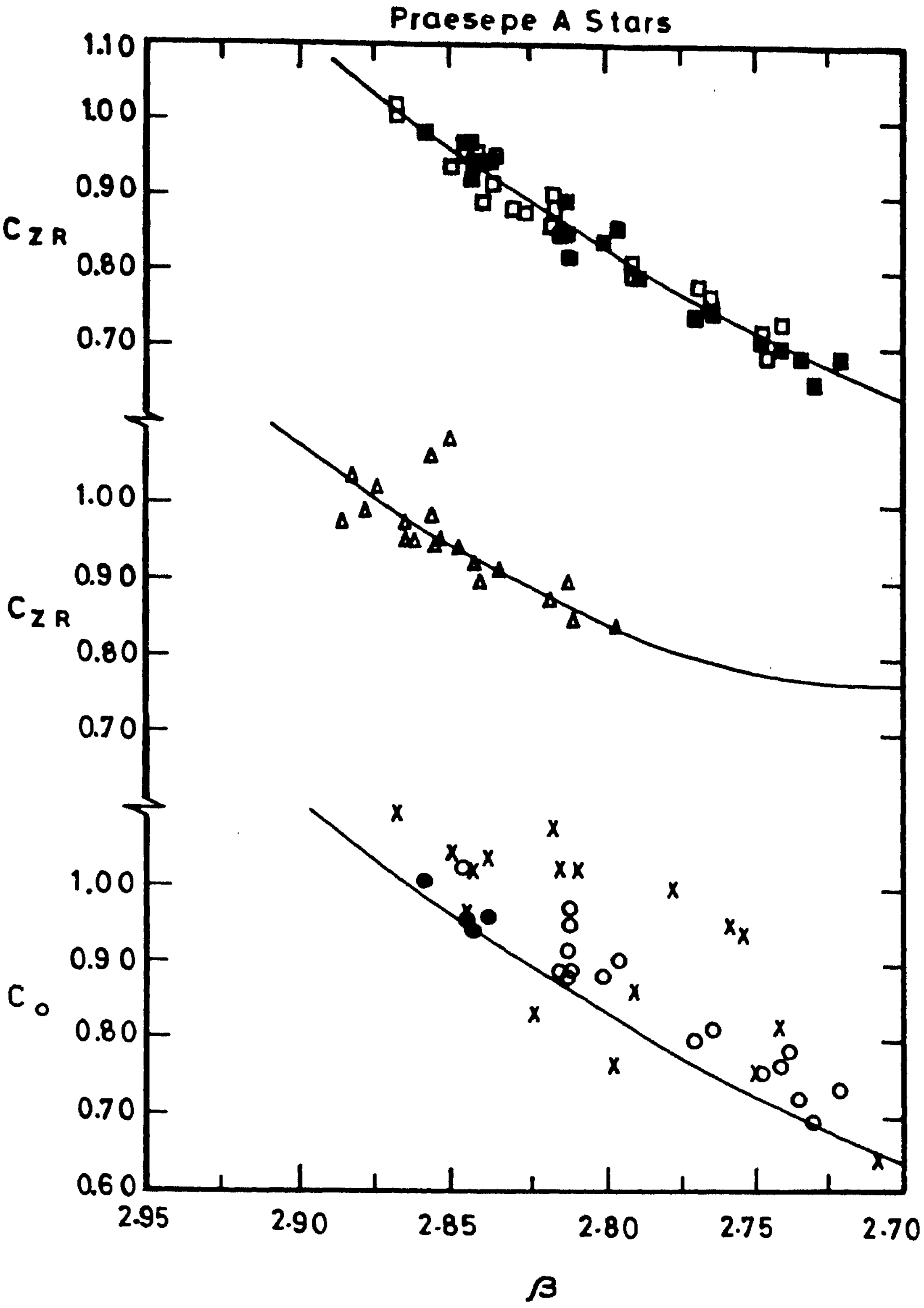

Fig IV–3 : *Same as Fig IV-1 for the Praesepe cluster. (a) ZRMS values of β and c_1 of Praesepe stars and the ZRMS curve from observed slopes of rotation effects. (b) ZRMS values of members and ZRMS curve from theoretical slopes of rotation effects. (c) Observed position of stars and the ZRMS curve from observed slopes of rotation effects.*

Table IV–3. Praesepe

β	$(b\text{-}y)_o$	m_o	c_o	$(u\text{-}b)_o$	M_v	$(b\text{-}y)_o$	m_o	c_o	$(u\text{-}b)_o$
	Observational ZRMS					Theoretical ZRMS			
2.680	.253	.148	.605	1.408	2.156	.261	−.018	.752	1.238
2.690	.245	.154	.619	1.418	2.287	.250	.013	.751	1.277
2.700	.236	.161	.633	1.428	2.400	.240	.041	.751	1.313
2.710	.227	.167	.649	1.438	2.494	.230	.067	.753	1.346
2.720	.218	.173	.665	1.448	2.570	.219	.091	.756	1.376
2.730	.208	.179	.683	1.457	2.628	.208	.113	.761	1.404
2.740	.199	.183	.701	1.466	2.667	.198	.133	.767	1.429
2.750	.189	.189	.720	1.475	2.688	.186	.152	.775	1.451
2.760	.179	.193	.740	1.484	2.690	.175	.167	.785	1.470
2.770	.170	.196	.761	1.493	2.674	.164	.182	.795	1.487
2.780	.161	.198	.782	1.501	2.639	.152	.194	.808	1.501
2.790	.151	.201	.805	1.509	2.587	.141	.204	.820	1.512
2.800	.141	.203	.828	1.517	2.515	.129	.212	.837	1.520
2.810	.131	.204	.853	1.524	2.425	.117	.218	.854	1.525
2.820	.122	.205	.878	1.532	2.317	.105	.223	.873	1.528
2.830	.113	.204	.904	1.539	2.191	.093	.225	.893	1.528
2.840	.103	.204	.931	1.546	2.046	.080	.225	.914	1.525
2.850	.095	.202	.959	1.553	1.882	.068	.223	.937	1.519
2.860	.086	.199	.988	1.559	1.701	.055	.219	.962	1.510
2.870	.077	.196	1.018	1.565	1.500	.042	.214	.988	1.499
2.880	.069	.192	1.048	1.571	1.282	.029	.206	1.016	1.485
2.890	.061	.187	1.080	1.577	1.045	.016	.195	1.045	1.468
2.900	.054	.181	1.112	1.583	0.789	.003	.184	1.075	1.449

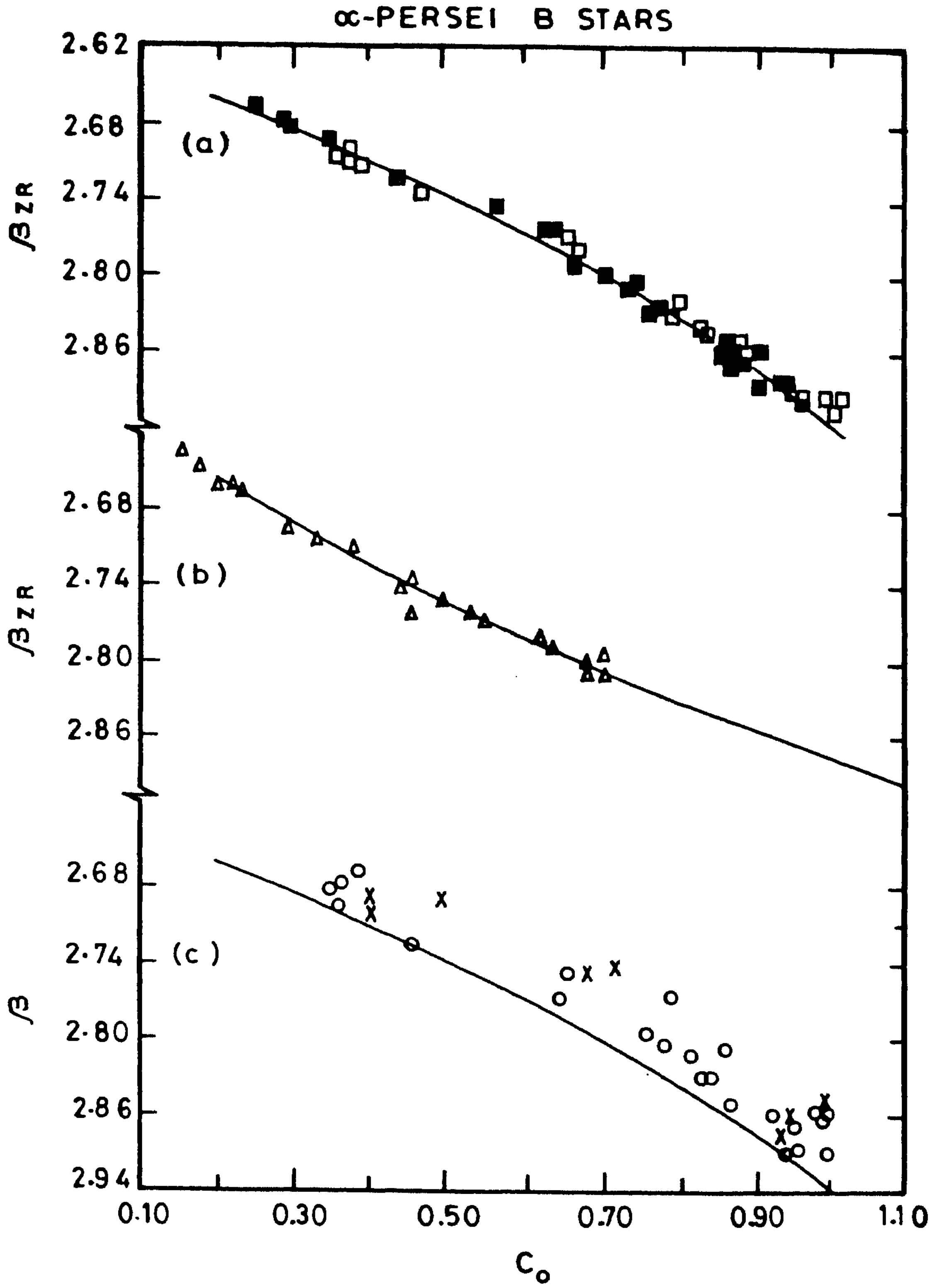

IV–4 : *Same as Figs IV–1 and IV–3 for α-Persei B-stars.*

Table IV–4. α-Persei B stars

β	$(b\text{-}y)_o$	m_o	c_o	$(u\text{-}b)_o$	M_v	$(b\text{-}y)_o$	m_o	c_o	$(u\text{-}b)_o$
	Observational ZRMS					Theoretical ZRMS			
2.660	−.090	.092	.192	.232	−.919	−.077	.092	.198	.228
2.670	−.089	.092	.233	.277	−.636	−.072	.092	.223	.262
2.680	−.087	.094	.273	.323	−.374	−.069	.093	.250	.297
2.690	−.087	.096	.312	.368	−.134	−.065	.094	.277	.334
2.700	−.085	.097	.350	.414	.086	−.061	.094	.306	.372
2.710	−.081	.099	.388	.459	.284	−.058	.096	.335	.412
2.720	−.079	.101	.424	.505	.460	−.054	.098	.366	.454
2.730	−.076	.103	.461	.550	.616	−.051	.100	.398	.497
2.740	−.071	.105	.496	.596	.750	−.048	.104	.431	.542
2.750	−.068	.107	.530	.641	.863	−.045	.107	.464	.588
2.760	−.064	.110	.564	.687	.954	−.043	.111	.499	.636
2.770	−.060	.111	.597	.732	1.024	−.040	.116	.535	.686
2.780	−.056	.114	.629	.777	1.073	−.037	.120	.572	.737
2.790	−.050	.117	.661	.823	1.101	−.035	.125	.610	.789
2.800	−.045	.119	.692	.868	1.107	−.033	.130	.649	.843
2.810	−.040	.122	.722	.914	1.092	−.031	.136	.689	.899
2.820	−.033	.125	.751	.959	1.056	−.029	.142	.730	.956
2.830	−.027	.127	.779	1.004		−.027	.148	.772	1.015
2.840	−.020	.132	.807	1.050		−.026	.156	.815	1.075
2.850	−.015	.134	.834	1.095		−.024	.163	.859	1.137
2.860	−.006	.138	.860	1.140		−.023	.171	.905	1.201
2.870	.001	.141	.886	1.185		−.022	.180	.951	1.266
2.880	.009	.145	.911	1.231		−.021	.188	.998	1.333
2.890	.018	.149	.935	1.276		−.020	.197	1.047	1.401
2.900	.027	.152	.958	1.321		−.019	.206	1.096	1.471
2.910	.035	.156	.980	1.366		−.019	.217	1.146	1.542
2.920	.045	.160	1.002	1.412					

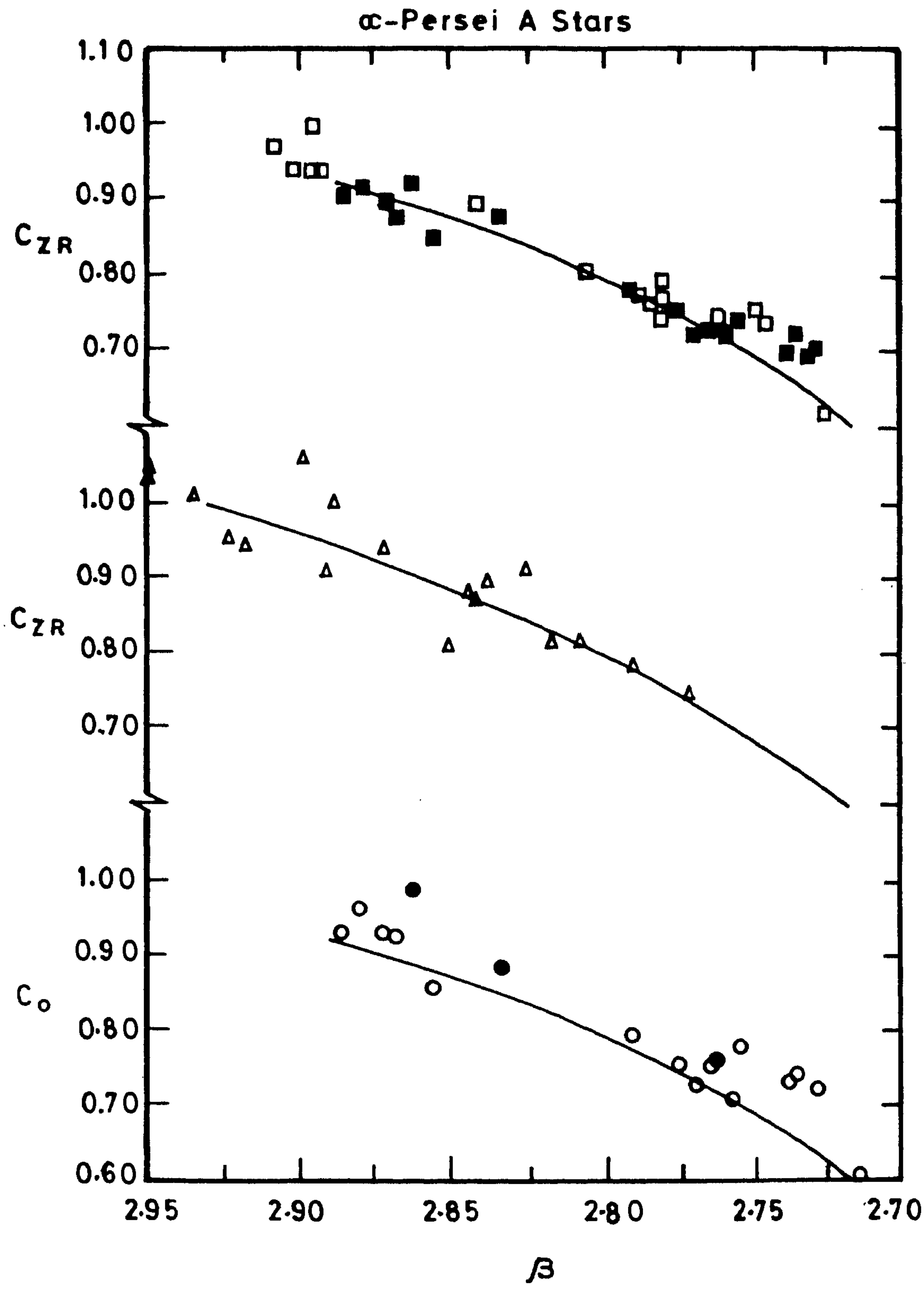

Fig IV–5 : *Same as Figs IV-1 and IV-3 for α-Persei A stars.*

Table IV–5. α-Persei A stars

β	$(b\text{-}y)_o$	m_o	c_o	$(u\text{-}b)_o$	M_v	$(b\text{-}y)_o$	m_o	c_o	$(u\text{-}b)_o$
	Observational ZRMS					Theoretical ZRMS			
2.650	.298	.151	.387	1.285	3.720	.304	.143	.389	1.283
2.660	.288	.150	.423	1.298	3.627	.291	.149	.421	1.301
2.670	.278	.149	.457	1.311	3.537	.278	.155	.453	1.319
2.680	.268	.149	.490	1.324	3.449	.266	.160	.484	1.336
2.690	.258	.149	.522	1.336	3.363	.254	.165	.514	1.353
2.700	.248	.150	.553	1.348	3.280	.242	.170	.544	1.368
2.710	.239	.150	.583	1.360	3.199	.230	.175	.572	1.383
2.720	.229	.151	.611	1.371	3.120	.219	.180	.600	1.397
2.730	.219	.152	.639	1.381	3.044	.208	.183	.627	1.410
2.740	.210	.153	.665	1.391	2.970	.197	.188	.653	1.423
2.750	.200	.156	.690	1.401	2.898	.186	.191	.679	1.434
2.760	.191	.157	.714	1.410	2.829	.176	.195	.703	1.445
2.770	.182	.159	.737	1.419	2.762	.166	.198	.727	1.455
2.780	.172	.163	.758	1.427	2.697	.156	.201	.750	1.464
2.790	.163	.165	.779	1.435	2.635	.146	.205	.772	1.473
2.800	.154	.168	.798	1.442	2.575	.137	.207	.793	1.481
2.810	.145	.172	.816	1.449	2.517	.128	.210	.813	1.488
2.820	.136	.175	.833	1.455	2.462	.119	.212	.833	1.494
2.830	.127	.179	.849	1.461	2.407	.111	.213	.852	1.499
2.840	.118	.184	.864	1.467	2.357	.102	.215	.870	1.504
2.850	.110	.188	.877	1.472	2.310	.094	.216	.887	1.507
2.860	.101	.193	.890	1.477	2.265	.086	.217	.904	1.510
2.870	.092	.198	.901	1.481	2.221	.079	.217	.919	1.512
2.880	.084	.203	.911	1.485	2.180	.072	.218	.934	1.514
2.890	.075	.209	.920	1.488	2.141	.065	.218	.948	1.515

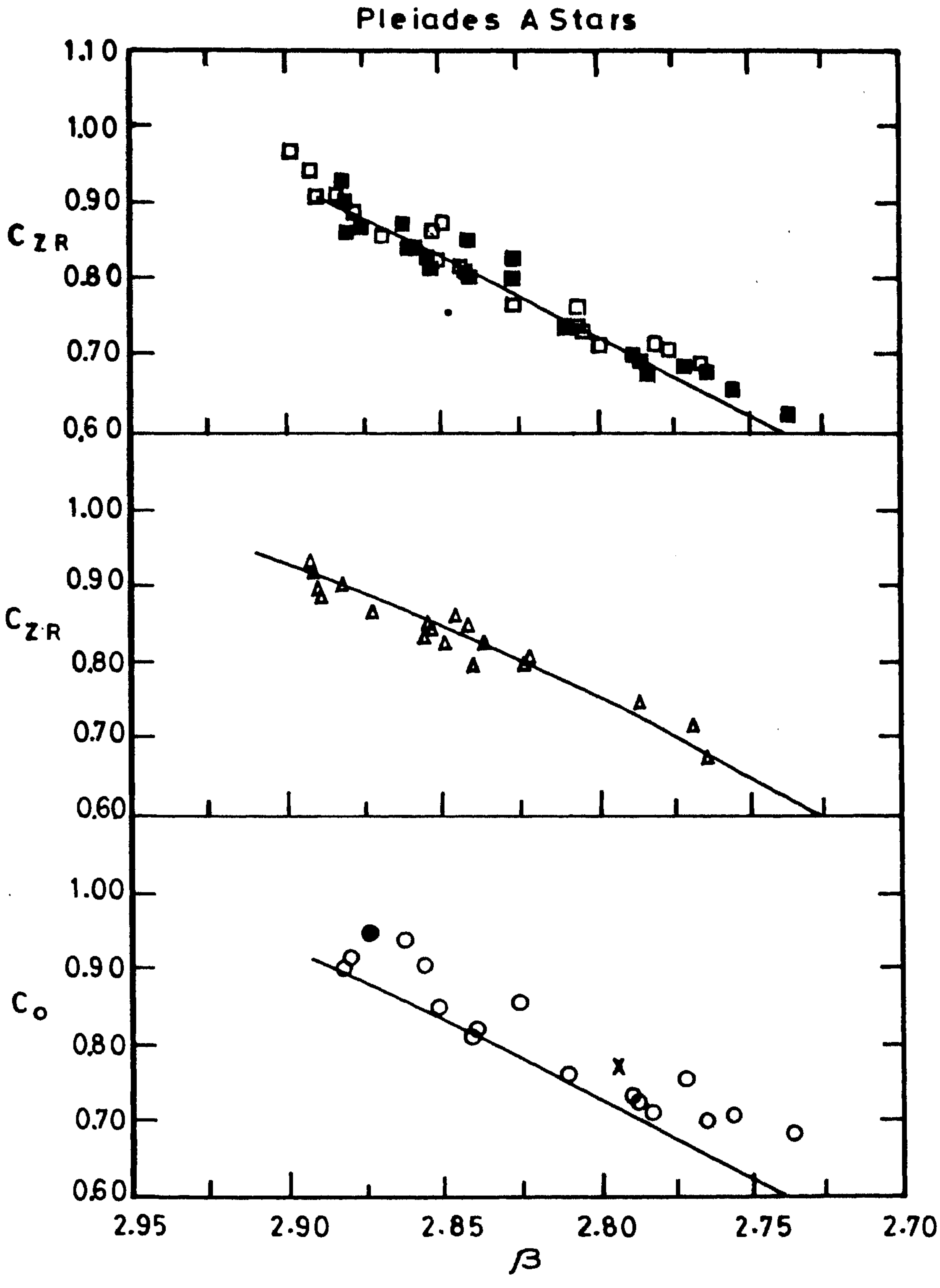

Fig IV–6 : *Same as Figs IV-1 and IV-3 for Pleiades A-stars.*

Table IV–6. Pleiades A stars

β	$(b-y)_o$	m_o	c_o	$(u-b)_o$	M_v	$(b-y)_o$	m_o	c_o	$(u-b)_o$
	Observational ZRMS					Theoretical ZRMS			
2.680	.253	.172	.467	1.318	3.824	.225	.149	.484	1.231
2.690	.244	.175	.490	1.329	3.687	.218	.158	.508	1.261
2.700	.235	.177	.512	1.337	3.555	.211	.167	.532	1.289
2.710	.226	.180	.534	1.347	3.429	.205	.174	.556	1.315
2.720	.217	.183	.556	1.357	3.308	.198	.182	.579	1.339
2.730	.208	.186	.578	1.367	3.192	.191	.189	.601	1.361
2.740	.199	.189	.600	1.377	3.081	.184	.195	.624	1.381
2.750	.190	.191	.621	1.384	2.976	.176	.200	.646	1.399
2.760	.180	.194	.643	1.392	2.876	.169	.204	.667	1.414
2.770	.171	.197	.664	1.401	2.781	.162	.208	.688	1.427
2.780	.162	.200	.685	1.410	2.691	.154	.211	.709	1.439
2.790	.152	.203	.706	1.417	2.607	.147	.212	.730	1.448
2.800	.142	.206	.727	1.424	2.528	.139	.214	.749	1.455
2.810	.133	.209	.748	1.433	2.455	.131	.214	.769	1.459
2.820	.123	.213	.768	1.441	2.386	.123	.214	.788	1.462
2.830	.113	.216	.789	1.448	2.323	.115	.213	.807	1.463
2.840	.103	.219	.809	1.454	2.265	.107	.211	.825	1.461
2.850	.093	.222	.829	1.460	2.213	.099	.208	.843	1.457
2.860	.082	.225	.849	1.464	2.166	.090	.205	.861	1.451
2.870	.072	.229	.869	1.472	2.124	.082	.200	.878	1.443
2.880	.062	.232	.888	1.477	2.087	.073	.196	.894	1.433
2.890	.051	.235	.908	1.481	2.056	.064	.191	.911	1.421

Table IV–7. Pleiades B stars

β	M_v	$(b\text{-}y)_o$	m_o	c_o	$(u\text{-}b)_o$
		Theoretical ZRMS			
2.640	−1.046	−.111	.103	.258	.242
2.650	−.876	−.107	.101	.276	.265
2.660	−.711	−.103	.100	.294	.289
2.670	−.550	−.099	.101	.312	.315
2.680	−.394	−.095	.101	.332	.343
2.690	−.243	−.091	.101	.351	.371
2.700	−.096	−.087	.102	.372	.401
2.710	.046	−.083	.102	.393	.432
2.720	.184	−.079	.105	.414	.465
2.730	.317	−.076	.107	.436	.499
2.740	.445	−.072	.110	.458	.534
2.750	.569	−.068	.113	.481	.571
2.760	.688	−.064	.116	.504	.608
2.770	.803	−.061	.121	.528	.648
2.780	.913	−.057	.125	.552	.688
2.790	1.019	−.053	.129	.577	.730
2.800	1.120	−.050	.135	.603	.773
2.810	1.216	−.046	.140	.629	.818
2.820	1.308	−.043	.147	.655	.864
2.830	1.395	−.039	.153	.682	.911
2.840	1.478	−.036	.160	.710	.959
2.850	1.556	−.032	.167	.738	1.009
2.860	1.629	−.029	.176	.766	1.060
2.870	1.698	−.025	.184	.795	1.113
2.880	1.762	−.022	.193	.825	1.167
2.890	1.822	−.019	.202	.855	1.222
2.900	1.877	−.015	.212	.885	1.278
2.910	1.928	−.012	.222	.916	1.336

5. The ZRMS of the Scorpio-Centaurus association & IC 4665

As the upper Scorpius sub-group is known to have highly variable reddening due to interstellar extinction, we decided to consider only the two other subgroups of this association for the derivation of ZRMS values. The lower Centaurus and upper Centaurus subgroups consist mainly of B2 and B3 main sequence stars which gave us opportunity of deriving accurate rotational effects for this mass range (see Chapter II).

The ZRMS values derived from observations and theory (methods 1a and 1b) for these two subgroups are listed in Table IV–8. The extinction for this subgroup appears to be extremely small (Glaspey 1971) and therefore needs no correction.

The (dereddened) ZRMS values derived for B-stars of IC 4665 from observed slopes and theory are given in Table IV–9.

Table IV–8. Lower-Cen + Upper-Cen B2, B3 stars

β	$(b-y)_o$	m_o	c_o	$(u-b)_o$	M_v	$(b-y)_o$	m_o	c_o	$(u-b)_o$
	Observational ZRMS					Theoretical ZRMS			
2.600	−.118	.065	−.020	−.125	−3.040	−.122	.081	−.029	−.111
2.610	−.114	.069	.014	−.077	−2.882	−.118	.084	.005	−.063
2.620	−.109	.070	.048	−.029	−2.706	−.115	.088	.037	−.017
2.630	−.105	.073	.081	.018	−2.512	−.111	.091	.067	.027
2.640	−.101	.077	.114	.066	−2.301	−.107	.095	.094	.070
2.650	−.097	.080	.147	.113	−2.071	−.103	.099	.120	.112
2.660	−.093	.084	.179	.160	−1.824	−.099	.104	.143	.152
2.670	−.089	.087	.211	.207	−1.560	−.095	.107	.165	.190
2.680	−.085	.091	.242	.253	−1.277	−.092	.113	.184	.227
2.690	−.082	.095	.273	.300	−.977	−.088	.119	.201	.263
2.700	−.078	.099	.304	.346	−.660	−.084	.125	.216	.297
2.710	−.075	.104	.334	.392	−.324	−.080	.131	.228	.329

Table IV–9. IC 4665 B Stars

β	$(b-y)_o$	m_o	c_o	$(u-b)_o$	M_v	$(b-y)_o$	m_o	c_o	$(u-b)_o$
	Observational ZRMS					Theoretical ZRMS			
2.680	−.050	.075	.251	.302	−.768	−.050	.076	.309	.361
2.690	−.057	.079	.287	.332	−.736	−.057	.080	.341	.387
2.700	−.063	.083	.323	.365	−.697	−.063	.083	.374	.414
2.710	−.069	.089	.358	.399	−.651	−.069	.088	.406	.444
2.720	−.072	.093	.392	.434	−.598	−.072	.091	.439	.477
2.730	−.075	.097	.426	.472	−.538	−.075	.095	.471	.511
2.740	−.077	.102	.460	.511	−.471	−.077	.100	.503	.549
2.750	−.077	.106	.493	.552	−.397	−.077	.104	.535	.588
2.760	−.076	.110	.526	.595	−.315	−.076	.108	.566	.630
2.770	−.074	.114	.558	.639	−.227	−.074	.112	.598	.674
2.780	−.070	.118	.590	.686	−.132	−.070	.116	.630	.721
2.790	−.065	.120	.622	.733	−.029	−.065	.120	.661	.770
2.800	−.060	.124	.653	.783	.080	−.060	.125	.692	.822
2.810	−.052	.128	.683	.835	.196	−.052	.128	.723	.875
2.820	−.044	.130	.714	.888	.320	−.044	.133	.754	.932
2.830	−.035	.134	.744	.943	.450	−.035	.138	.785	.990
2.840	−.024	.136	.773	.999	.588	−.024	.142	.816	1.051
2.850	−.012	.139	.802	1.058	.732	−.012	.147	.846	1.115
2.860	.001	.142	.830	1.118	.884	.001	.152	.876	1.181
2.870	.016	.144	.858	1.179	1.042	.016	.155	.907	1.249
2.880	.032	.146	.886	1.243	1.208	.032	.159	.937	1.319
2.890	.049	.148	.913	1.308	1.381	.049	.164	.967	1.392
2.900	.067	.150	.940	1.375	1.560	.067	.178	.997	1.486

6. The ZRZAMS

6.1. Interstellar Reddening

As both rotation and interstellar extinction redden the stars, we decided to check the E(b-y) values given in the literature for various clusters.

For the A-stars, β and (b-y) are linearly related as both are functions of effective temperature. Crawford (1977) finds a slight dependence of this relationship on δc_1 and δm_1 terms. The δc_1 term refers to reddening due to evolution and δm_1 the differences in line blanketting with respect to Hyades values. The largest correction involved due to blanketting differences is of the order of 0.02 magnitudes only. The δc_1 term would be zero for unevolved members.

Rotation does not produce a shift away from the β, (b-y) relation whereas extinction would shift the entire sequence along the (b-y) axis only. Hence mean extinction values derived from A-stars in the β, (b-y) plane should be independant of rotation effects.

Table IV–10. E(b-y) & Distance Modulus for clusters

Cluster	E(b-y)	m-M	Cluster	E(b-y)	m-M
Hyades		3.2	NGC 2422	0.06	8.01
Praesepe	<0.01	6.1	Coma		4.5
α-Persei	0.07	6.1	IC 2602	0.021	5.94
Pleiades	0.04	5.54	Cep OB3	0.6	9.3
Sco-Cen		6.0	NGC 2287	0.018	9.10
IC 4665	0.14	7.5	NGC 6475	0.067	7.02
NGC 2516	0.088	8.01	NGC 2244	0.34	10.96
IC 4756	0.161	8.05	h & χ-Persei	0.41	11.8
NGC 2264	0.057	9.5	NGC 4755	0.28	11.4
IC 2391	0.000	5.90	NGC 6025	0.110	9.40

We plotted the ZRMS values of β and (b-y) for various clusters and estimated their relative shift along the (b-y) axis with respect to the Hyades relation. The E(b-y) values derived by us for a few selected clusters were compared with the values quoted in the original papers. The agreement between the two estimates was found to be good excepting for α-Persei where we find our estimate to be smaller by about 0.03 magnitudes. For all the clusters the E(b-y) taken from literature was used for extinction corrections excepting for α-persei for which we use a value of 0.045 instead of the value 0.07 given by Crawford and Barns (1974). In Table IV–10, we list the E(b-y) values and distance moduli of various clusters taken from the original literature listed in Table II–1

6.2. Absolute magnitudes

The distance moduli of the clusters used for deriving the ZRZAMS are also listed in Table IV–10. These have been taken from the references listed in Table II–1. The absolute magnitudes and dereddened colours for all stars were derived using the following relationship (Stromgren 1966).

$$\begin{aligned} E(b-y) &= 0.70E(B-V) \\ E(m_1) &= -0.18E(b-y) \\ E(c_1) &= 0.20E(b-y) \\ E(u-b) &= 1.84E(b-y) \\ A_v &= 4.57E(b-y). \end{aligned}$$

The ZRMS values listed in this chapter have all been corrected for average extinction using the above relationship.

6.3. The ZRZAMS : from observed slopes of rotation effects

The ZRMS values of various indices as a function of β derived for different clusters were all supperposed to derive the mean ZRZAMS for B and A stars separately. In Fig IV–7 we show in the β, c plane the ZRMS curves for B stars of α-Persei, Upper Centaurus and IC 4665. Similar diagram for the A stars is shown in Fig IV–8 where the values for α-Persei, Pleiades, Hyades and Praesepe are plotted. ZRMS values for the B and A stars are plotted in the β, (b-y), and β, (u-b) planes respectively in Figures IV–9 and IV–10. Preliminary ZRZAMS values derived from this set of clusters are listed in Table IV–11 and IV–12 for B and A stars respectively. We expect that this would be highly representative of the true

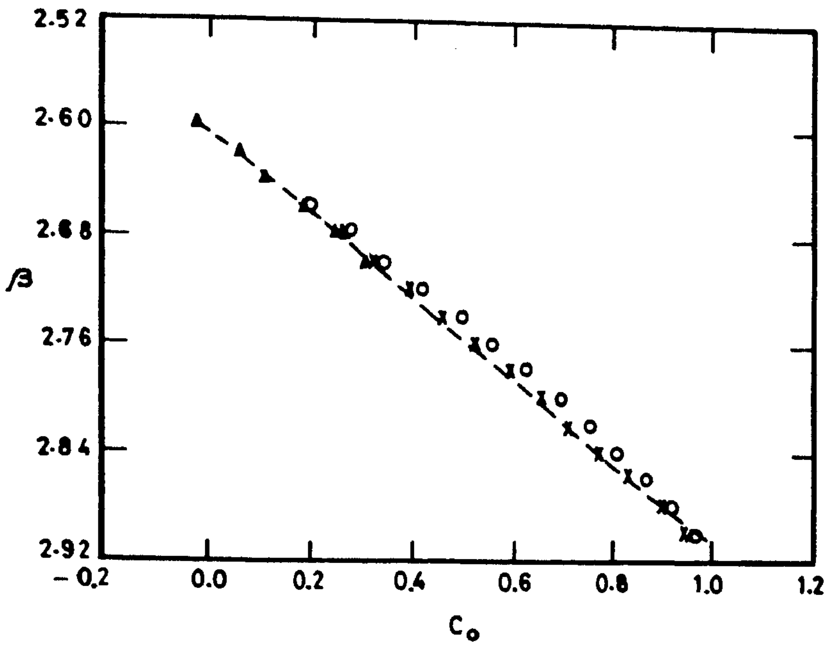

Fig IV–7 : *The ZRMS curves in the β, c_o plane determined from observed rotational effects for α-Persei B stars, Lower & Upper Centaurus B2, B3 stars and IC 4665 B-stars are shown. The adopted ZRZAMS values of c_o as a function of β are shown by a dotted line.*

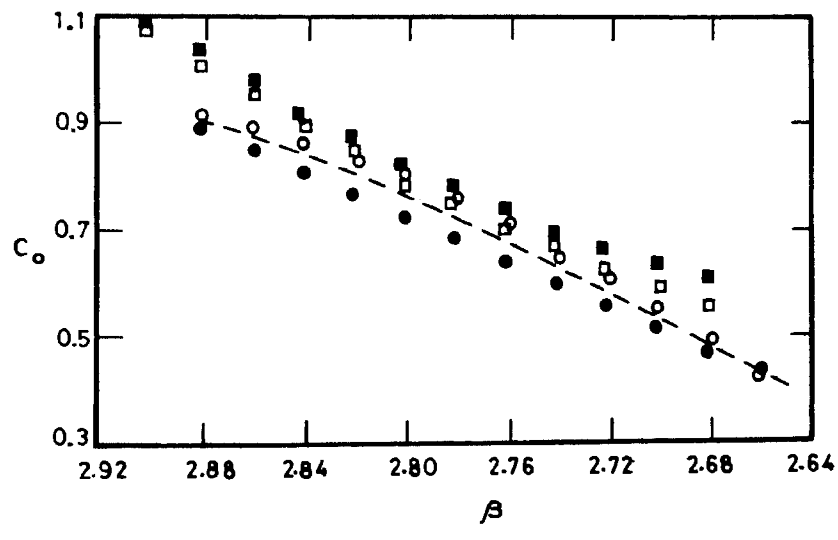

Fig IV–8 : *Same as Fig IV-7 for A-stars. The ZRMS from observed slopes of rotation effects of α-Persei, Pleiades, Hyades and Praesepe are plotted. The adopted ZRZAMS curve is shown by a dotted line.*

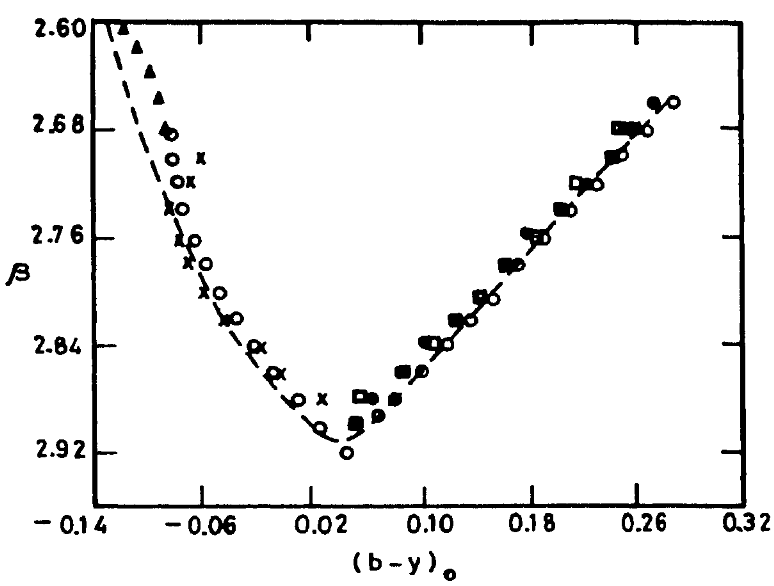

Fig IV–9 : *The ZRMS (observational) in the β, (b-y) plane for A and B-type stars of all clusters plotted in Fig IV–7 and IV–8 is shown. The adopted ZRZAMS values of (b-y) as a function of β are shown by the dotted line.*

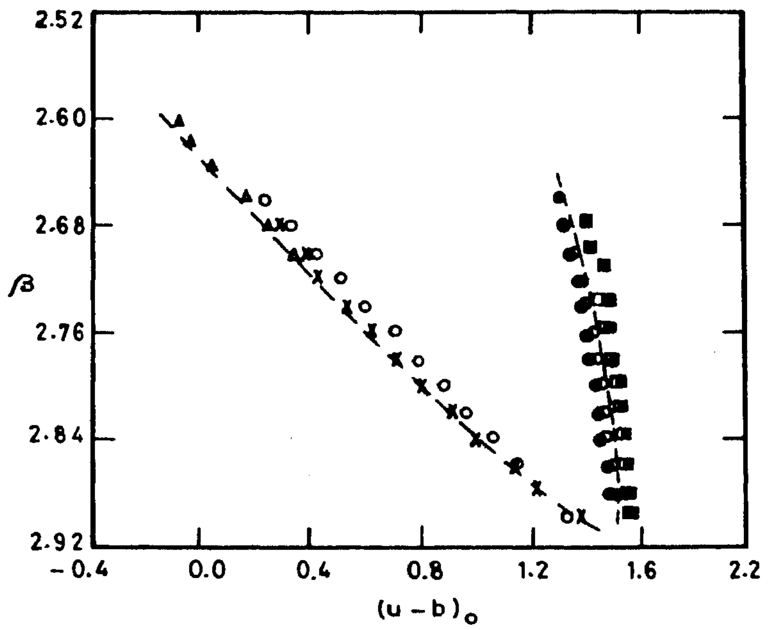

Fig IV–10 : *Same as Fig IV-9 in the β, (u-b) plane.*

values from mid B to late A and early F-star ranges. The B2, B3 type stars are represented only by the Lower Centaurus and Upper Centaurus group.

6.4. ZRZAMS : from theoretical corrections

ZRZAMS from theoretical corrections also was derived by superposing the theoretical ZRMS curves for various clusters. In addition to α-Persei, Pleiades, Hyades, Praesepe, Upper Centaurus and IC 4665, we have used Cep OB3, Coma, IC 2602, IC 2391, IC 4756, NGC 2264, NGC 2516 and NGC 4755 to check the derived ZRZAMS by correcting the indices using the theoretical predictions of Collins & Sonneborn for i=60°.

Because we are assuming a value of $i = 60^o$ for all stars, we are likely to leave uncorrected, all such stars which are rotating fast but seen pole-on. For example, in an M_v versus c_o plane for B-stars, these will be more than half a magnitude above the non rotators at a given c_o. These objects would add to the scatter that would be introduced by the inclusion of visual and double lined spectroscopic binaries.

We checked the derived ZRZAMS values using stars that have $Vsin\ i$ values greater than or equal to 100 km s^{-1}. We compared these determinations with those derived by using all stars without any discrimination. Fig IV–11 shows, for fast rotating ($Vsin\ i \geq 100$ km s^{-1}) B stars, the plot of β_{ZR} and c_{ZR} values corrected for rotation. The theoretical ZRZAMS curve is also shown. The relationship appears extremely smooth as expected. In Fig IV–12 stars of all $Vsin\ i$ values are plotted. α-Persei, Pleiades, Upper and Lower Centaurus, Cep OB 3, IC 4665, IC 2602, IC 2391, NGC 2264 and NGC 4755 have been included. Similar diagrams in the M_v, β and M_v, (b-y) planes are shown in Figs IV–13 to IV–16. Fig IV–17 is a plot of β_{ZR}, $(b\text{-}y)_{ZR}$ for stars of all $Vsin\ i$ values and c_{ZR}, $(u\text{-}b)_{ZR}$, for fast rotators is plotted in Fig IV–18.

Similarly from a superposition of various clusters containing A-stars the ZRZAMS values were determined. The following clusters were used; α-Persei, Pleiades, Hyades, Praesepe, IC 4665 and Coma. The theoretical ZRZAMS values are also listed in Table IV–11 and IV–12 for B and A stars respectively. Adopted ZRZAMS values are the averages of the observational and theoretical ZRZAMS values and are listed in Table IV-13 and IV–14 for B and A-type stars respectively.

A comparison of our adopted ZRZAMS values is made with the zero age main sequence values derived by Crawford (1975, 1978, 1979). Crawford has listed the

ZAMS values derived from the locus of the blue envelope of B and A stars. We can easily anticipate that such a blue envelope should also represent the zero rotation zero age main-sequence and hence must agree with our values derived by correcting for rotation effects. In Figures 19, 20, 21 and 22 we have compared these two independant determinations. The agreement is excellent and supports the fact that rotation affects all the observed parameters and our procedures in determining the ZRZAMS values should be valid.

Table IV–11. B-type stars

β	$(b-y)_o$	m_o	c_o	$(u-b)_o$	M_v	$(b-y)_o$	m_o	c_o	$(u-b)_o$
	Observational ZRZAMS					Theoretical ZRZAMS			
2.60	−.130	0.067	−0.020	−0.146	−4.00	−0.120	0.047	−0.030	−0.175
2.62	−.125	0.073	0.046	−0.058	−2.90	−0.112	0.056	0.030	−0.082
2.64	−.118	0.079	0.111	−0.033	−2.00	−0.104	0.065	0.090	0.012
2.66	−.110	0.084	0.177	0.125	−1.45	−0.097	0.074	0.150	0.104
2.68	−.102	0.090	0.243	0.219	−0.90	−0.090	0.083	0.210	0.196
2.70	−.094	0.096	0.308	0.312	−0.40	−0.081	0.092	0.270	0.292
2.72	−.087	0.102	0.374	0.404	0.00	−0.073	0.101	0.330	0.386
2.74	−.080	0.108	0.440	0.496	0.45	−0.066	0.110	0.395	0.483
2.76	−.071	0.114	0.506	0.592	0.80	−0.058	0.119	0.460	0.582
2.78	−.062	0.120	0.571	0.687	1.00	−0.050	0.128	0.530	0.686
2.80	−.057	0.128	0.637	0.791	1.20	−0.042	0.136	0.600	0.788
2.82	−.040	0.137	0.702	0.896	1.30	−0.034	0.145	0.670	0.892
2.84	−.028	0.146	0.768	1.004	1.40	−0.026	0.154	0.740	0.996
2.86	−.014	0.155	0.834	1.116	1.50	−0.019	0.163	0.810	1.108
2.88	.002	0.166	0.900	1.236	1.75	−0.011	0.172	0.880	1.202
2.90	.020	0.176	0.966	1.358	1.80	−0.003	0.183	0.950	1.310

Table IV–12. A-type stars

β	$(b-y)_o$	m_o	c_o	$(u-b)_o$	M_v	$(b-y)_o$	m_o	c_o	$(u-b)_o$
	Observational ZRZAMS					Theoretical ZRZAMS			
2.64						0.312	0.133	0.405	1.295
2.66	0.281	0.157	0.422	1.298	3.66	0.291	0.144	0.448	1.318
2.68	0.262	0.164	0.478	1.330	3.54	0.270	0.155	0.491	1.341
2.70	0.242	0.172	0.532	1.360	3.42	0.249	0.166	0.533	1.363
2.72	0.223	0.179	0.583	1.387	3.30	0.228	0.176	0.577	1.385
2.74	0.205	0.186	0.632	1.414	3.18	0.206	0.186	0.620	1.404
2.76	0.186	0.194	0.678	1.438	3.06	0.185	0.196	0.662	1.424
2.78	0.168	0.199	0.721	1.455	2.94	0.163	0.203	0.705	1.437
2.80	0.151	0.205	0.762	1.474	2.82	0.142	0.209	0.748	1.450
2.82	0.133	0.211	0.800	1.488	2.70	0.120	0.214	0.791	1.459
2.84	0.115	0.215	0.836	1.496	2.58	0.099	0.218	0.834	1.468
2.86	0.096	0.219	0.870	1.500	2.46	0.078	0.221	0.877	1.475
2.88	0.078	0.222	0.900	1.500	2.28	0.057	0.222	0.920	1.478
2.90		0.225				0.036	0.221	0.970	1.484

Table IV–13. Adopted ZRZAMS for B-type stars

β	M_v	$(b\text{-}y)_o$	m_o	c_o	$(u\text{-}b)_o$
2.60	−4.00	−0.125	0.057	−0.025	−0.161
2.62	−2.90	−0.119	0.065	0.038	−0.070
2.64	−2.00	−0.111	0.072	0.100	0.023
2.66	−1.45	−0.104	0.079	0.164	0.115
2.68	−0.90	−0.096	0.087	0.226	0.208
2.70	−0.40	−0.088	0.094	0.289	0.302
2.72	0.00	−0.082	0.102	0.352	0.392
2.74	0.45	−0.073	0.109	0.417	0.490
2.76	0.80	−0.065	0.117	0.483	0.587
2.78	1.00	−0.056	0.124	0.550	0.687
2.80	1.20	−0.050	0.132	0.618	0.790
2.82	1.30	−0.037	0.141	0.686	0.894
2.84	1.40	−0.027	0.150	0.754	1.000
2.86	1.50	−0.017	0.159	0.822	1.112
2.88	1.75	−0.005	0.169	0.890	1.219
2.90	1.80	0.009	0.180	0.958	1.334

Table IV–14. Adopted ZRZAMS for A-type stars

β	M_v	$(b\text{-}y)_o$	m_o	c_o	$(u\text{-}b)_o$
2.66	3.66	0.286	0.150	0.435	1.308
2.68	3.54	0.266	0.160	0.484	1.336
2.70	3.42	0.246	0.169	0.532	1.362
2.72	3.30	0.226	0.178	0.580	1.386
2.74	3.18	0.206	0.186	0.626	1.409
2.76	3.06	0.186	0.195	0.670	1.431
2.78	2.94	0.166	0.201	0.713	1.446
2.80	2.82	0.148	0.207	0.755	1.462
2.82	2.70	0.127	0.212	0.795	1.469
2.84	2.58	0.107	0.216	0.835	1.482
2.86	2.46	0.087	0.220	0.874	1.488
2.88	2.28	0.068	0.222	0.910	1.489

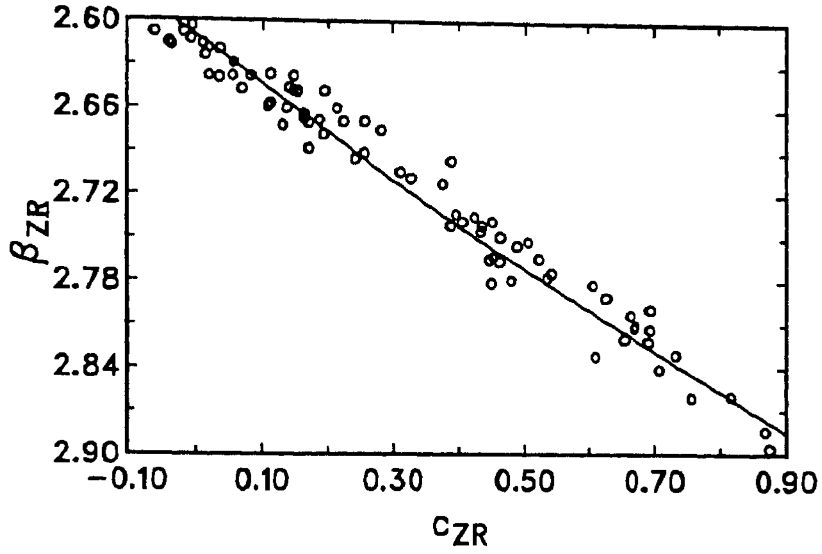

Fig IV−11 : *The theoretically corrected values of β and c_o for B-stars in various cluster stars with $V\sin i \geq 100$ km s^{-1} have been plotted. The adopted ZRZAMS theoretical curve is shown as a line.*

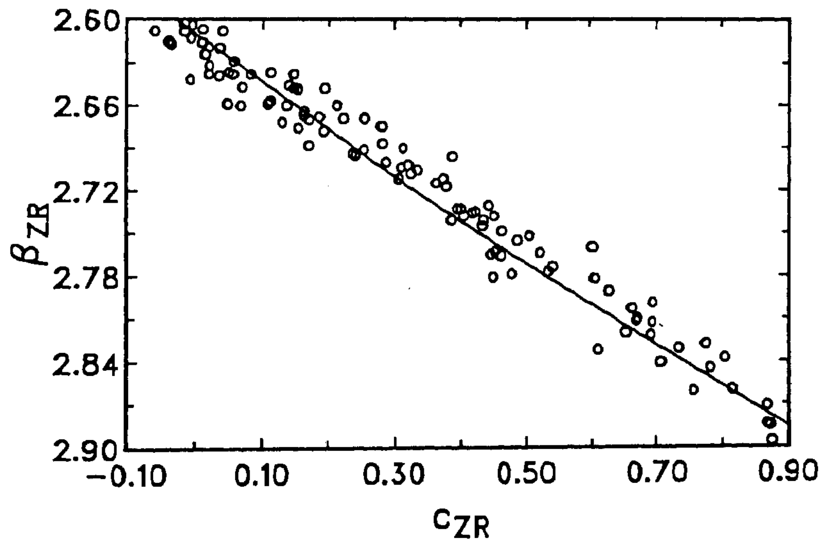

Fig IV−12 : *Same as Fig IV-11. Stars with all $V\sin i$ values have been plotted.*

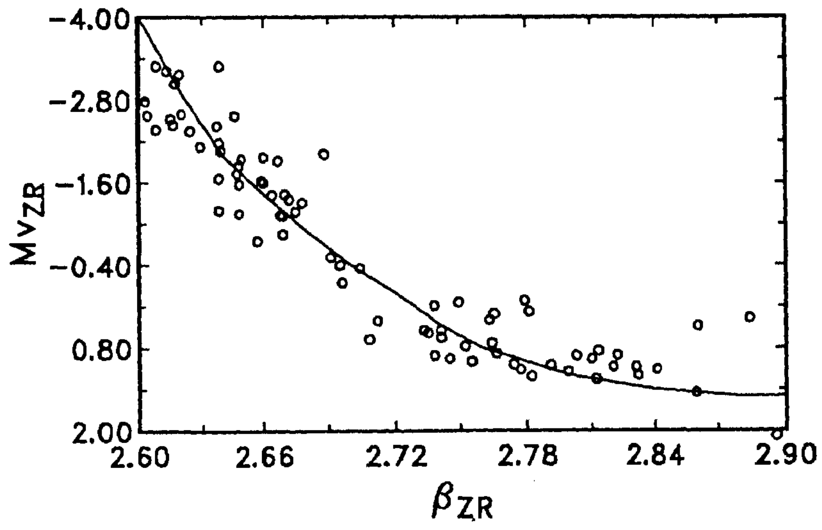

Fig IV–13 : *The theoretically corrected values of M_v and β for B stars, with $V \sin i \geq 100$ km s^{-1}, in various clusters have been plotted. The adopted ZRZAMS curve (theoretical) is shown as a line.*

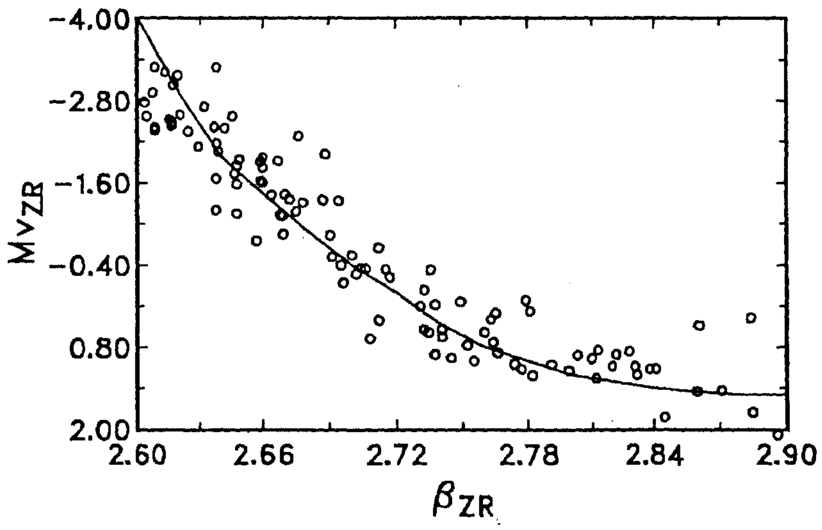

Fig IV–14 : *Same as Fig IV–13. Stars with all $V \sin i$ values have been plotted.*

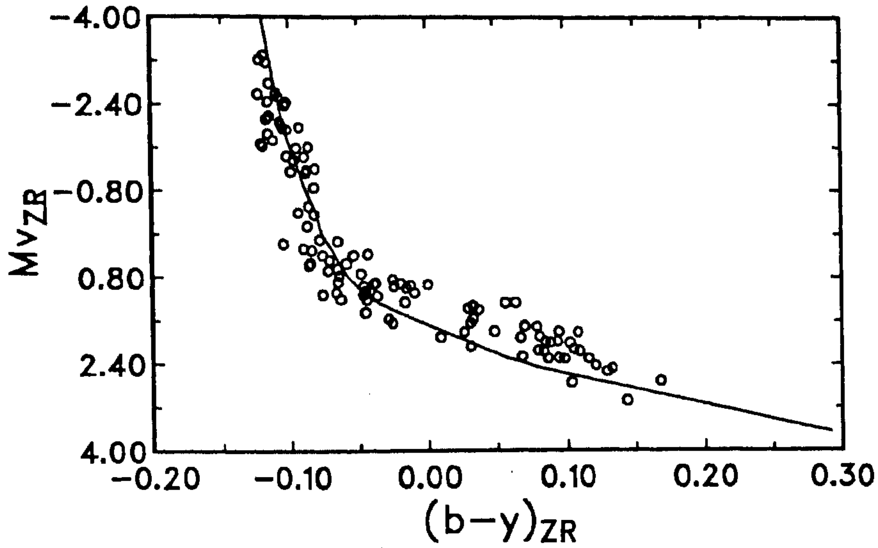

Fig IV–15 : *The theoretically corrected values of M_v and (b-y) for B and A stars, with $V sin\ i \geq 100\ km\ s^{-1}$, in various clusters have been plotted. The adopted ZRZAMS (theoretical) curve is also shown.*

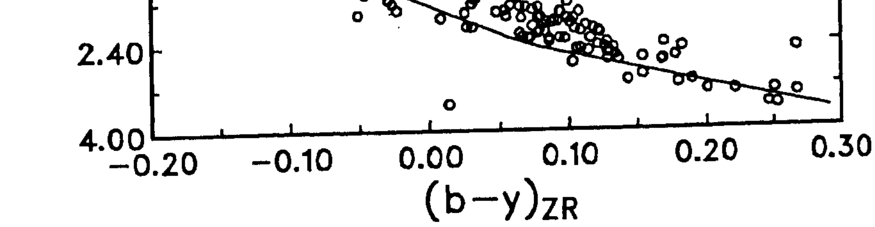

Fig IV–16 : *Same as Fig IV-15. Stars with all $V sin\ i$ values have been plotted.*

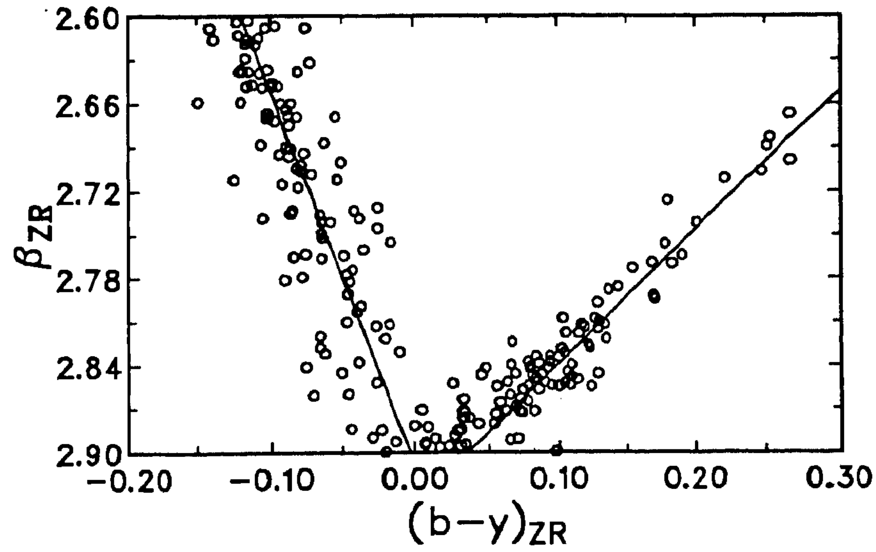

Fig IV–17 : *The theoretically corrected values of β and (b-y) for B and A stars in various clusters have been plotted. The adopted ZRZAMS (theoretical) values are shown by lines.*

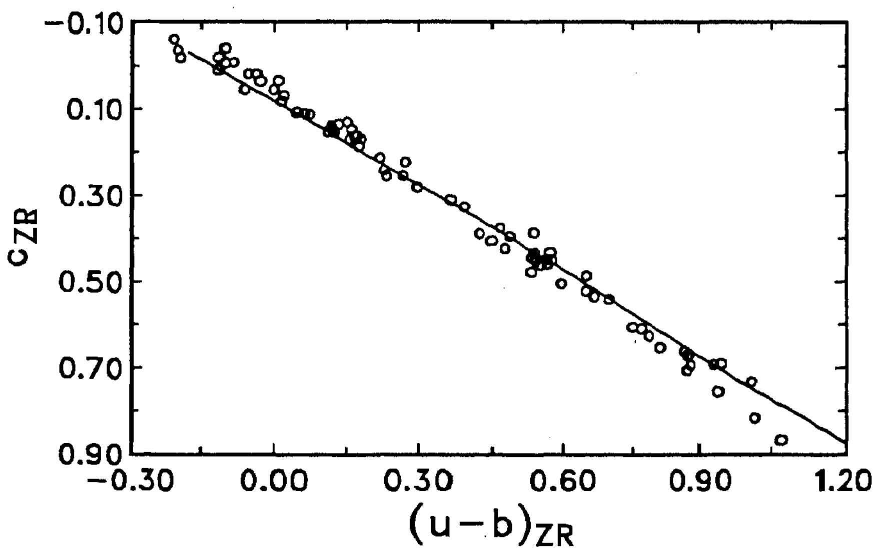

Fig IV–18 : *The theoretically corrected c_o and $(u\text{-}b)_o$ values for cluster B-stars with $V \sin i \geq 100$ km s^{-1} have been plotted. The adopted ZRZAMS values (theoretical) are shown by a line.*

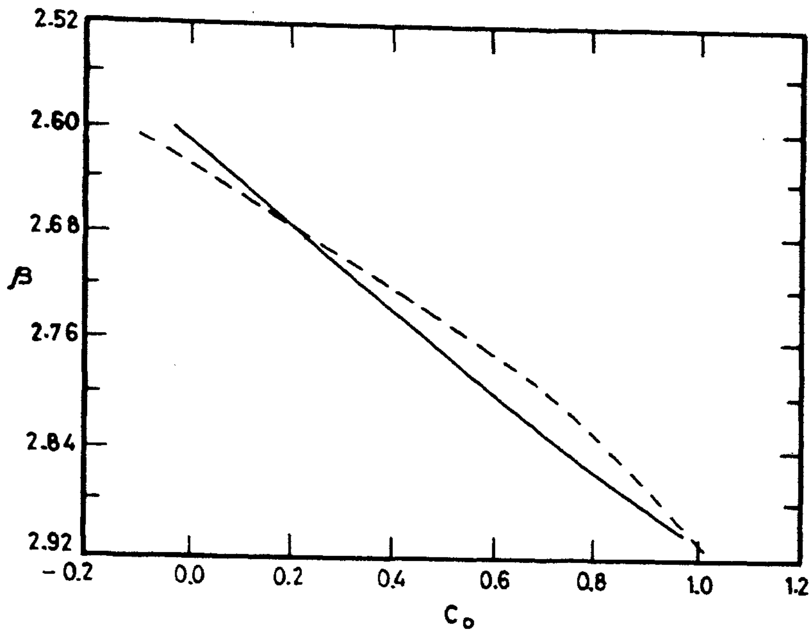

Fig IV–19 : *The ZRZAMS values for B stars derived in this study are compared with the values derived by Crawford (1978, 1979) from the lower envelope of field and cluster stars (dotted line), in the β, c_o plane.*

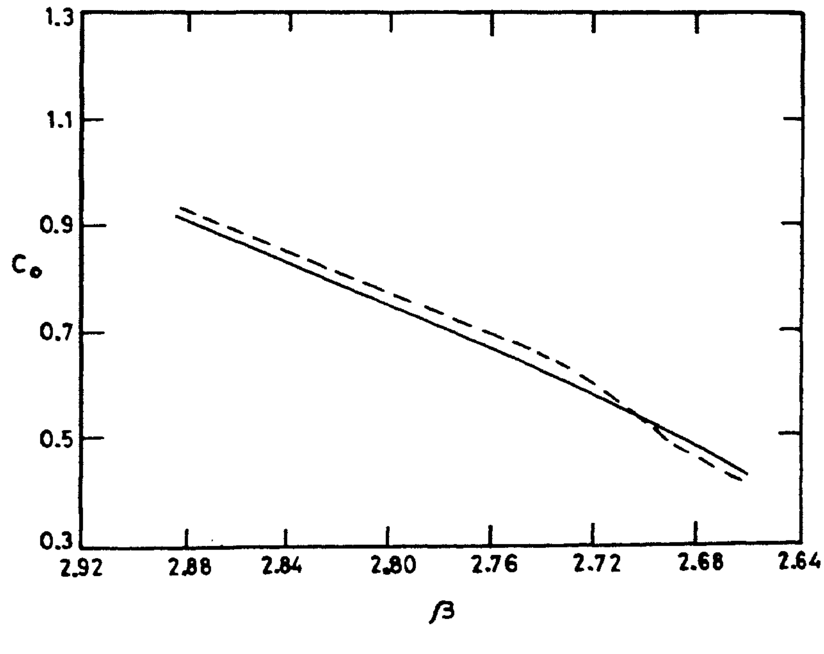

Fig IV–20 : *Same as Fig IV–19 for A-type stars.*

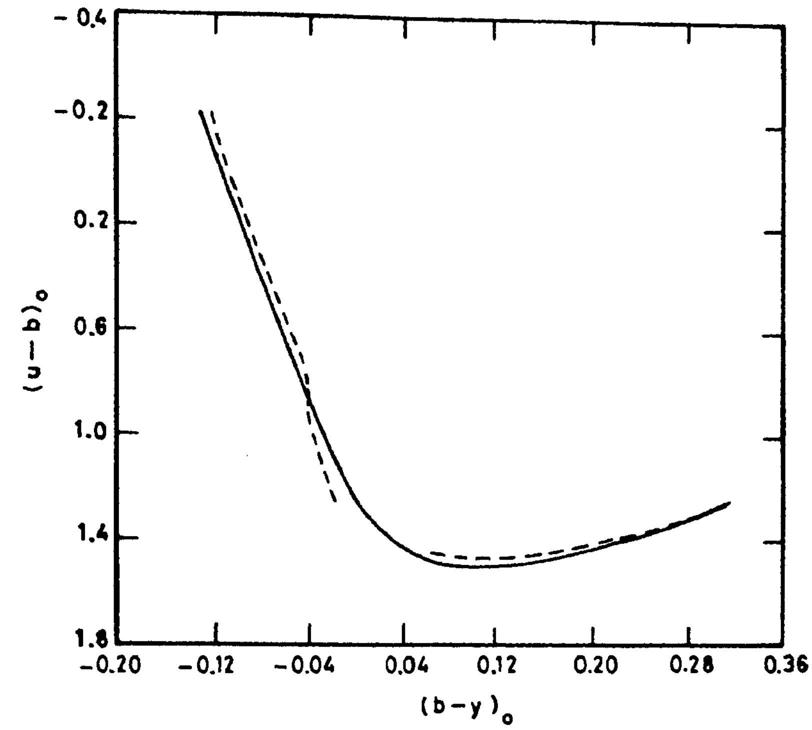

Fig IV–21 : *Same as Figs IV-19 and IV-20 in the (u-b), (b-y) plane for B and A-type stars.*

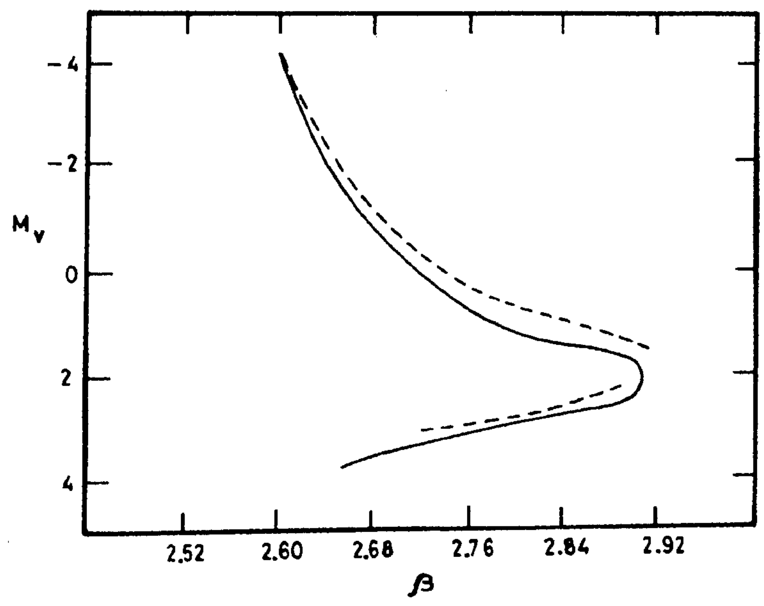

Fig IV–22 : *Same as Fig IV-19 in the M_v, β plane for B and A type stars.*

V. BLUE STRAGGLERS

1. Introduction

Blue stragglers are stars that occupy a position in a cluster colour magnitude diagram above and to the left of the cluster main sequence. They appear bluer than the presumed cluster turn off, obviously contradicting the assumption that all cluster members are coeval. Various theories have been put forward to explain their anomalous position with respect to the cluster main sequence.

Williams (1964a) in his delayed formation theory suggested that these objects were formed later than other cluster members and that the assumption that cluster members are coeval is erroneous. This theory is not favoured any longer since there is no independant observational evidence especially in old open clusters for ongoing star formation such as the occurence of T-Tauri stars, emission or reflection nebulae and differential reddening due to clumps of dusty gas (Wheeler 1979a).

Williams (1964b) proposed the theory of accretion in which a main sequence star accretes matter from high density regions and moves along the main sequence to become a bluer star. The interaction of the interstellar matter already present in the cluster with the mass ejected by supergiant members is supposed to produce such regions. For this mechanism to be operative such clusters must be fairly old while the blue Straggler seems to occur in clusters of all ages.

Mass transfer in close binaries proposed by McCrea (1964) and quasi homogeneous evolution proposed by Wheeler (1979b) are more viable but the evidence in support of them is not conclusive. While some blue stragglers do show radial velocity variations, an equal number have constant radial velocity indicating that duplicity is not a necessary condition for their existence.

Maeder (1987) hypothesized extra-mixing by rotationally induced turbulent diffusion in OBN stars giving rise to nearly homogeneous evolution. This suggestion is analogous to the extensive mixing hypothesis proposed by Wheeler. Another mechanism that may lead to homogeneous evolution is extensive core overshooting as suggested by Stothers & Chin (1979). Stellar coalescence suggested by Leonard (1989) attributes the formation of blue stragglers to binary-binary collisions in globular clusters. A blue straggler formed from the above mechanism must not be a slow rotator as the merger of binaries should produce a rapidly rotating star.

Blue stragglers on the other hand have a wide range of observed $V sini$ values.

Mermilliod (1982) compiled a list of blue stragglers in clusters younger than the Hyades which show a large spread in properties indicating that no unique model would be able to explain all the observations.

Mermilliod (1982) has shown that there are no observable differences between the blue stragglers and corresponding normal main sequence stars, except for the distribution of their rotational velocities. He also finds that the blue stragglers cannot be identified spectroscopically and can only be discovered from their position in the colour magnitude diagram.

An interesting feature that has emerged out of the work on blue stragglers (Pendl and Seggewiss 1975, Mermilliod 1982) is that more than half of them belong to the class of chemically peculiar (CP) stars of spectral types B7 and later ones. This group in general are slow rotators. The blue stragglers earlier than B5 in general have a range in their observed rotational velocities and some of them are also Be stars. This marked characteristic in the rotational velocity distribution of the blue stragglers and the fact that even in the old galactic cluster M 67 (Mathy's 1991) they are all slow rotators, lead us to investigate the possibility of rotation effects on colours of cluster stars as a primary cause for their observed positions.

The blue stragglers that fall in the early A-type domain the intrinsic slow rotators – are discussed in Section 2, and the B-type stragglers with a wide range in rotational characteristics are discussed in Section 3.

2. The A-type blue stragglers

The zero rotation zero age main sequence used has been derived by us, using selected galactic clusters as described in Chapter IV. The early B type stars in a cluster have maximum observed rotational velocities close to their break up speeds, while the maximum observed rotational velocity for stars in the spectral range B5-F0 is close to ω=0.9 (Rajamohan 1978; Kawaler 1987). The effect of rotation on the main sequence of a cluster, is to displace it from its non-rotating counterpart and broaden it by about twice the displacement (Collins & Smith 1985). The maximum displacement that a main sequence star would suffer, depends directly on the maximum rotational velocity that it can have; this corresponds to the balance between centrifugal force and gravity at the equator. The observed distribution of main sequence stars in a cluster between the zero rotation main sequence curve and the main sequence curve for ω=1.0 therefore, depends on the spread in the true rotational velocities of the stars. Also the observed dispersion along the main

Table V–1. Change in the indices from ω=0.0 to ω=0.90

		ΔM_v		Δ(b-y)		Δ(u-b)		Δc_1	
$M/M_\odot$	Sp. Type	$i = 0$	$i = 90$	$i = 0$	$i = 90$	$i = 0$	$i = 90$	$i = 0$	$i = 90$
14.5	B0	0.07	0.23	0.025	0.029	0.149	0.158	0.097	0.098
11.0	B1	−0.01	0.15	0.027	0.031	0.208	0.085	0.152	0.156
8.3	B2	−0.05	0.12	0.028	0.033	0.247	0.265	0.185	0.193
6.3	B3	−0.07	0.10	0.028	0.034	0.291	0.314	0.229	0.242
4.9	B5	−0.09	0.09	0.029	0.035	0.347	0.379	0.281	0.300
3.9	B7	−0.06	0.12	0.032	0.039	0.391	0.430	0.311	0.336
3.3	B8	0.03	0.21	0.039	0.047	0.401	0.442	0.303	0.324
2.8	B9	0.23	0.43	0.056	0.068	0.374	0.401	0.246	0.247
2.5	A0	0.55	0.32	0.091	0.117	0.237	0.217	0.077	0.025
2.3	A1	0.64	0.93	0.104	0.137	0.152	0.114	−0.004	−0.082
2.1	A2	0.68	0.97	0.115	0.153	0.086	0.026	−0.078	−0.172
1.9	A3	0.72	1.01	0.129	0.174	−0.009	−0.086	−0.173	−0.290
1.8	A5	0.45	0.74	0.119	0.173	−0.107	−0.189	−0.239	−0.367
1.7	A7	0.31	0.59	0.120	0.179	−0.146	−0.217	−0.274	−0.403

sequence would be a function of mass as the effects on different indices peak in different mass ranges.

The maximum effects predicted for the (u-b) index are for stars in the B7-A0 spectral range (Collins & Sonneborn 1979). The presence of a slow rotator in any cluster where the turn-up occurs for stars in the above spectral range, would make the slow rotator appear bluer than other normally rotating main sequence stars. Since the effects of rotation and revolution both act in the same direction, this observed colour difference would make the stars on the main sequence appear more evolved than the blue straggler itself. We have in the following analyses, taken this differential reddening effect due to rotation into account in judging how blue the blue stragglers really are, and how much really are the nearby cluster members evolved.

Table V–1 gives the theoretically predicted changes for inclination i=0° and i=90° in the various photometric indices for a non-rotator and a star of the same spectral type rotating with ω=0.9. This table was derived from the work of Collins & Sonneborn (1977). They have listed the values of (b-y), c, m, β, M_v and (u-b) for various values of i ranging from 0 to 90° and fractional velocites ω=0.0, 0.5, 0.8, 0.9 and 1.0. These values have been tabulated for the mass range that corresponds to the main sequence stars in the spectral type domain B0 to A7. Table V–1 shows that the effects of rotation on the colour indices are almost independent of i in the B0 to A2 spectral domain.

Table V–2 lists the blue stragglers belonging to the class of slow rotators taken from a list compiled by Mermilliod (1982). Column 2 lists the cluster to which the blue straggler belongs, column 3 gives its HD number, column 4 its spectral type and column 5 its observed $V sin\ i$ value. The last column contains remarks if any on binary nature, membership probability, radial velocity variations etc. of the blue stragglers under consideration. The $V sin\ i$ values of the stragglers in NGC 6633 and NGC 6281 have been taken from Abt (1985). The spectral types, $V sin\ i$ values and other remarks for the clusters in the table are as given by Mermilliod.

Table V–2. List of the A-type blue stragglers

S.No	Cluster	Star No. HD(E)	Spectral type	$V sin\ i$	Remarks
1.	Hyades	27962	AIVm	<30	Constant V_r D 1".4, $3^m.3$
2.	Coma	108662	A0p(Sr,Cr)	15	Constant V_r, α CV_n type var.
3.	Praesepe	73666	AIV	10	Constant V_r
4.	NGC 3532	96213	A0IV		D 0".4, $0^m.5$
5.	NGC 6281	153947	A0p(Si)	~30	Probable non member
6.	NGC 6633	169959	A0III	<40	
		170563	Am		Probable non member
7.	NGC 2281	49010	Ap		

Mermilliod's listing contains a few more clusters. We have considered only those for which intermediate and narrow band photometric data along with $V sin\ i$ values for the blue straggler were readily available. The membership probability of star No.161 (HD 170563) in NGC 6633 (Abt 1985) and star No.9 (HD 153947) in NGC 6281 (Feinstein and Forte 1974) is low.

From Table V–1 it can be seen that rotation effects on the (u-b) index are larger than on (b-y) at B7-A0 spectral range. In a given cluster the members in these spectral ranges, rotating with an average velocity, typical of their spectral class should thus suffer a change in both the (u-b) and (b-y) indices due to rotation and be pushed away from the main sequence. This rotational reddening in (u-b) is especially large for this spectral range. Most of the blue stragglers listed in Table 2, being peculiar, are intrinsic slow rotators (Abt 1979) and have anomalously low observed $V sin\ i$ for their spectral type. They fall in the above mentioned spectral range where rotation effects on the (u-b) index reach a maximum.

A plot in the M_v vs (b-y) or M_v vs (u-b) plane of any of these clusters containing an intrinsic slow rotator in the B9-A0 spectral range would therefore, show the slow rotators in a position that is relatively blue when compared to other stars in the same spectral range rotating with an average velocity of the order of 150 km s^{-1}. The slow rotator would thus appear as a blue straggler, the effect being more pronounced in the M_v vs (u-b) plane since rotation affects the (u-b) index considerably.

Figs V–1 to V–5 show the clusters listed in Table V–2 plotted in the M_v, (b-y); M_v, (u-b); (u-b), (b-y) planes. The observed (b-y) index of each of the blue stragglers in the clusters was corrected for interstellar reddening using the average E(b-y) given for each of these clusters in the original papers giving photometric data. The rotational correction for ω=0.9 at the observed $(b\text{-}y)_o$ was taken for i=0 and i=90 from Table V–1. We have indicated by means of a triangle in each of these figures the change in position of the blue straggler if it were to be rotating with a velocity ranging anywhere from zero to a maximum velocity corresponding to ω=0.9. Rotation effects in the (u-b) vs (b-y) plane, push the stars along the main sequence curve. For the B0 to A2 stars the (u-b) index is affected by a larger extent than the (b-y) index. A slow rotator in this plane would therefore maintain its position on the curve, whereas the other normally rotating stars would be pushed downwards. This would cause a large gap between the slow rotators and the others. Correction of the blue straggler in this plane causes a significant reduction in this gap as shown in Fig V–Ib for Hyades and Coma and in Fig V–2c for Praesepe and NGC 3532. An exception to these results is the cluster NGC 6633. The blue stragglers in this cluster are discussed in the next section.

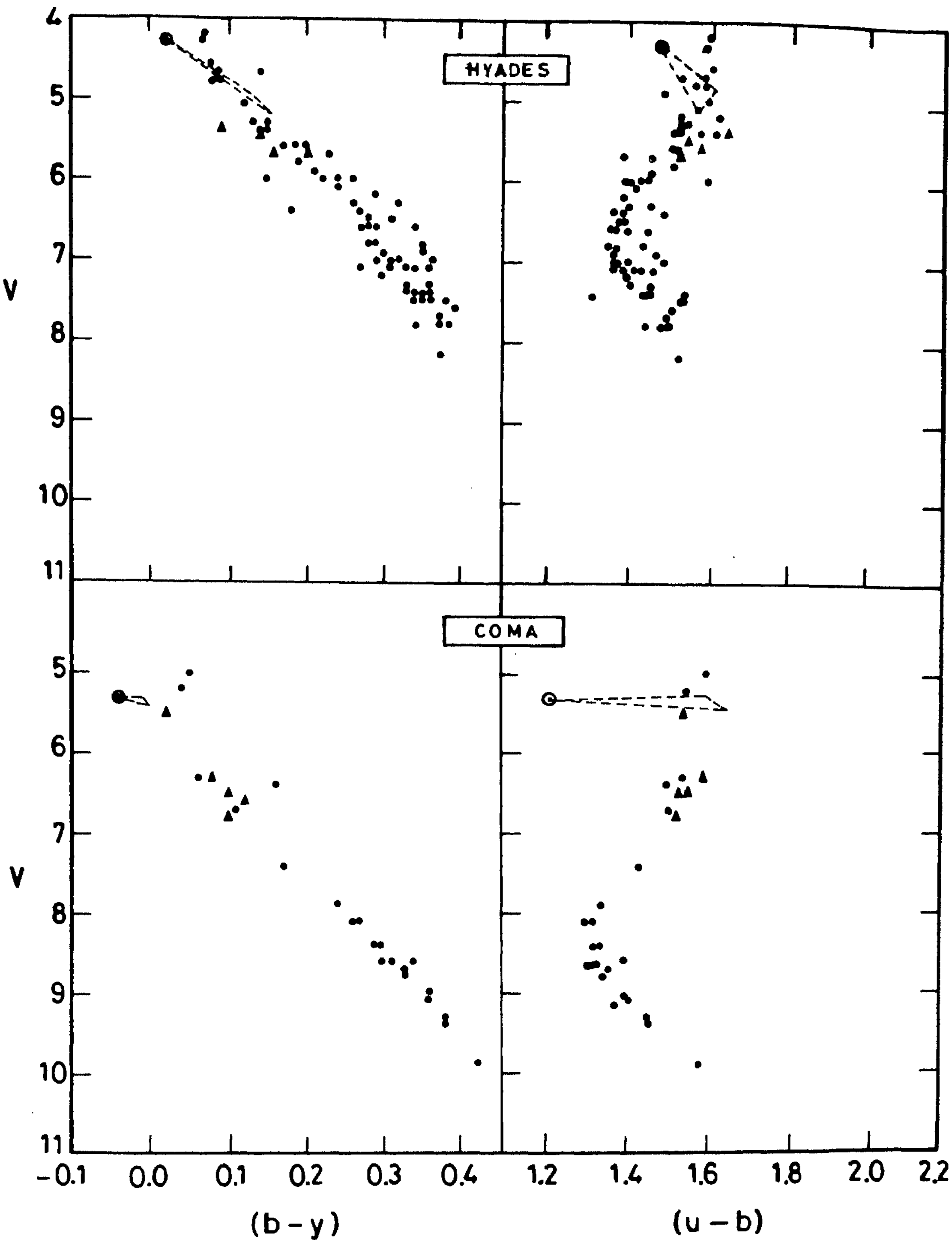

Fig V–1a : *Hyades and Coma in the V vs (b-y) and V vs (u-b) plane. The filled circles represent the cluster members and the filled triangles the Ap and Am stars in the cluster. The blue straggler is denoted by a dot inside an open circle. The triangle represents the correction for ω=0.9 for angles of inclination i=0° and i=90°.*

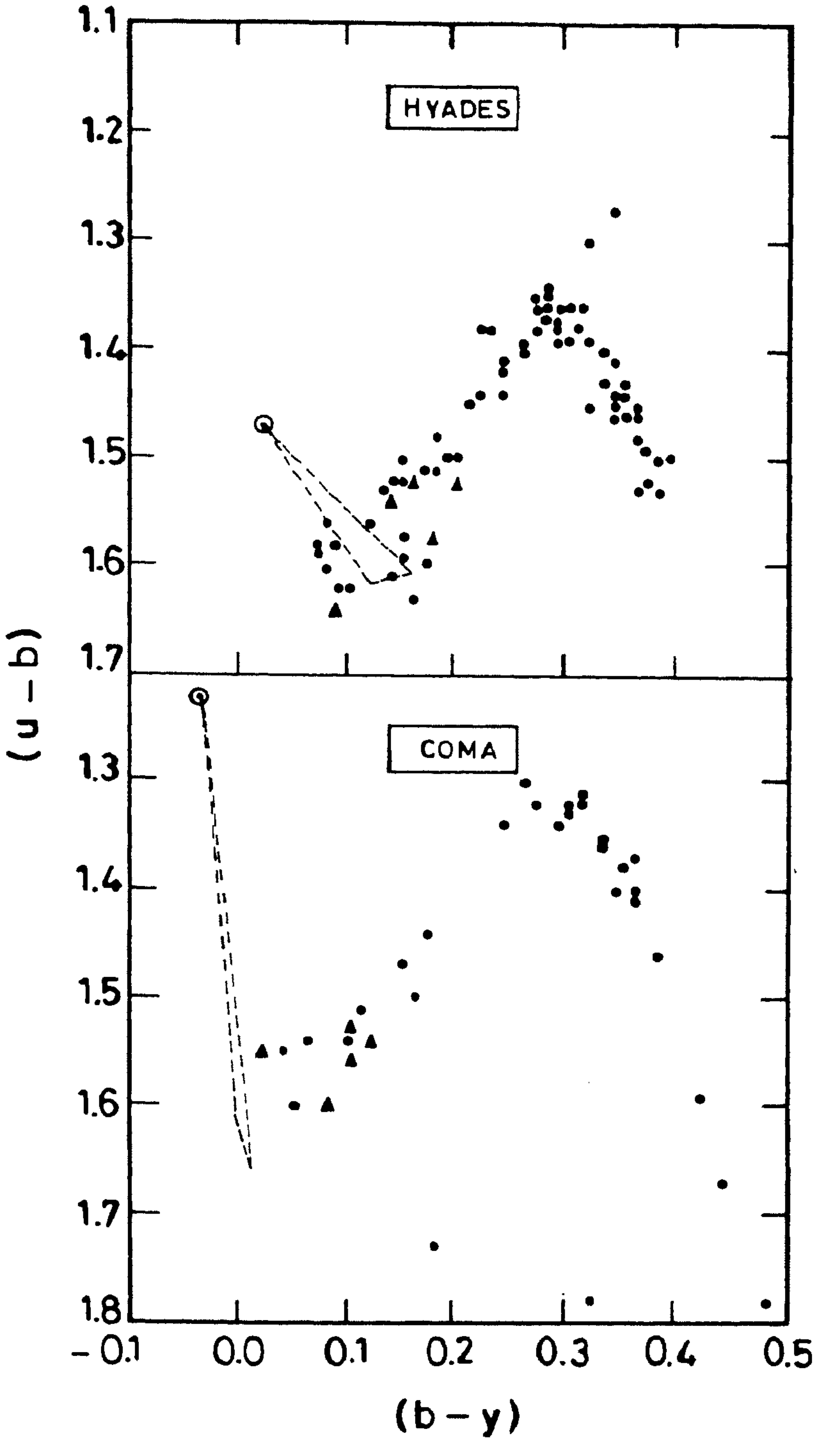

Fig V–1b : *Hyades and Coma clusters in the (u-b) vs (b-y) plane. Symbol representation is the same as in Fig V–1a.*

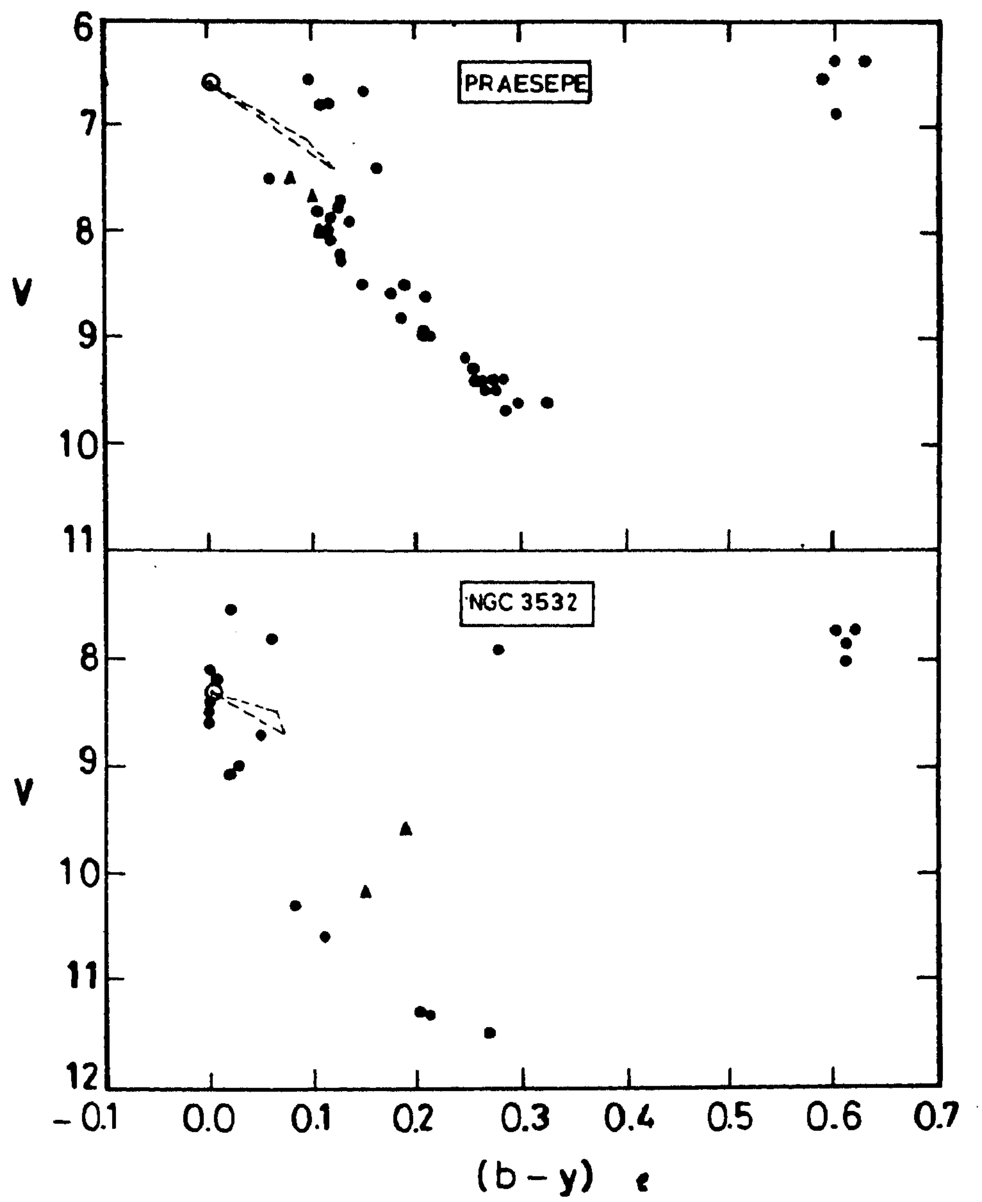

Fig V–2a : *Praesepe and NGC 3532 in the V vs (b-y) plane. Symbol representation is the same as in Fig V–1a. Data for NGC 3532 was taken from Eggen (1981).*

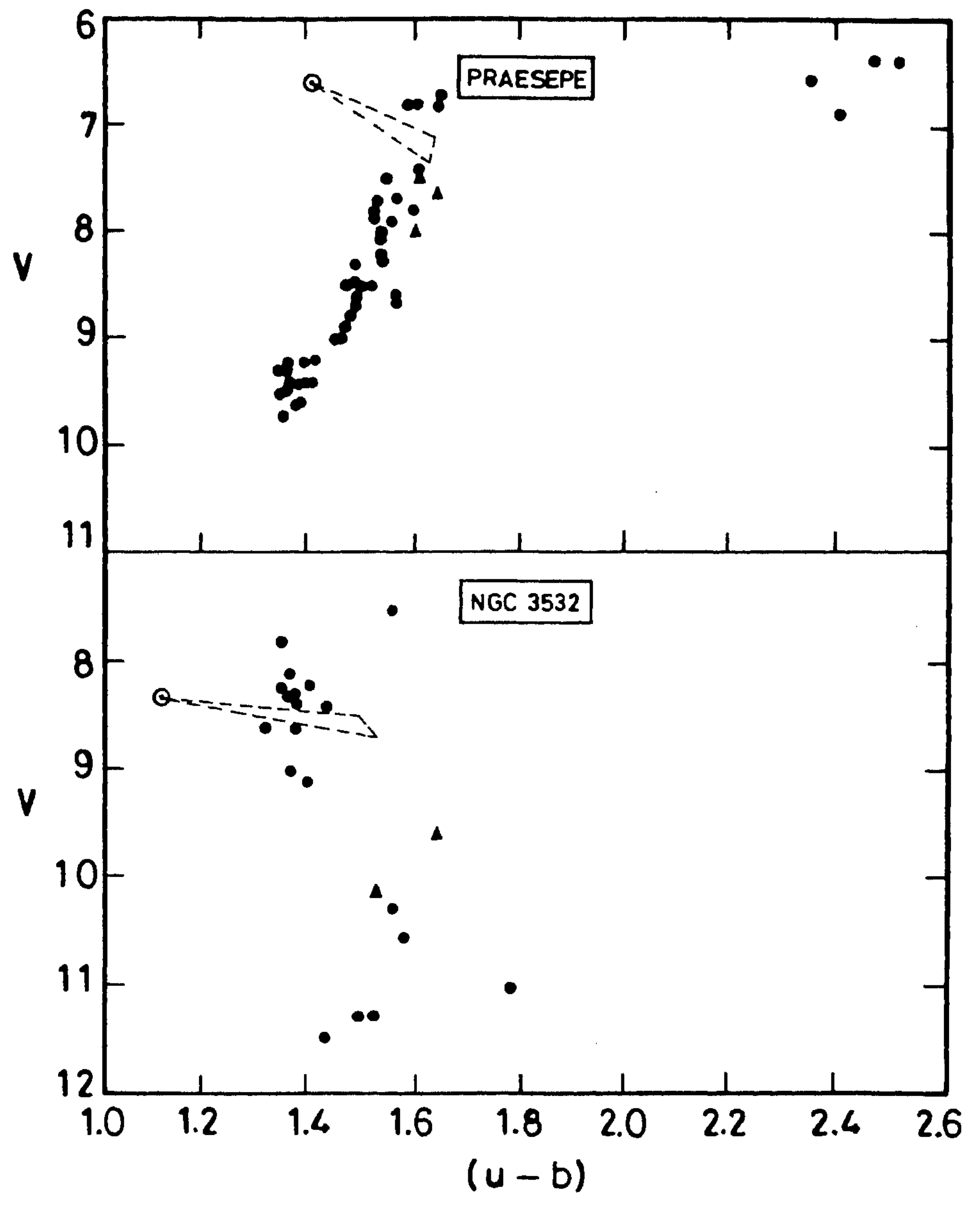

Fig V–2b : *Praesepe and NGC 3532 in the V vs (u-b) plane. Symbol representation is the same as in Fig V–1a.*

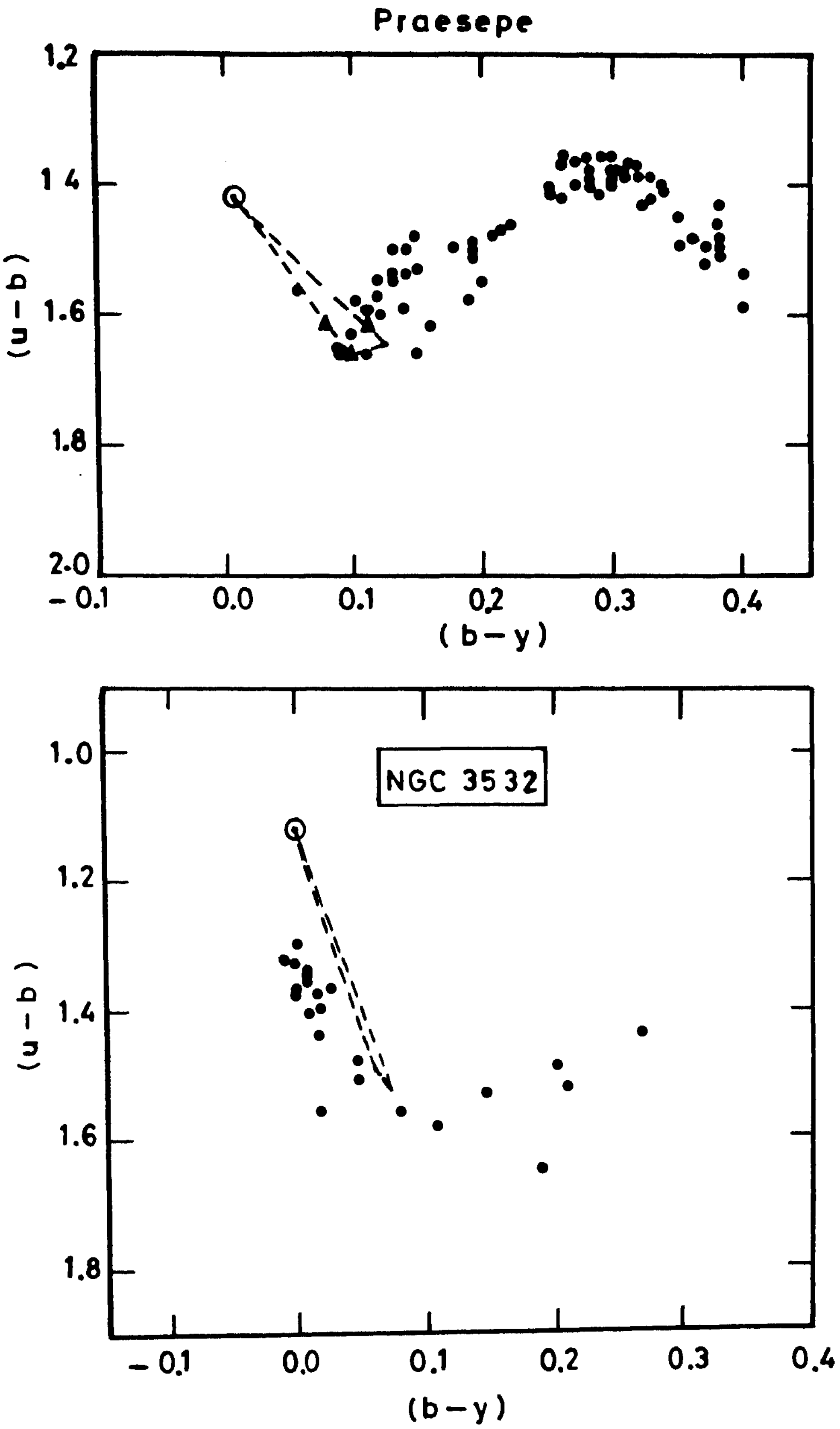

Fig V–2c : *Praesepe and NGC 3532 in the (u-b) vs (b-y) plane. Symbol representation is the same as in Fig V–1a.*

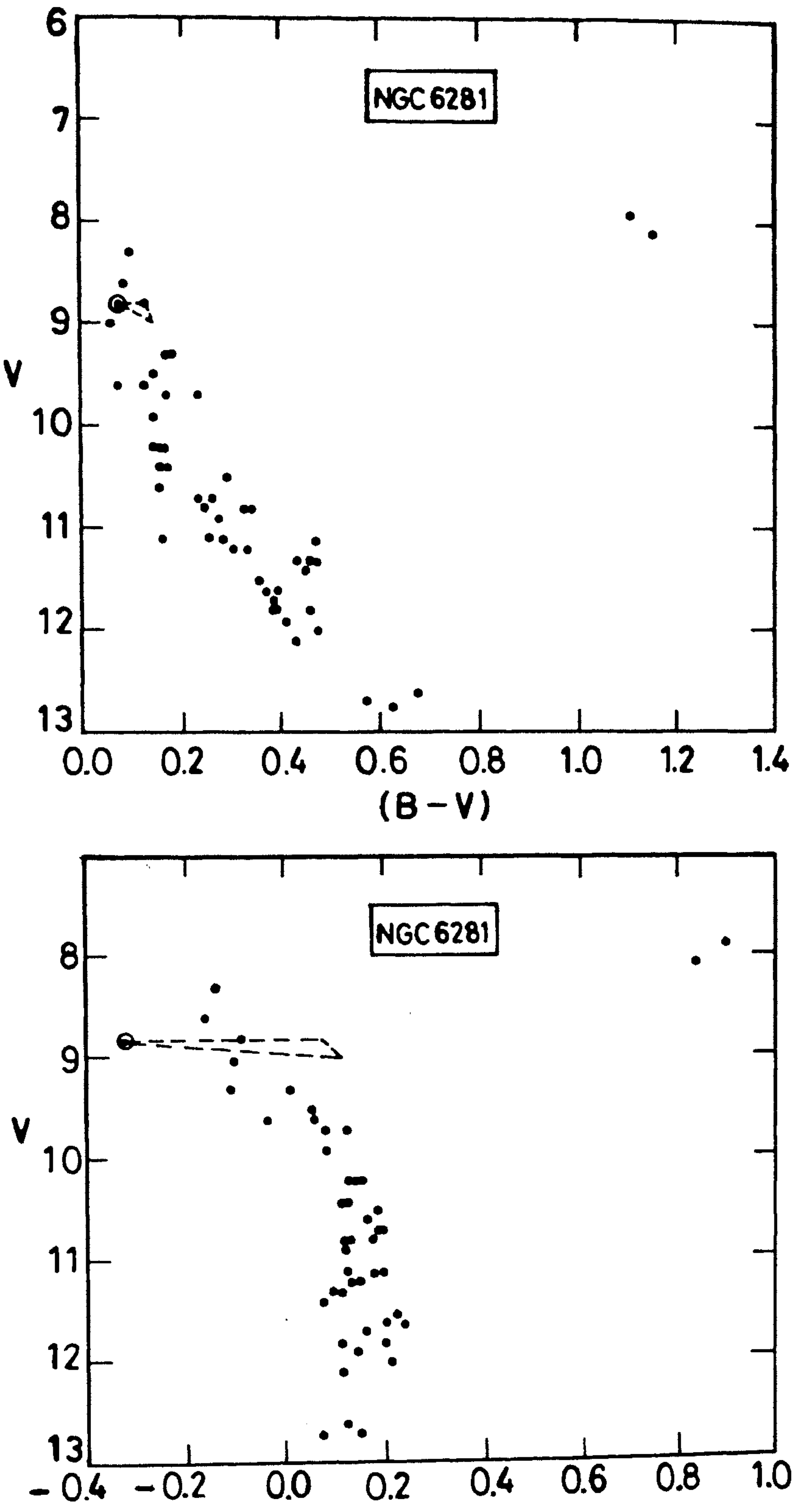

Fig V–3 : *NGC 6281 in the V vs (B-V)and V vs (U-B) planes. Symbol representation is the same as in Fig V–1a. Data for NGC 6281 was taken from Feinstein & Forte (1974).*

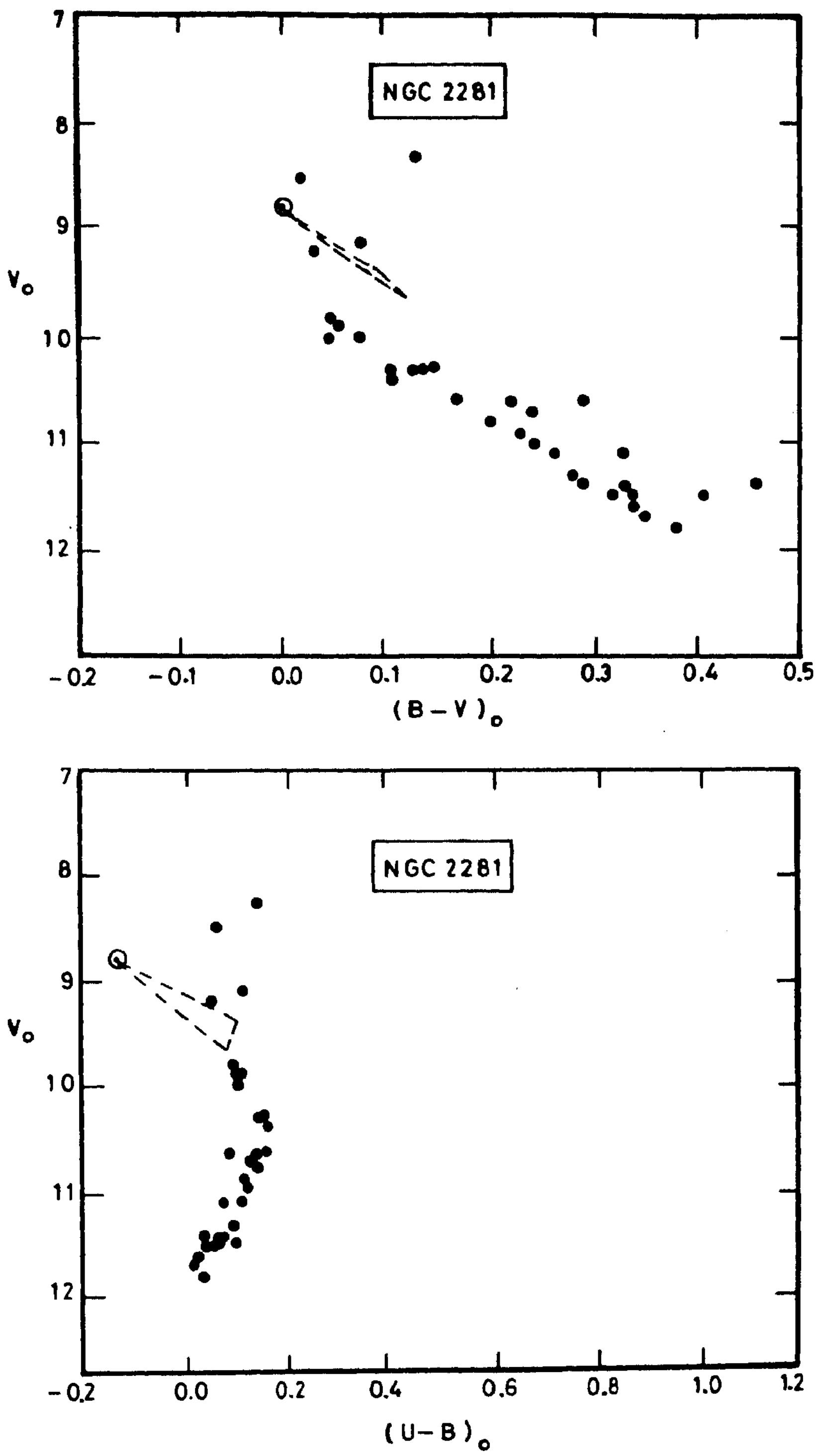

Fig V–4 : *NGC 2281 in the V_o vs $(B\text{-}V)_o$ and V_o vs $(U\text{-}B)_o$ planes. Symbols are the same as in Fig V-1a. Data taken from Pesch (1961).*

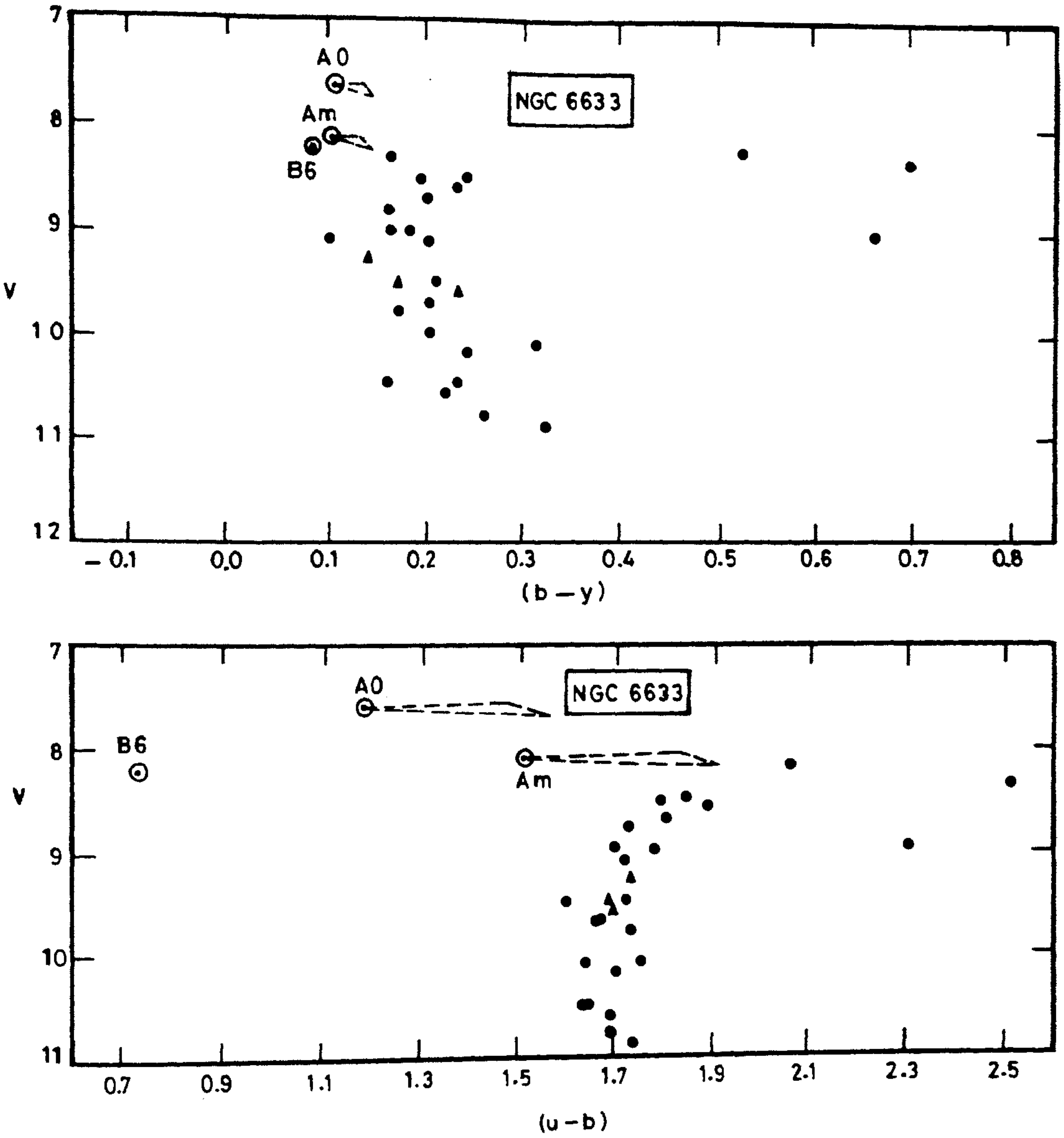

Fig V–5 :*NGC 6633in the V vs (b-y) and V vs (u-b) planes. Symbol representation is the same as in Fig V-1a.*

NGC 2281 has been analysed using UBV data since narrow band data for this cluster is not available. Similarly for NGC 6281 broad band indices have been plotted as narrow band data for the blue straggler in this cluster is not available. The corrections applied to the blue stragglers in these cases would be underestimated since larger effects due to rotation on the broad band colours are predicted (Collins & Smith 1985). The analysis of rotation effects on the broad band UBV colours of α-Persei and Pleiades cluster (Mathew & Rajamohan 1991) show that the effects are of the order of 0.05 mag. per 100 km s^{-1} in (U-B).

The cluster colour-colour and colour-magnitude diagrams show clearly that the anomalous position of all the blue stragglers listed in Table V–2 with the exception of the blue stragglers in NGC 6633 can be explained purely differences in the rotational velocities between the straggler and its nearest main sequence neighbours. The fact that blue stragglers in the B and early A spectral type domain appear bluer because of their low rotation seems to have been noted by Strittmatter & Sargent (1965) more than 25 years ago! They corrected the metallic-line stars in the Hyades, Praesepe and Coma clusters for blanketting effects and found that they lie to the left of the main sequence. They suggested that this was because they were slow rotators and that other stars of similar masses have been shifted to the red due to rotation.

We would also like to draw attention here to the blue stragglers in IC 4756, IC 4651, NGC 752 and M 67. The stragglers studied by Pendl & Seggewiss (1975) in IC 4756 are all spectroscopically peculiar and these authors were the first to suggest strongly that the two phenomena appear to be related. What is actually common to the two phenomena is slow rotation. Slow rotation is indirectly responsible for these objects to appear bluer and it is well known that almost all chemically peculiar stars on the upper main sequence are slow rotators.

In M 67 Mathys (1991) find that all the blue stragglers are slow rotators and the blue straggler phenomenon seems to be related to the Am phenomenon even though only two of the eleven stragglers are known Am stars (Pesch 1967). As noted by Pendl & Seggewiss (1975) the blue stragglers have not been studied carefully to recognize Ap, Am characteristics and it would not be surprising if a large fraction of the M 67 stragglers turn out to be Ap stars of the Hg-Mn type. A comparison of IC 4651 and M 67 in the M_v versus (B-V) plane also indicates that the stragglers in IC 4651 could possibly be explained in terms of rotation effects if they were to be intrinsic slow rotators. The position of the bue straggler in NGC 752 however does indicate that it cannot be explained by rotation effects alone.

3. The B-type blue stragglers

A listing of the blue stragglers in the B0-B6 spectral range is given in Table V–3. The third column gives the HD number of the blue straggler, followed by its spectral type and observed $Vsin\ i$ values in Columns 4 and 5 respectively. The last column is similar to that in Table V–2 and gives details regarding duplicity etc. The nine clusters listed in Table V–3 along with the above data have been taken from Mermilliod's (1982) listing of blue stragglers. Unlike the A-type stragglers discussed in Section 2, the B-type stragglers have a random $Vsin\ i$ distribution. Out of the nine clusters listed in the table, NGC 6633 and NGC 6475 stragglers have low observed $Vsin\ i$'s. The rotational velocities of the stragglers in NGC 6025 and NGC 2439 are not available. Out of the remaining five clusters, four contain emission-line objects, indicating rotation at a velocity close to their break-up speeds, while the blue straggler in IC 2602 has a $Vsin\ i$ typical of stars belonging to the spectral type B0.

Table V–3. List of the B-type blue stragglers

No	Cluster	Star No	Spectral type	$Vsin\ i$	Remarks
1.	NGC 6633	170054	B6IV	<20	Constant Vr
2.	NGC 6475	162374	B5IVp	<40	He weak, Constant Vr
		162586	B6V	<40	D:0".5, $0^m.0$
3.	NGC 2287	49333	B4p	100	He weak, probable non-member.
4.	NGC 2516	66194	B2IVne	250	
5.	NGC 6025	143448	B3IVne		
6.	Pleiades	23630	B8IIIe	230	Alcyone
7.	NGC 2422	60855	B21Ve	320	D:5".2, $6^m.8$
8.	IC 2602	93030	B0IVp	195	SBI
9.	NGC 2439	DM31°4911	B1.5Ib		

The effect of rotation, in general, on the early B type (B0-B3) stars, is small in comparison with the effect on the late B type (B5-B9) stars. The reddening due to rotation in the $(u\text{-}b)_o$ and c_o indices in particular shows a steep increasse in the B5-B9 spectral range relative to the early B type stars. The blue stragglers that are fast rotators, except for Alcyone in Pleiades fall in the B0-B3 mass domain where the rotation effects are not pronounced. It is therefore possible that in a few of these clusters, differential rotational reddening, may cause the stars that are of slightly lower mass than the straggler, to appear redder and therefore more evolved.

To check that the above effect may be a possible cause for some of the stars to be designated blue stragglers we attempted to correct the brightest cluster stars on the main sequence for the effects of rotation. We do find that the bright main sequence stars close to the stragglers are indeed fast rotators and fall in the spectral type range where the rotational effects on their colours are large.

To correct each star for rotation effects, we need to know the individual values of V and i. We have assumed a value of $i = 45^o$ to get an approximate estimate of the velocity V with which the star is rotating from the observed $Vsin\ i$ value. Table V–4 contains the average corrections for 100 km s^{-1} of rotation that have to be applied in the M_v, $(u-b)_o$ and M_v, $(b-y)_o$ plane calculated from the work of Collins & Sonneborn (1977). These corrections have been listed as a funcation of $(u-b)_o$ since masses of the stars are unknown. The ZRZAMS values of $(u-b)_o$ as a function of mass is taken from Chapter IV. The observed $(u-b)_o$ for each star was used to get the first set of corrections in $(u-b)_o$ and Mv. These corrected indices were then used to derive the second set of corrections in$(u-b)_o$ and M_v. The average of these two sets was used to correct the stars in the M_v range 0.0 to −2.0 magnitude for which rotational velocity data are available. Some of the stars in this magnitude range have low observed $Vsin\ i(< 50kms^{-1})$. These appear considerably displaced from the ZRMS and are probably fast rotators seen pole-on. The velocities obtained from the $Vsin\ i$ values in these cases are obviously underestimated leaving these stars uncorrected.

Six of the nine clusters listed in Table V–3 are shown in the M_v versus $(u-b)_o$ plane in Figs V–6 to V–11. The straggler in NGC 2287 is considered a non-member by Mermilliod (1982), as it lies outside the cluster radius and its membership based on available radial velocities is difficult to assess. Intermediate-band photometric indices are not available for NGC 2439. The stragglers in the remaining seven clusters are discussed below in relation to the rotational reddening effects as a possible cause contributing to their erroneous designation as blue stragglers. More

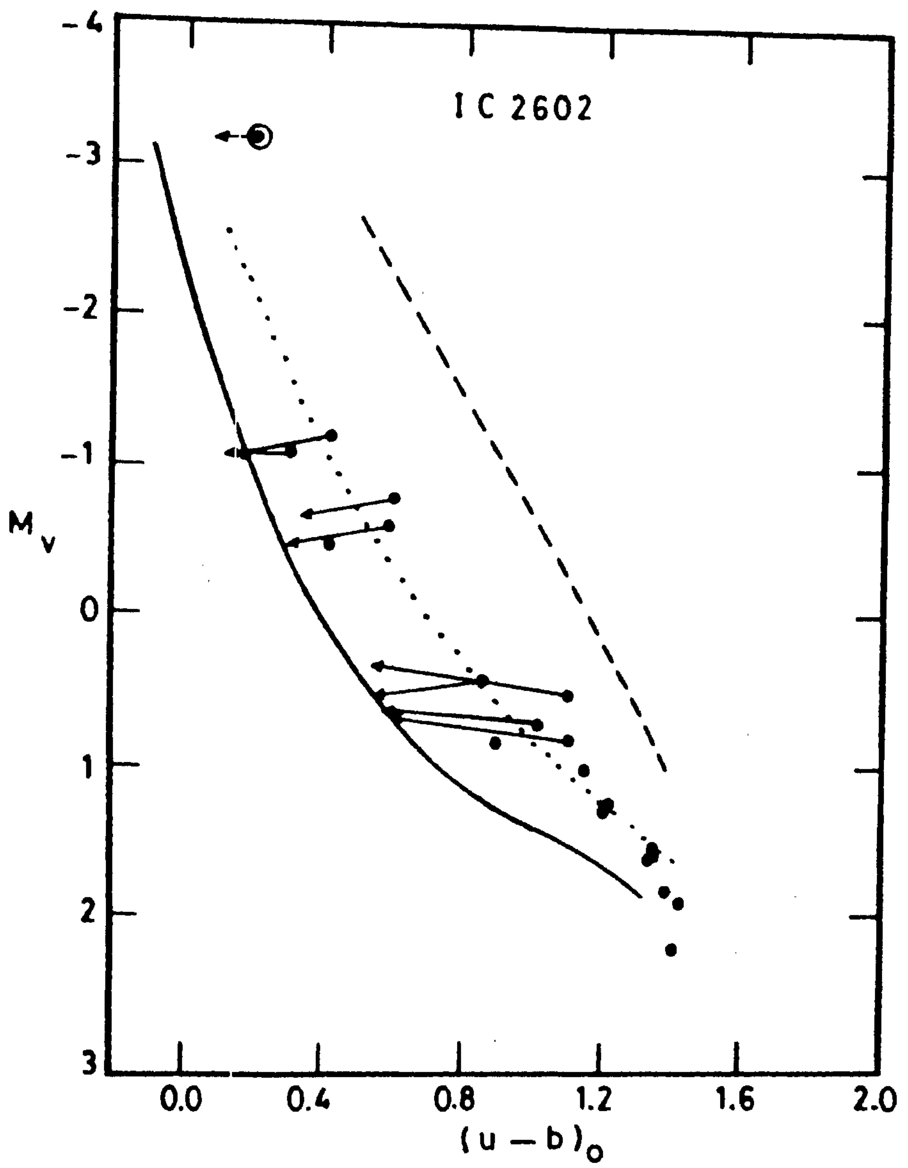

Fig. V–6: *IC 2602 in the M_v versus $(u-b)_o$ plane. The blue straggler is denoted by a dot inside an open circle. The continuous line represents the zero rotation main sequence used by us. The theoretical sequence for $\omega = 0.9$ and 1.0 are denoted by the dotted and broken lines respectively. The arrow heads indicate the position of the stars, when corrected for rotation.*

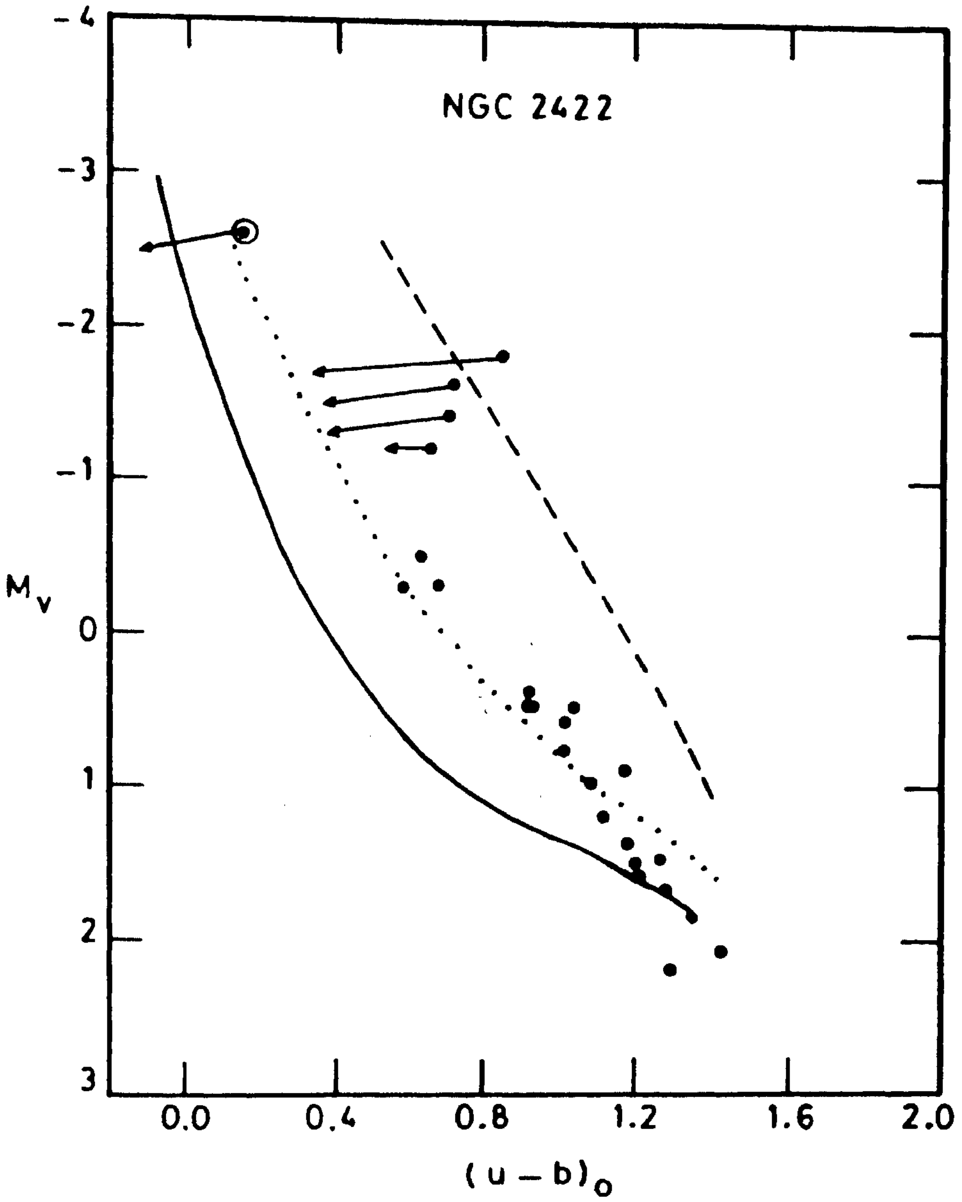

Fig. V–7: *NGC 2422 in the M_v versus $(u-b)_o$ plane. Symbols are the same as in Fig. V–6.*

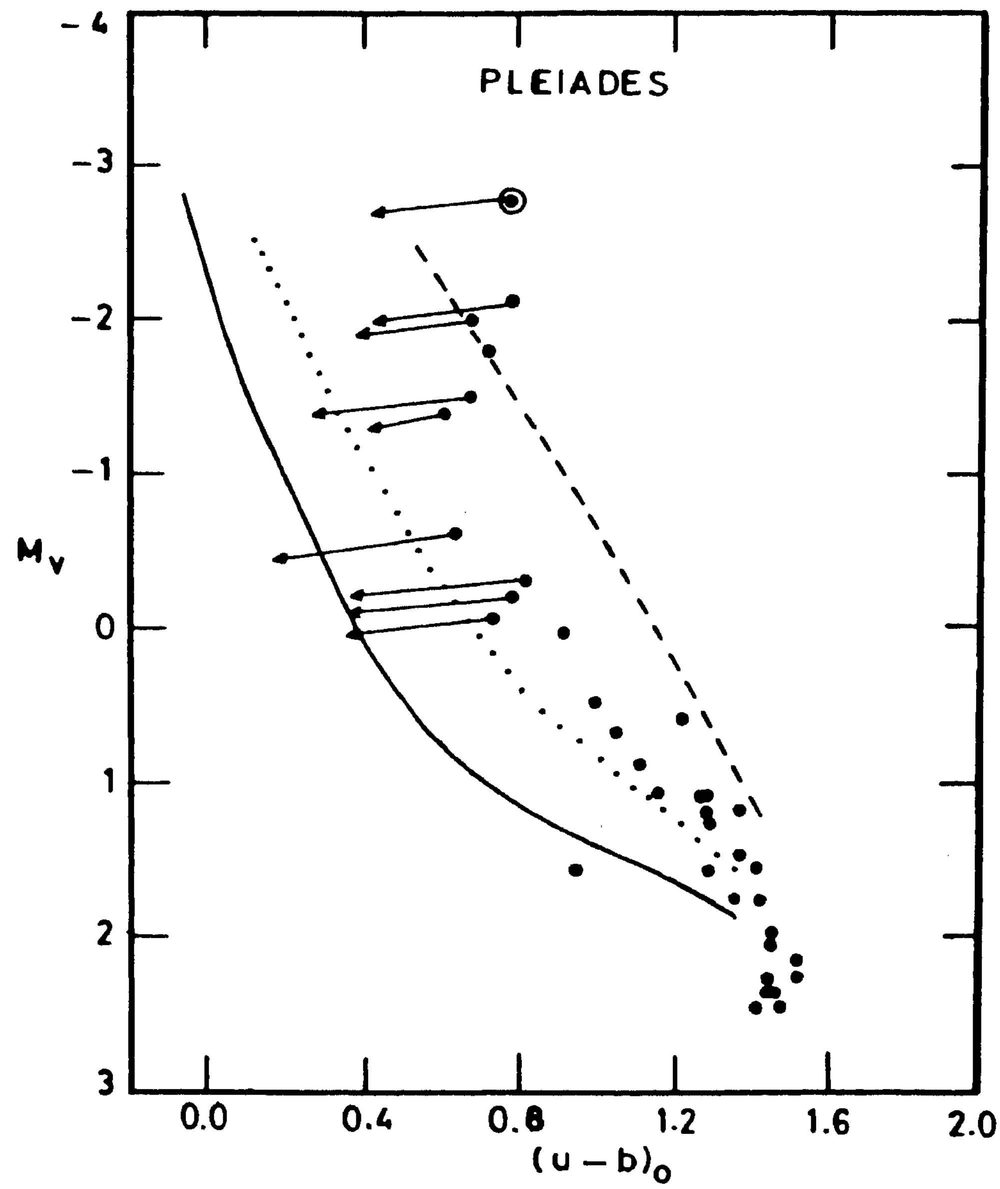

Fig. V–8: *The Pleiades cluster in the M_v versus $(u-b)_o$ plane. Symbols are the same as in Fig. V–6.*

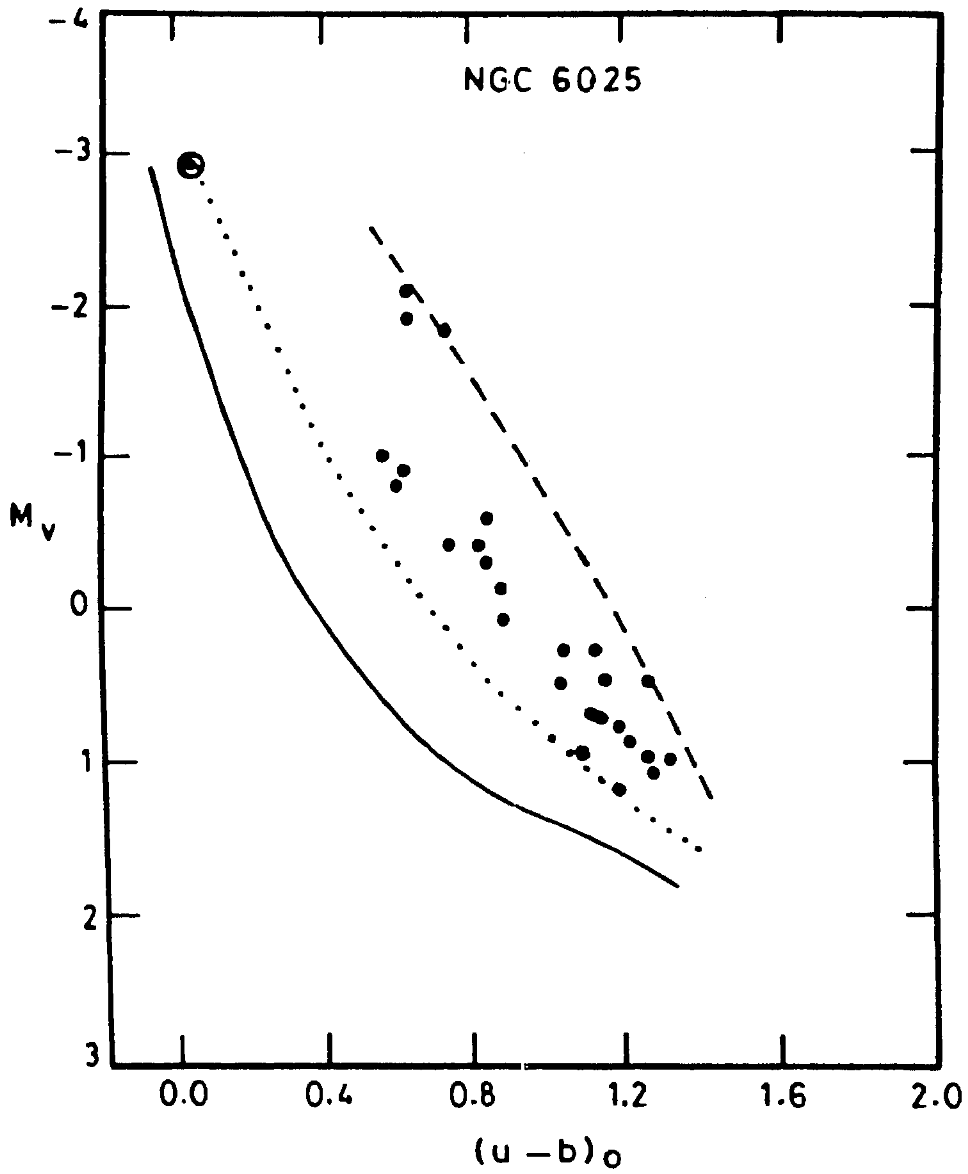

Fig. V–9: *NGC 6025 in the M_v versus $(u-b)_o$ plane. Symbols are the same as in Fig. V–6.*

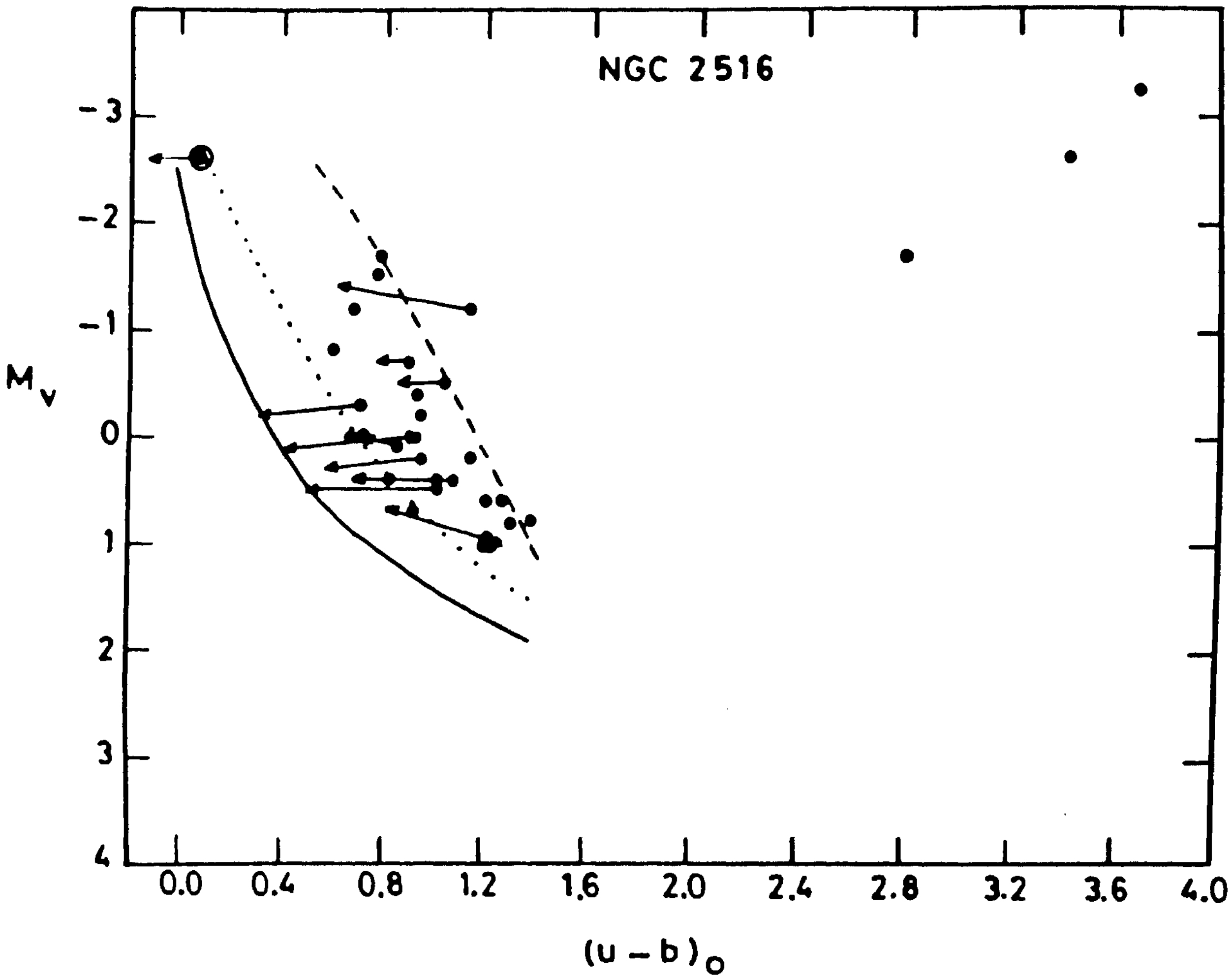

Fig. V–10: *NGC 2516 in the M_v versus $(u-b)_o$ plane. Symbols are the same as in Fig. V–6.*

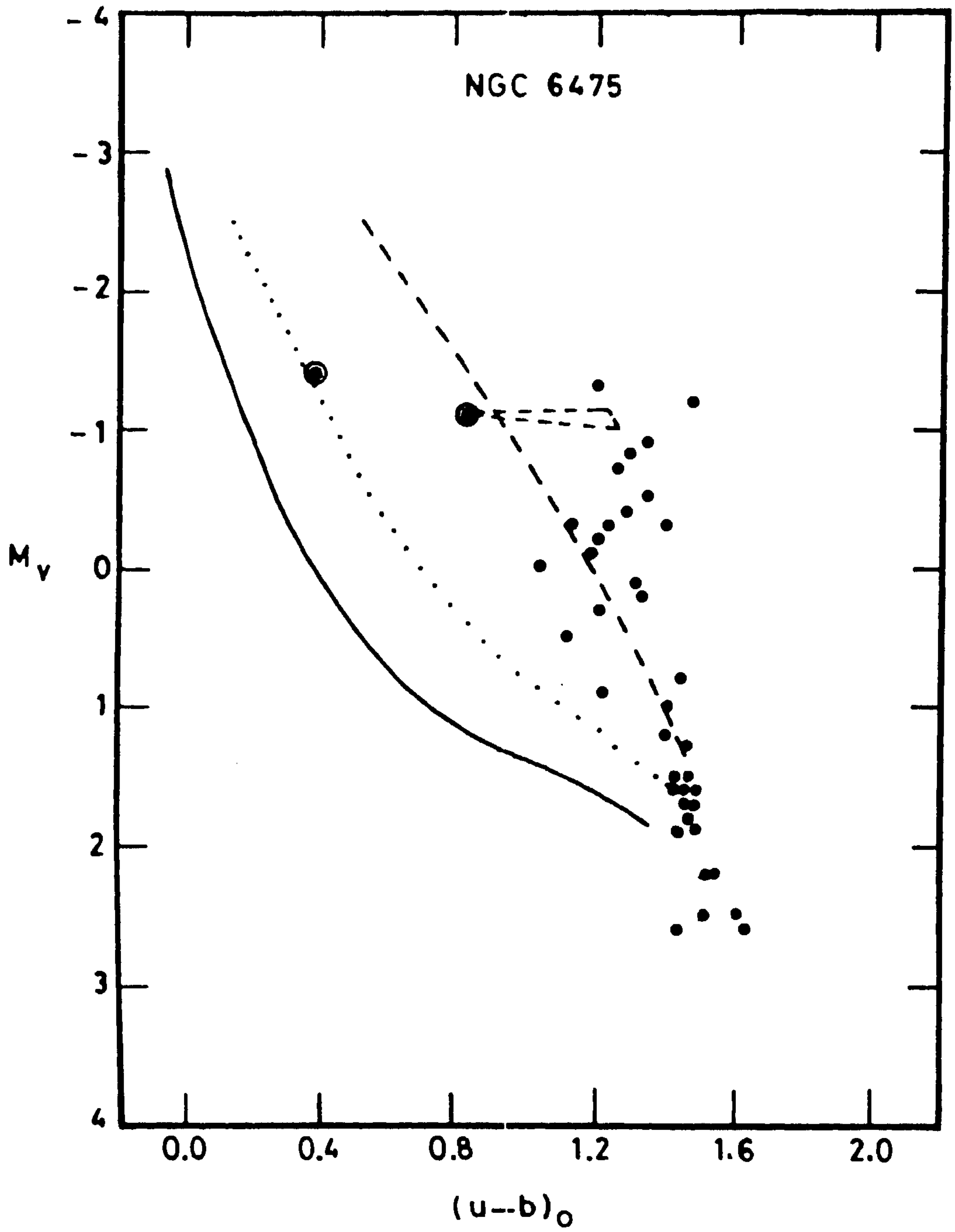

Fig. V–11: *NGC 6475 in the M_v versus $(u-b)_o$ plane. Symbols are the same as in Fig. V–6. The triangle with one apex as the blue straggler (HD 162586) represents the correction for ω = 0.9 for angles of inclination $i = 0^o$ and $i = 90^o$.*

detailed discussion on other properties of these stragglers have been listed by Mermilliod (1982).

(a) HD 93030 in IC 2602: This bright southern object has been found by Walborn (1979) to be a short period binary (P=1.7788 days) with a relatively low mass companion. Mass transfer phenomenon is supposed to account both for its spectral peculiarity and observed location in the HR diagram. The upper main sequence of the IC 2602 stars is shown in Fig V–6. Also shown, are the zero rotation zero age main sequence (ZRZAMS) from Chapter IV, the zero age main sequence (ZAMS) for ω=0.9 and the ZAMS for ω=1.0. The reddening effects predicted by Collins & Sonneborn (1977) for ω=0.9 and 1.0 were appropriately combined with the adopted ZRZAMS to derive the two ZAMS curves. The arrow heads indicate the position which the stars indicated would occupy if they were to be non-rotators. The rotational velocities for these stars were taken from Levato (1975) and were corrected using Table V–4. It can be noticed that the majority of the stars scatter around the ZAMS for ω=0.9 and would lie along the ZRZAMS if rotational reddening can be properly taken into account. The position of the blue straggler shows it is slightly evolved and cannot be considered anomalous.

(b) HD 60855 in NGC 2422: The upper main sequence of the stars in NGC 2422 is shown in Fig V–7. Rotational reddening corrections for the brightest members are indicated by arrows. Rotational velocities were taken from Dworetsky (1975). These corrections are a lower estimate if these stars have fractional velocities greater than ω=0.9. The reddening effect due to rotation is highly non-linear for $\omega > 0.9$ (Collins & Sonneborn 1977; Collins & Smith 1985). On the other hand, if the stars on the upper main sequence are evolved, then they would be rotating with less than 0.9, as an increase in the radius would diminish the rotational velocity of the star. Our corrections in this case would be slightly over-estimated. However, an ultraviolet excess of 0.15 magnitudes is not unusual for Be stars (Mermilliod 1982; Feinstein 1968). Therefore HD 60855 should be considered only as a probable blue straggler until detailed evolutionary tracks that take rotation into account become available.

(c) HD 23630 in Pleiades: The Pleiades data are plotted in Fig V–8, and the observed position of the stars appear to be consistent with the fact that they are fast rotators (Anderson, Stoeckly & Kraft 1966). The rotation corrections applied to the bright stars indicate that the age has to be revised downwards by a larger amount than that estimated by Maeder (1970). Remarks similar to the ones made in connection with NGC 2422 regarding the estimates for these corrections also apply to Pleiades. Given the uncertainties in the position of the bright members, HD 23630 should not be considered a blue straggler.

(d) HD143448 in NGC 6025: The data for this cluster is plotted in Fig V–9 which seems to indicate that the majority of the stars are fast rotators. No rotational velocity data is available for this cluster. The cluster appears similar to that of NGC 2422 and the same remarks as before apply to this cluster.

(e) HD 66194 in NGC 2516: The data for this cluster is plotted in Fig V–10. The large scatter of the stars in the M_v, $(u-b)_o$ plane appears to be directly correlated to the large spread in their rotational velocities. The $V sin\ i$ values were taken from Abt et al. (1989). The slowly rotating peculiar stars in this cluster are found closer to the ZRZAMS. This fact has already been noted by Eggen (1972) and Snowden (1975). Both of them call the CP stars in this cluster as stragglers! We find that a large number of slow rotators lie well above the main sequence indicating that they are probably fast rotators seen pole-on. For a few of the bright members, rotational velocities are not available. The age estimates for this cluster by Eggen (1972) and Snowden (1975) must be considered highly uncertain due to the large observed spread in the rotational velocity distribution for this cluster. However, the position in the colour-magnitude diagram of one of the evolved giants in this cluster indicates that HD 66194 should be considered as a blue straggler, as the giant appears to have evolved from a star less massive than the blue straggler itself.

(f) HD 162374 and HD 162586 in NGC 6475: The data for this cluster is plotted in Fig V–11. As both are slow rotators we can consider what would be their position if their rotational velocities were to be high as we have done for the A-type stragglers. If HD 162586 is an intrinsic slow rotator, a fact which we cannot prove, then it cannot be considered as a blue straggler. HD 162374 appears to be a definite blue straggler whatever be its true rotational velocity unless its helium weak nature can account for its large observed excess in the $(u-b)_o$ index. The ultraviolet excess may not be able to account for the observed $(u-b)_o$ index for HD 162374 unless it is also an intrinsic slow rotator while the other members of the cluster are fast rotators.

(g) HD 170054 in NGC 6633: This cluster has two blue stragglers in the A-type domain and one blue straggler in the B-domain. Fig V–5 in Section 2 shows that the position of the Am star (HD 170563) can easily be accounted for in terms of rotation effects. This star is a probable non-member. There are six red giants in the cluster, whose membership has been established from radial velocity measures by Mermilliod & Mayor (1989). The observed position of the giants in the colour-magnitude diagram of this cluster surely indicates that HD 169959 and

Table V–4. Average change in indices for change in velocity of 100 km s^{-1}.

$(u-b)_o$	ΔM_v	$\Delta(b-y)$	$\Delta(u-b)$
−0.058	−0.009	0.005	0.045
0.185	−0.019	0.006	0.059
0.436	−0.026	0.007	0.078
0.654	−0.034	0.007	0.103
0.830	−0.027	0.008	0.122
0.926	0.000	0.011	0.129
1.129	0.062	0.016	0.122
1.301	0.170	0.028	0.072
1.379	0.200	0.031	0.043
1.488	0.206	0.035	0.020

HD 170054 are definite blue stragglers.

If some of the stragglers in the B0-B3 class are real, then they are probably produced by the mechanism of mass-exchange in binary stars proposed by McCrea (1964). Quasi-homogeneous evolution proposed by Wheeler (1979b) appears ruled out as these few candidate stragglers, which are all in the early B-spectral range have a wide range in their observed $V sin\ i$ distribution.

VI. DISCUSSION

The effect of rotation on colours and line indices of stars has been a subject of some controversy, though not actually appreciated as such. Empirical calibrations of broad band and narrow band indices available in the literature have all been carried out without taking rotation effects into account. (e.g. u v b y and β by Crawford 1978, 1979). The discordant results in this field until 1970 have been nicely summarised by Collins (1970). The basic reason, that rotation effects on colours and line indices of stars could not be established firmly, seems to be due to the smallness of the effect for moderate rotational velocities. Further, the effects on observed indices by other causes such as duplicity, chemical peculiarity, evolutionary effects and variable interstellar extinction appear to have introduced a large uncertainity in the determination of rotation effects.

The problem is further complicated by the fact that the effects are a function of the mass of the stars. Theoretical work especially by Collins and his collaborators shows that each index is affected differently and very large effects should be observable for the A stars even for moderate rotational velocities. Also, there is no observable parameter which is not affected by rotation. The problem gets further confounded with the fact that only $V sin\ i$ is observable and there appears to be no way of determining V and i independantly.

We decided therefore to take an approach that would take care of most of these complications. In principle, it is similar to the method followed by Strittmatter (1966) in his analysis of the Praesepe cluster. At a given (B-V) value, he measured ΔV defined as the difference between the observed value and an assumed zero rotation main sequence. But we decided to make no assumption as far as the ZRMS is concerned. We wanted to determine the ZRMS after deriving the rotation effects.

We decided to analyse each cluster data separately as the members are coeval. We first derived a mean main sequence defined by the rotating stars and measured the deviations in the observed positions with respect to this mean main sequence. This is where we essentially differ in our analysis from the earlier workers. For example, Crawford & Barnes (1974) measured the deviations in c_1 from a preliminary calibration of zero age main sequence. In α-Persei cluster, they found the deviations in c_1 to show the rotation effects while the B-stars of the same cluster did not appear to be affected by rotation effects. Whereas, we find that our approach clearly demonstrates the rotation effects for both B and A stars. Similarly the analysis of field stars by Hartwick & Hesser (1974) and by Gray & Garrison (1988, 1989, 1990) demonstrates the effect on c_1 but the spread is large as they have not taken into account the reddening due to other causes.

The evolutionary effects even on the main sequence are brought out clearly in our analysis of the Scorpio-Centaurus association (see also Mathew & Rajamohan 1990). We have established firmly the rotation effects for various mass ranges by analysing a large number of clusters for which sufficient data was available. This was made possible by rejecting the spectroscopic doubles, and visual binaries with $\Delta m < 2.0$ magnitudes. We chose to analyse in detail — the intermediate band indices only — as we have detailed theoretical calculations by Collins and Sonneborn (1977), to compare. We also analysed the broad band U B V colours of α-Persei, Pleiades and the Scorpio-Centaurus association (Mathew & Rajamohan 1991). The results are compatible with our analysis of the intermediate band indices.

A basic assumption which underlies all our calculations is that the rotation effects are linear. This is not true for ω values greater than 0.9. Hence we would be underestimating the corrections for B0 to B3 stars and overestimating it slightly for the late A stars. In all our comparisons with the theoretical work of Collins and Sonneborn, we did not make any assumption on the distribution of v and i values. In our calculation of slopes of rotation effects from theory for a given value of i, we assumed distribution of equal number of stars at each ω. ($\omega \leq 0.9$).

Similarly in the calculations of ZRMS from theory, we have assumed that all stars in a cluster rotate with a value of i=60°. In spite of these assumptions, the agreement between observations and theory is very good. But the true ZRZAMS values for the early B stars is likely to be slightly in error. One must take the non linearity of the rotation effects into account for the B0-B3 stars to derive accurate ZRZAMS values.

The majority of the Lower Centaurus and Upper Centaurus main-sequence stars are of spectral type B2 and B3. The analysis of these stars is in excellent agreement with theoretical predictions by Collins & Sonneborn (1977). Similarly the B5 to B9 main sequence stars of the Alpha Persei cluster show perfect agreement with the theoretical calculations. The A3-F0 main sequence stars in Hyades, Praesepe, α-Persei and Pleiades agree very well with the calculations of Collins & Sonneborn (1977). The A0-A2 type stars have not been analysed. This is the range in which almost all indices are a function of both the effective temperature and gravity. Further, the procedures we have adopted are not suitable for this type. At these types, both β and c_1 reach a maximum value and the rotation effect on (u-b) starts reducing after reaching a maximum value around B9 and the effect on (b-y) starts becoming more pronounced after A0.

We derived ZRZAMS by two methods. In the first method we derived the ZRMS of each cluster using observed slopes of rotation effects. These were superposed to derive ZRZAMS. Similarly theoretical corrections for each star were made to derive ZRMS for each cluster. These were superposed to derive the ZRZAMS as derived from theoretical predictions (for i=60°). The two sets were found to agree with each other. The absolute magnitudes were corrected only using theoretical predictions. The β, M_v relation for ZRZAMS derived by us is in excellent agreement with the values for the lower envelope of B-stars in the β, M_v plane derived by Crawford (1978). This is as expected since the slow rotators in such a plane would lie along the blue envelope.

We have established for the first time the empirical zero rotation zero age values for the intermediate band indices u v b y and H_β. We also carried out extensive comparison with theoretical prediction for these indices with the calculations of Collins & Sonneborn. The agreement was very good and gave us enough confidence to look into enigmatic blue Straggler phenomena anew.

More than 25 years ago Strittmatter & Sargent (1966) had already suggested the possibility that relative rotation effects may be responsible for the observed position of the blue Stragglers in the HR diagram. We looked into this possibility for many of the blue Stragglers listed by Mermilloid (1982). We find that all the slow rotating blue Stragglers later than B5 can not be considered blue Stragglers at all. The average observed rotational velocity of about 150 km s^{-1} for the rest of the members shift them redward relative to the blue Stragglers. As the rotation effect in (u-b) index is maximum at spectral type B9, this effect appears very pronounced for the A-stars. There are no fast rotating A-type blue Stragglers at all. This is fully in conformity with the suggestion that rotation is responsible indirectly for these stars to be termed as blue Stragglers !

The fast rotators amongst blue Stragglers are all earlier than B7. We find that they too can be explained in terms of relative rotational velocity effects on colours. The ages of these clusters have been grossly overestimated because rotation effects have not been taken into account. Even Maeder's (1970) estimate of the errors in age determinations is low as his models predict lower effects in (U-B) and (B-V) than what is actually observed. Collins & Smith's (1985) work shows larger effects on the broadband indices than on the intermediate indices. Thus the effects on the (U-B) index must atleast be as much as in (u-b). The clusters with blue Stragglers of type B when plotted in the M_v, (b-y), M_v, (u-b) and M_v, c_o planes show that mostly all stars in a cluster, lie within the zero age band defined for ω=0 and ω=1.0. The early B-stars fall in the range of ω=0.9 and ω=1.0. The higher incidence of Be stars in this spectral type range also favours high rotational velocities for them. As the rotation effects are highly non linear, the early B-stars appear as more evolved. This leads to considerable overestimates of their ages and the position of a B-star that is rotating slightly slowly appears closer to the ZRZAMS.

We find that the blue Straggler phenomenon is not real. They are all normal stars rotating slower than their immediate main sequence counter parts.

VII. CONCLUSIONS

Effects of rotation on the intermediate band indices uvby and H_β are firmly established empirically from published data for many clusters. The observed positions of single main-sequence stars and single-lined spectroscopic binaries in a given plane defined by any two of the indices were used to establish the relative displacements due to rotation.

As interstellar extinction also reddens the stars, the Alpha Persei Cluster was analysed using both observed and dereddened indices. It was found that for Alpha Persei, where non-uniformity of extinction is not large, both reddened and dereddened indices lead to similar results. However, as suggested by Gray and Garrison, we used the observed indices for other clusters as dereddening procedures for A-stars are based on an assumed calibration which may be in error due to rotational reddening.

Evolutionary effects will introduce a scatter if the cluster members are not coeval. This is evident from our results for the Scorpio-Centaurus association. Here the upper Scorpius members which are younger than the Lower Centaurus and Upper Centaurus subgroups were found to be separated in all diagrams of colour excess due to reddening versus v sin i diagrams. Also the scatter for upper Scorpius was large where the interstellar extinction was highly non-uniform. The upper Centaurus and lower Centaurus group which are unreddened, consisting mostly of B2 and B3 type-stars show the reddening effect due to rotation in perfect agreement with theoretical predictions by Collins & Sonneborn (1977) for stars in the similar mass range.

As the predicted effects are a function of the mass, we analysed all clusters grouping them into three mass ranges corresponding to the spectral type ranges B0-B3, B5-B9 and A3-F0. The predicted indices for these ranges by Collins and Sonneborn were analysed the same way as we did our observational data.

In our analysis of the theoretically derived indices we did not assume any distribution in V or i. Instead, for each value of i (30^o, 45^o, 60^o and 90^o) we took sixteen values corresponding to ω=0.2, 0.5, 0.8 and 0.9 for the mass range corresponding to the spectral types from B0-B3, B5-B9 and A3-F0 and derived the rotation effects in different planes (such as β, c_1, β,(u-b) etc.). We found that the rotation effects determined from observed data points for clusters, very closely matched the predictions for the various mass ranges. We have established very firmly that not only rotation effects can be discerned from observations but also that the agreement is excellent with theoretical predictions of Collins & Sonneborn

(1977) for rigidly rotating stars.

The observed rotation effects, together with theoretical predictions were used to derive ZRMS for various clusters. The sequences were combined to derive a preliminary ZAZRMS values of the various indices.

The most dramatic result that we have obtained is that the blue straggler phenomenon in young galactic clusters can be completely interpreted in terms of rotation effects in colour magnitude diagrams; at least in the large majority of clusters with ages less than or equal to Hyades.

These results also raise some basic questions, such as the possible errors in estimates of ages of galactic clusters. Rotation affects the various indices differently and all indices do not show peak effects at the same spectral type. They would introduce great errors in age estimates, much greater than those calculated by Maeder (1970). This and other questons such as the errors in distance modulus estimated purely from photometry etc have to be considered in future work on this subject.

References

Abney, W. de W., 1877, Mon. Not. R. Astr. Soc., **37**, 278.

Abt, H.A., 1965, Astrophys. J. Suppl., **11**, 429.

Abt, H.A., 1970, in IAU Coll. 4 : Stellar Rotation ed. Slettebak, A., D.Reidel, Dordrecht, p.193.

Abt, H.A., 1979, Astrophys. J., **230**, 485.

Abt, H.A., 1985, Astrophys. J. Lett., **294**, No. L 103.

Abt, H.A., and Chaffee, F.H., 1967, Astrophys. J., **148**, 459.

Abt, H.A., Clements, A.E., Doose, L.R., and Harris, D.H., 1969, Astron. J., **74**, 1153.

Abt, H.A., and Hunter, J.H., Jr. 1962, Astrophys. J., **136**, 381.

Abt, H.A., and Jewsbury, Cp.P., 1969, Astrophys. J., **156**, 983.

Abt, H.A., and Levato, H., 1977, Publ. Astron. Soc. Pacific, **89**, 648.

Abt, H.A., and Levato, H., 1977, Publ. Astron. Soc. Pacific, **89**, 797.

Abt, H.A., and Morgan, W.W., 1969, Astron. J., **74**, 813.

Abt, H.A., Muncaster, G.W., and Thompson, L.A., 1970, Astron. J., **75**, 1095.

Anderson, C.M., Stoeckly,R., and Kraft, R.P., 1966, Astrophys. J., **143**, 299.

Atkinson, R. d'E., 1937, Observatory, **60**, 299.

Balona, L.A., 1975, Mem. Roy. Astron. Soc., **78**, 51.

Bidelman,W.P., 1956, Publ. Astron. Soc. Pacific., **68**, 318.

Blaauw, A., 1959, IAU Symp. 10. The Hertzsprung - Russell Diagram. J. Greenstein, Ed. p.105.

Blaauw, A., 1964, A. Rev. Astr. Astrophys. **2**, 213.

Blaauw, A., Hiltner, W.A. and Johnson, H.L., 1959, Astrophys. J., **130**, 69, Ap. J., **131**, 527, (erratum).

Braes, L.L.E., 1962, Bull. Astron. Inst. Neth., **16**, 297.

Canterna, R., and Perry, C.L., 1979, Publ. Astron. Soc. Pacific, **91**, 263.

Collins, G.W., II, 1963, Astrophys. J., **138**, 1136.

Collins, G.W., II, 1965, Astrophys. J., **142**, 265.

Collins, G.W., II, 1970, Stellar Rotation. Procee. of IAU Coll. ed. Stettebak, p.85.

Collins, G.W., II and Harrington, J.P., 1966, Astrophys. J., **146**, 152.

Collins, G.W., II and Sonneborn, G.H., 1977, Astrophys. J. Suppl., **34**, 41.

Collins, G.W., II and Smith, R.C., 1985, Mon. Not. R. Astr. Soc., **213**, 519.

Collins, G.W., II., Traux, R.J. and Cranmer, S.R., 1991, Astrophys. J. Suppl., **77**, 541.

Crawford, D.L., 1978, Astron. J., **83**, 48.

Crawford, D.L., 1979, Astron. J., **84**, 1858.
Crawford, D.L., and Barnes, J.V., 1969, Astron. J., **74**, 818.
Crawford, D.L., and Barnes, J.V., 1969, Astron. J., **74**, 407.
Crawford, D.L., and Barnes, J.V., 1970, Astron. J., **75**, 952.
Crawford, D.L., and Barnes, J.V., 1972, Astron. J., **77**, 862.
Crawford, D.L., and Barnes, J.V., 1974, Astron. J., **79**, 687.
Crawford, D.L., and Mander, J., 1966, Astron. J., **71**, 114.
Crawford, D.L., and Perry, C.L., 1966, Astron. J., **71**, 206.
Crawford, D.L., and Perry, C.L., 1976, Astron. J., **81**, 419.
Dickens, R., Kraft, R., and Krzeminski, W., 1968, Astr. J., **73**, 6.
Dworetsky, M., 1975, Astron. J., **80**, 131.
Eggen, O.J., 1972, Astrophys. J., **173**, 63.
Eggen, O.J., 1974, Astrophys. J., **188**, 59.
Eggen, O.J., 1981, Astrophys. J., **247**, 507.
Eggen, O.J., 1981, Astrophys. J., **246**, 817.
Feast, M.W., 1963, Mon. Not. R. Astr. Soc., **126**, 11.
Feinstein, A., 1968, Z. Astrophys., **68**, 29.
Feinstein, A., Forte, J.C., 1974, Publ. Astron. Soc. Pacific, **86**, 284.
Garmany, C.D., 1973, Astron. J., **78**, 185.
Garrison, R.F., 1967, Astrophys. J., **147**, 1003.
Glaspey, J.W., 1971, Astron. J., **76**, 1041.
Gray, R.O., and Garrison, R.F., 1987, Astrophys. J. Suppl., **65**, 581.
Gray, R.O., and Garrison, R.F., 1989, Astrophys. J. Suppl., **69**, 301.
Gray, R.O., and Garrison, R.F., 1989, Astrophys. J. Suppl., **70**, 623.
Guthrie, B.N.G., 1963, Pub. Roy. Obs. Edinburgh, **3**, 84.
Hardorp, J., and Strittmatter, P., 1968a, Astrophys. J., **151**, 203.
Hartoog, M.R., 1976, Astrophys. J., **205**, 807.
Hartwick, F.D.A., and Hesser, J.E., 1974, Astrophys. J., **192**, 391.
Heckmann, O., Dieckvoss, W., and Kox, H., 1956, Astr. Nachr., **283**, 109.
Hertzsprung, E., 1947, Ann. Sterrew, Leiden, **19**, pt.1.
Herzog, A.D., Sanders, W.L., and Seggewiss, W., 1975, Astron. Astrophys. Suppl. **19**, 211.
Hill, G., and Perry, C.L., 1969, Astron. J., **74**, 1011.
Hintzen, P., Scott, J., 1974, Astrophys. J., **194**, 657.
Hoffleit, D., and Jaschek, C., 1982, The Bright Star Catalogue, Yale Univ. Obs., New Haven (BSC).
Hoag, A.A., Johnson, H.L., Iriate, B., Hallam, K., and Sharpless, S., 1961. Publs. US Naval Obs., **17**, 347.
Hogg, A.R., and Kron, G.E., 1955, Astron. J., **60**, 365.

Huang, S.S., and Struve, O., 1960, Stellar Atmosphere, ed. Greenstein, p.321.
Ianna, P.A., 1970, Publ. Astron. Soc. Pacific, **82**, 825.
Johnson, H.L., 1952, Astrophys. J., **116**, 640.
Johnson, H.L., and Knuckles, C.F., 1955, Astrophys. J., **122**, 209.
Johnson, H.L., and Mitchell, R.I., 1958, Astrophys. J., **128**, 31.
Kawaler, S.D., 1987, Publ. Astr. Soc. Pacific, **99**, 1322.
Kilambi, G.C., 1975, Publ. Astron. Soc. Pacific, **87**, 975.
Kraft, R.P., 1965, Astrophys. J., **142**, 681.
Kraft, R.P., 1967, Astrophys. J., **148**, 129.
Kraft, R.P., 1969, Struve Memo. Vol. p.385.
Kraft, R.P., and Wrubel, M., 1965, Astrophys. J., **142**, 703.
Levato, H., 1974, Publ. Astron. Soc. Pacific, **86**, 940.
Levato, H., 1975, Astrophys. J., **195**, 825.
Levato, H., and Abt, H.A., 1977, Publ. Astron. Soc. Pacific, **89**, 274.
Levato, H., and Garcia, B., 1984, Astrophys. Letters., **24**, 161.
Maeder, A., 1971, Astron. & Astrophys., **10**, 354.
Maeder, A., 1987, Astron. & Astrophys., **178**, 159.
Maeder, A., and Peytreman, E., 1972, Astron. & Astrophys., **21**, 279.
Mathew, A., and Rajamohan, R., 1990a, J. Astrophys. Astr. **11**, 167.
Mathew, A., and Rajamohan, R., 1990b, Bull. Astron. Soc. India, **18**, 329.
Mathys, G., 1991. (to be published in Astron. & Astrophys.).
McCrea, W.H., 1964, Mon. Not. R. Astr. Soc., **128**, 147.
Mc Gee, J.D., Khogali, A., Baum, W.A., and Kraft, R.P., 1967, Mon. Not. R. Astr. Soc., **137**, 303.
Mc Namora, D.H., and Larsson, H.J., 1961, Astrophys. J., **135**, 748.
Mendoza, E.E., 1956, Astrophys. J., **123**, 54.
Mendoza, E.E., 1963, Bol. Obs. Tonantzintla y. Tacubaya **3**, 137.
Mermilliod, J.C., 1982, Astron. & Astrophys., **109**, 37.
Mermilliod, J.C., Mayor, M., 1989, Astron. & Astrophys., **219**, 125.
Mitchell, R.I., 1960, Astrophys. J., **132**, 68.
Moreno, A., and Moreno, H., 1968, Astrophys. J. Suppl. **15**, 459.
Morgan, W.W., and Hiltner, W.A., 1965, Astrophys. J. Suppl. **141**, 177.
Morgan, W.W., Hiltner, W.A., and Garrison, R.F., 1971, Astron. J., **76**, 242.
Nissen, P.E., 1988, Astron. Astrophys., **199**, 146.
Pendl, E.S., and Seggeswiss, W., 1975, IAU Coll. 32 : Physics of Ap. Stars. eds. W.W.Weiss, H.Jenker, H.J.Wood, Universitasstern Warte Weim, p.357.
Perry, C.L., and Bond, H.E., 1969, Publ. Astron. Soc. Pacific, **81**, 629.
Perry, C.L., Franklin, C.B.Jr., Landolt, A.U., and Crawford, D.L., 1976, Astron. J., **81**, 632.

Perry, C.L., and Hill, G., 1969, Astron. J., **74**, 899.
Pesch, P., 1961, Astrophys. J., **134**, 602.
Petrie, R.M., 1964, Pub. Dom. Astrophys. Obs. **12**, 317.
Plavec, M., 1970, in IAU Coll. 4 : Stellar Rotation, ed. Slettebak, A., D.Reidel, Dordrecht, p.133.
Rajamohan, R., 1976, Pramana, **7**, 160.
Rajamohan, R., 1978, Mon. Not. R. Astr. Soc., **184**, 743.
Rajamohan, R., and Mathew, A., 1988, J. Astrophys. Astr. **9**, 107.
Roxburgh, I.W., 1970, in IAU Coll. 4 : Stellar Rotation, ed. Slettebak, A., D.Reidel, Dordrecht, p.318.
Roxburgh, I.W., Griffith, J., & Sweet, P., 1965, Zs. f. Ap. **61**, 203.
Roxburgh, I.W., & Strittmatter, P.A., 1965, Z. Astrophys., **63**, 15.
Roxburgh, I.W., & Strittmatter, P.A., 1966, Mon. Not. R. Astr. Soc., **133**, 345.
Sargent, W.L.W., & Strittmatter, P.A., 1966, Astrophys. J., **145**, 938.
Schild, R.E., 1970, Astrophys. J., **161**, 855.
Schmidt, E.G., 1976, Pub. Astron. Soc. Pacific, **88**, 63.
Schmidt, E.G., 1978, Pub. Astron. Soc. Pacific., **90**, 157.
Schmidt, E.G., & Forbes, D., 1984, Mon. Not. R. Astr. Soc., **208**, 83.
Shobbrook, R.R., 1984, Mon. Not. R. Astr. Soc., **206**, 273.
Shobbrook, R.R., 1984, Mon. Not. R. Astr. Soc., **211**, 659.
Slettebak, A., 1968, Astrophys. J., **151**, 1043.
Slettebak, A., 1970, in IAU Coll. 4 : Stellar Rotation, ed. Slettebak,A., Reidel.D., Dordrecht, p.3.
Smyth, M.J., & Nandy, K., 1962, Publs. R. Obs., Edinburgh, **3**, No.2, 23.
Snowden, M.S., 1975, Publs. Astron. Soc. Pacific., **87**, 721.
Snowden, M.S., 1976, Publs. Astron. Soc. Pacific., **88**, 174.
Stother, R., Chin, C.W., 1979, Astrophys. J., **233**, 267.
Strittmatter, P.A., 1966, Astrophys. J., **144**, 430.
Strittmatter, P.A., and Sargent, W.W., 1965, Astrophys. J., **145**, 130.
Strom, K.M., Strom, S.E., & Yost, J., 1971, Astrophys. J. **165**, 479.
Stromgren, B., 1966, Ann. Rev. Astron. Astrophys. **4**, 433.
Stromgren, B., 1967, Magnetic and Related Stars, p.461.
Sweet, P.A., and Roy, A.E., 1953, Mon. Not. R. Astr. Soc., **113**, 701.
Trimble, V.L., & Ostriker, J.P., 1978, Astron. & Astrophys., **63**, 433.
Trimble, V.L., & Ostriker, J.P., 1981, Astron. & Astrophys., **97**, 403.
Uesugi, A., & Fukuda, I., 1982, Revised Catalogue of Stellar Rotational Velocities, Kyoto Univ. Japan.
Vogel, S.N., & Kuhi, L.V., 1981, Astrophys. J., **245**, 960.
Walborn, N.R., 1979, Publ. Astr. Soc. Pacific, **91**, 442.

Walker, M.F., 1956, Astrophys. J. Suppl., **2**, 365.
Warren, W.H., 1976, Mon. Not. R. Astr. Soc., **174**, 111.
Warren, W.H., & Hesser, J.E., 1977, Astrophys. J. Suppl., **34**, 115.
Wheeler, J.C., 1979a, Comments, Astrophys., **8**, 133.
Wheeler, J.C., 1979b, Astrophys. J., **234**, 569.
Williams, I.P., 1964a, Mon. Not. R. Astr. Soc., **128**, 389.
Williams, I.P., 1964b, Ann. d'Astrophys, **27**, 198.
Yong, A., 1978, Publs. Astron. Soc. Pacific, **90**, 144.